THE EFFECT OF ANTECEDENT MOISTURE CONDITION ON HEC-HMS MODEL PERFORMANCE: A CASE STUDY IN KELANI RIVER BASIN, SRI LANKA

Karma Yangzom Dorji

(179233D)

Degree of Master of Science

Department of Civil Engineering

University of Moratuwa
Sri Lanka

April 2018

THE EFFECT OF ANTECEDENT MOISTURE CONDITION ON HEC-HMS MODEL PERFORMANCE: A CASE STUDY IN KELANI RIVER BASIN, SRI LANKA

Karma Yangzom Dorji

(179233D)

Thesis submitted in partial fulfilment of the requirements for the degree
Master of Science in Water Resources Engineering and Management

Supervised by

Dr. R. L. H. L. Rajapakse

UNESCO Madanjeet Singh Centre for
South Asia Water Management (UMCSAWM)

Department of Civil Engineering

University of Moratuwa

Sri Lanka

April 2018

DECLARATION

I declare that this is my own work and this thesis does not incorporate without acknowledging any material previously submitted for a Degree or Diploma in any other University or institute of higher learning and to the best of my knowledge and belief it does not contain any material previously published or written by another person except where the acknowledgement is made in the text.

Also, I hereby grant to University of Moratuwa the non-exclusive right to reproduce and distribute my thesis, in whole or in part in print, electronic or other medium. I retain the right to use this content in whole or part in future works (such as articles or books).

Signature: Date: 16th April 2018

The above candidate has carried out research for the Master's thesis under my supervision.

Signature of the supervisor: Date

ACKNOWLEDGEMENT

I would first like to thank my research supervisor Dr. R. L. H. L. Rajapakse for the patient guidance, encouragement and advices he provided me on my research. Without his dedicated supervision and continuous guidance, successful completion of this thesis would not have been possible. I take this opportunity to humbly extend my sincere gratitude to my research supervisor for spending his valuable time with me in materializing this research work.

I must thank Senior Professor N.T.S Wijesekera for being my source of inspiration and always bringing out the best in me. His continuous encouragement and advices kept me framed in achieving my Master's degree.

Mr. Wajira Kumarasinghe and Mrs. Gayani Edirisinghe and all other Centre staff will be remembered for providing all necessary assistance during the course and helping me during my sickness.

I would also like to thank my husband and my family members for their unconditional love, support and believe in me which encouraged me to work up to my level best during my stay in Sri Lanka. Had they not been the source of my motivation, I would not have been where I am now.

Lastly, I would like to thank South Asian Foundation (SAF) for providing financial support through scholarship, SAF Founder, late Shri Madanjeet Singh and the University of Moratuwa for furnishing this outstanding opportunity for me to study towards the Master's Degree in Water Resource Engineering and Management, at UNESCO Madanjeet Singh Centre for South Asia Water Management (UMCSAWM), Department of Civil Engineering, University of Moratuwa, Sri Lanka.

The Effect of Antecedent Moisture Condition on HEC-HMS Model Performance: A Case Study in Kelani River Basin, Sri Lanka

ABSTRACT

Among all observed natural hazards, water-related disasters are the most frequent and they pose major threats to people and while hindering socio-economic development. Flood forecasting is one the most challenging and difficult problems in hydrology. However, it is also one of the most important problems in hydrology due to its critical contribution in reducing economic damages and loss of life losses. In many regions of the world, flood forecasting is one among the few feasible options to manage floods. In Soil Conservation Service Curve Number (SCS-CN) method, Antecedent Moisture Condition (AMC) of the soil plays a very consequential role because the curve number varies according to the soil, land cover and soil moisture content, and that is considered while estimating runoff depth. Soil water represents only a minimal part of the water on our planet, but it is certainly one of the most imperative factors when it comes to flood forecasting since soil saturation directly affects runoff generation.

Kelani river basin was selected for the study because of the nature of the basin with respect to the vulnerability to floods and availability of data at finer resolution. Ten years of daily rainfall, streamflow and evaporation data from 2007 to 2017 water year were used for the study. Events separation was carried out using Minimum Inter-event Time (MIT) method. There are 38 selected events, out of which the first half events were used for model calibration and the second half events were used for model verification. The univariate gradient search method was applied to optimize the parameters by minimizing the Sum of Absolute Residual Error (SARE) objective function. Manual calibration was carried out using Nash-Sutcliffe model efficiency coefficient (NASH) as an objective function for comparison.

The average NASH value in model calibration and validation were 0.63 and 0.62 while the lowest Root Mean Square Error (RMSE) obtained in model calibration and validation were 1.31 and 2.82 respectively. The closer the model efficiency is to NASH value of 1, the more accurate the model is. The calibration data set performed better than the model verification data set as depicted by lower RMSE value. Random events were selected to incorporate different soil moisture conditions to check the model performances. It has been observed that the events that falls in Maha season performs better when AMC III is applied whereas the model performance neither improves nor deteriorate when the events falls in Yala season.

The present work reveals and confirms that while conducting event rainfall-runoff modelling for flood management using HEC-HMS, AMC should be considered in order to improve the model efficiency and performance. The study findings are applicable to other hydrologically similar basins in the same region or elsewhere and the findings from model sensitivity analysis are useful for fine tuning model performance and opting for better flood management strategies.

Keywords: Event based modelling, Inter-event time, Model sensitivity and efficiency

TABLE OF CONTENTS

TABLE OF FIGURES

LIST OF TABLES

1. INTRODUCTION

1.1 General

The term hydrology can be treated as an important subject for the people and their environment. It treats water of the earth, their occurrence, circulation and distribution, their chemical and physical properties and their reaction with the environment including their relation to living things (Ray, 1975). Due to rapid urbanisation and industrialisation including deforestation, land cover change and irrigation, various changes have been incurred on hydrologic systems. Along with climate change, soil heterogeneity as well as soil saturation has direct impact on the discharges of many rivers in and around the world (Devi et al., 2015).

Among all observed natural hazards, water-related disasters are the most frequent and they pose major threats to people and socio-economic development (ICHARM, 2009). International Centre for Water Hazard and Risk Management (ICHRM) reports that water-related disasters account for about 72% of the total economic damages caused by natural disasters, out of which 26% of all the damages are attributed to floods. These losses are expected to escalate in the future due to climate change, land use change, deforestation, rising sea levels, and population growth in flood-prone areas, causing the number of people vulnerable to flood disasters globally to increase to two billion by 2050 (Bogardi, 2004, ICHARM, 2009, Vogel et al., 2011).

Development of optimal flood forecasting and viable flood risk management systems have been advocated as measures of flood preparedness (Arduino et al., 2005, WMO, 2011). Due to the uncertainties surrounding the magnitude, timing and place of occurrence, geographical extent, and geophysical interactions of floods, it is often not possible to completely control them. As a result, complete protection from flood is not always considered as a viable alternative (Moore et al., 2005).

Flood forecasting is one of the most challenging and difficult problems in hydrology. However, it is also one of the most important problems in hydrology due to its critical contribution in reducing economic damages and loss of life . In many regions of the world, flood forecasting is one among the few feasible options to manage floods (Jain, et al., 2018).

Soil water represents a minimal part of the water on our planet, but it is certainly one of the most imperative factors when it comes to flood forecasting since soil saturation directly affects runoff generation. The soil plays a central role in the terrestrial water cycle by controlling the partitioning of rainfall among evapotranspiration, runoff, and deep infiltration in a strongly nonlinear way. Soil moisture dynamics directly or indirectly controls meteorological processes, plants conditions, soil biogeochemistry, groundwater dynamics, and the exchanges of nutrients and contaminants in the soil (Daly & Porporato, 2005). Soil water content in the upper soil layer prior to a rain event which is called as Antecedent Moisture Content (AMC) can be an important factor affecting the relationship between rainfall and runoff (Zhang, Wei, & Nearing, 2011). However, for modelling purposes using Soil conservation Service's Curve Number (SCS-CN) method, watersheds are mostly considered to be AMC II, which is essentially an average moisture condition (Walker et al., 2018). For example, a study carried out by Li (2010) used only CN II which is also considered as AMC II condition in HEC-HMS model for flood forecasting in Misai and Wan'an catchments in China. Similarly, a study conducted using HEC-HMS for flood forecasting and flood estimation in Kabkian basin and Delibajak sub-basin in Iran and for Johor River, Malaysia considered SCS curve number method (Soil conservation Service, 1972) for the rainfall-runoff modelling but the use of specific Antecedent Moisture Condition (AMC) was not reflected (Asadi & Boostani, 2013).

In SCS Curve Number method, antecedent moisture condition of the soil plays a very consequential role because CN number varies according to the soil and that is considered while estimating runoff depth (Kumar et al., 2017). It is applied on a continuous based modelling for watershed management and natural resources development purposes. In event based modelling in HEC-HMS for Kelani river basin, Sri Lanka, the Green and Ampt infiltration loss method was used to account for infiltration loss (De Silva, Weerakoon, & Herath, 2014). Kelani river basin is the most vulnerable river basin for floods in Sri Lanka. Therefore, it is very important to develop an effective event based model platform for flood management purposes especially incorporating AMC into the model to improve the model performances.

1.2 Problem Statement

Extreme low pressure conditions in the Bay of Bengal and two monsoon systems, Northeast (May ~ September) and Southwest (November ~ February) monsoons, have direct impact on the rainfall patterns in Sri Lanka. Anomalously high seasonal precipitation typically associated with La Nina phenomenon and cyclonic storms which originate from the Bay of Bengal are usually the main reasons for the devastating floods in the island.

The annual rainfall distribution in Kelani basin varies from 500 mm to 5,000 mm with an average mean annual rainfall about 3,450 mm. The watersheds in the middle of the basin receive the highest rainfall. The total volume of water falling within the basin is estimated at 7,865 Million Cubic Meters (MCM) with about 43% of rainfall ending in the Indian Ocean (Survey Department of Sri Lanka, 2007). It is one of the most vulnerable river basins for floods in Sri Lanka. The flood damages caused are relatively high as the river flows through the commercial capital of the country. Therefore, it is necessary to develop an effective rainfall-runoff modelling system for better flood management in Kelani Basin.

The key reason for selecting Kelani river basin is the nature of the basin with respect to the vulnerability to floods and availability of data at finer resolution.

1.3 Objective of the Study

1.3.1 Overall objective

The overall objective of this research is to incorporate the effect of antecedent moisture condition to improve the HEC-HMS model performance for better flood forecasting and management.

1.3.2 Specific objectives

The specific objectives of the study to achieve the aforementioned overall objective of the study are as listed below.

1. Comprehensive Literature Review to assess present status of Rainfall-runoff modelling, HEC-HMS modelling, Event based modelling and Antecedent moisture condition.
2. To collect data, perform data checking and selection of events for analysis.
3. Development of HEC-HMS model for Kelani river basin.
4. Incorporation of Antecedent Moisture Conditions (AMC) in HEC-HMS model.
5. Calibration and Verification of the hydrologic model for Kelani river basin.
6. Making suitable recommendations for better flood management.

2 LITERATURE REVIEW

2.1 Hydrological Models

A model is a simplified representation of real world system. The best model is the one which give results close to the reality with the use of the least parameters and model complexity. Models are mainly used for predicting system behaviour and understanding various hydrological processes. A model consists of various parameters that define the characteristics of the model (Sorooshian & Moradkhani, 2008). A runoff model can be defined as a set of equations that helps in the estimation of runoff as a function of various parameters used for describing watershed characteristics. The two important inputs required for all models are rainfall data and drainage area. Along with these, watershed characteristics like soil properties, vegetation cover, topography, soil moisture content, characteristics of groundwater aquifer are also considered. Hydrological models are nowadays considered as an important and necessary tool for water and environmental resource management (Gyathri et al. 2015).

2.1.1 Types of models

Rainfall-runoff models are classified based on model input and parameters and the extent of physical principles applied in the model. They can be classified as lumped and distributed models based on the model parameters as a function of space and time and deterministic and stochastic models based on the other criteria. Deterministic models will give same output for a single set of input values whereas in stochastic models, different values of output can be produced for a single set of inputs. According to Sorooshian and Moradkhani (2008) in lumped models, the entire river basin is taken as a single unit where spatial variability is disregarded and hence the outputs are generated without considering the spatial processes whereas a distributed model can make predictions that are distributed in space by dividing the entire catchment into small units, usually square cells or triangulated irregular network, so that the parameters, inputs and outputs can vary spatially. Another classification is static and dynamic models based on time factor. Static models exclude time while dynamic model include time. Wheater et al., (2007) had classified the models as event based and continuous models. The former one produce output only for specific time periods while the latter produces a continuous output. One of the most important classifications is empirical model, conceptual models and physically based models as described in Table 2-1.

Table 2-1 Characteristics of three model

Empirical model	Conceptual model	Physically based model
Data based or metric or black box model	Parametric or grey box models.	Mechanistic or white box models.
Involve mathematical equations, derive values from available time series.	Based on modelling of reservoirs and include semi empirical equations with a physical basis.	Based on spatial distribution, evaluation of parameters describing physical characteristics.
Little consideration of features and processes of system.	Parameters are derived from field data and calibration.	Require data about initial state of the model and morphology of catchment.
High predictive power, low explanatory depth.	Simple and can be easily implemented in computer code.	Complex model, requires human expertise and computation capability.
Cannot be generated to other catchment.	Require large hydrological and meteorological data sets.	Suffer from scale related problems.
ANN, Unit hydrograph.	HBV model, TOPMODEL.	SHE or MIKESHE model, SWAT.
Valid within the boundary of the given domain.	Calibration involves curve fitting making difficult physical interpretation.	Valid for wide range of situations.

Source: Department of Applied Mechanics and Hydraulics, National Institute of Technology Karnataka

2.2 Hydrologic Modelling System (HEC-HMS)

The Hydrologic Modelling System (HEC-HMS) is designed to simulate the precipitation-runoff processes of dendritic drainage basins. It is designed to be applicable in a wide range of geographic areas for solving the widest possible range of problems. This includes large river basin water supply and flood hydrology and small urban or natural watershed runoff. Hydrographs produced by the program are used directly or in conjunction with other software for studies of water availability, urban drainage, flow forecasting, future urbanization impact, reservoir spillway design, flood damage reduction, floodplain regulation, and systems operation. HEC-HMS model computes the runoff volumes by computing the volume of water that is intercepted, infiltrated, stored, evaporated or transpired and subtracting it from the precipitation (USACE, 2000).

HEC-HMS has three main components, as listed below:

1. Basin Model
2. Precipitation Model
3. Control Specification

The components of the basin model are Precipitation loss model, Transform model, Baseflow model and Routing model.

2.2.1 Precipitation loss model

There are 11 loss methods in HEC-HMS, namely, Deficit and constant, Exponential, Green and Ampt, Gridded deficit constant, Gridded SCS curve number, Gridded soil moisture accounting, Initial and constant, SCS curve number, Smith Parlange and Soil moisture accounting. Selecting a loss model and estimating the model parameters are critical steps in developing a HEC-HMS model. Not all loss models can be used with all transforms (Feldman, 2000).

Chow, Maidment and Mays (1988) explained the abstractions or losses as the difference between observed total rainfall hyetograph and excess rainfall hyetograph. The SCS curve number method, Green and Ampt method, Average storm method, Horton method and Phi index method are methods of separating effective component from the total rainfall but among all methods, Phi index is the constant rate of abstraction that will yield excess rainfall hyetograph with a total depth which equals the depth of direct runoff over the watershed and it is determined by trial and error (Chow et al., 1988).

Sardoii et al. (2012) interpreted that Green & Ampt infiltration model is a conceptual model in HEC-HMS that calculates precipitation loss in permissible surfaces. Required parameters in this method are initial loss, conductivity, wetting front suction and volume moisture deficit. The initial and constant loss model includes two parameters of constant rate and initial loss. These parameters show the soil physical characteristics, land use and previous wet conditions of basin, respectively. If basin is in saturated condition, initial loss tends to zero and when basin is in dry condition, initial loss increases and majority of precipitation is not converted to runoff. The SCS method classifies soil into four groups based on their infiltration capacity. The SCS model estimates surplus precipitation as a function of cumulative precipitation, soil cover, land use and previous moisture condition.

Manchanayake, Sumanaweera and Jayaratne (1985) evaluated the loss rates for some Sri Lankan catchments by using Horton method and Average storm method for selected storm periods and compared the results. The study concluded that the Average storm method gives considerable differences with Horton method and if temporal and aerial distribution of rainfall are uniform over the catchment, the Average storm method would give quite satisfactory results.

In the study carried out for Attanagalu Oya basin, the Deficit constant loss method performed better than SCS Curve number method (Halwatura & Najim, 2013). An assortment of different methods is available to simulate infiltration losses. Options for event modelling include Initial constant, SCS curve number, exponential, Green Ampt, and Smith Parlange. Deficit and constant loss method and soil moisture accounting method can be used for continuous hydrologic modelling (Cunderlik and Simonovic, 2004). A canopy component can be added to represent interception and transpiration. A surface component can be added to represent depression storage.

USACE (2000) stated several pros and cons of different loss methods in HEC-HMS. Initial and constant rate method is easy to set up and use but it is difficult to apply to ungauged areas due to lack of direct physical relationship of parameters and watershed properties. Deficit and constant rate method can be used for long term simulation but the model may be too simple to predict losses. The SCS-CN method is a simple and stable well established method, widely accepted for use in United States (US) and abroad but it is developed with data from small agricultural watersheds in Midwestern US, so its applicability to elsewhere is uncertain.

2.2.2 Transform model

There are seven methods for transforming excess precipitation into surface runoff. Unit hydrograph methods include the Clark, Snyder, and SCS techniques. User-specified unit hydrograph or S-graph ordinates can also be used. The modified Clark method (ModClark), is a linear quasi-distributed unit hydrograph method that can be used with gridded meteorological data. An implementation of the kinematic wave method with multiple planes and channels is also included.

Halwathura and Najim (2013) concluded that Snyder unit hydrograph method simulates more reliable flow compared to the Clark unit hydrograph method in their study carried out for Attanagalu Oya basin. In SCS unit hydrograph, lag time is the only parameter. Lag time is proportional to the time of concentration, T_c which is calculated using Kirpich formula (Chow et al., 1998)

2.2.3 Baseflow model

Five methods are included for representing baseflow contributions to sub-basin outflow. The recession method gives an exponentially decreasing baseflow from a single event or multiple sequential events. The constant monthly method can work well for continuous simulation. The linear reservoir method conserves mass by routing infiltrated precipitation to the channel. The nonlinear Boussinesq method provides a response similar to the recession method but the parameters can be estimated from measurable qualities of the watershed. Recession baseflow model is intended primarily for event simulation, it has the ability to automatically reset after each storm event and consequently may be used for continuous simulation (USACE, 2000).

2.2.4 Routing model

Six hydrologic routing methods are included for simulating flow in open channels. Routing with no attenuation can be modelled with the lag method. The traditional Muskingum method is included along with the Straddle stagger method for simple approximations of attenuation. The Modified Puls method can be used to model a reach as a series of cascading, level pools with a user-specified storage-discharge relationship. Channels with trapezoidal, rectangular, triangular, or circular cross sections can be modelled with the kinematic wave or Muskingum-Cunge methods. Channels with overbank areas can be modelled with the Muskingum-Cunge method and an 8-point cross section. Additionally, channel losses can also be included in the routing. The constant loss method can be added to any routing method while the percolation method can be used only with the Modified Puls or Muskingum-Cunge methods (USACE, 1992).

The kinematic wave and Muskingam models cannot account for the influence of backwater on the flood wave because these are based on uniform flow assumptions and only Modified Pulse model can simulate backwater effects (USACE, 2000). Further, it states that flood flows through extremely flat and wide flood plains may not be modelled accurately as one dimensional flow. Nandalal and Ratnayake (2010) mentioned that Muskingam model accounts clearly for channel storage only and not total storage along a river reach which may include lateral inflows or outflows, losses and temporal changes in bank storage and hence the model may generate impractical values for Muskingam parameters.

2.3 Automatic Parameter Optimization in HEC HMS

The HEC-HMS automatic calibration capabilities include the ability to specify one of six different objective functions and one of two different search algorithms. Four of the six objective function definitions currently available within HEC-HMS are 1-norm, 2-norm squared, percentage error in peak and peak-weighted root mean square error (Skahil, 2006).

In automatic parameter optimization, HEC HMS model has default constraints that limit the ranges of optimized values. The two search algorithms within HEC-HMS include the univariate-gradient search algorithm and the derivative-free minimization algorithm (Nelder & Mead, 1965). According to Skahill (2006), the Nelder and Mead local search algorithm is a widely used derivative-free minimization algorithm that works in multiple dimensions. It is sometimes referred to as an "amoeba" method because it works by setting up rules that allow a cloud of points in parameter space to "crawl" to an objective function minimum in a vaguely amoeboid fashion. Rather than starting with a single initial guess for the optimized model, as with the univariate-gradient search algorithm.

Skahill (2006) after calibrating the model using automated parameter optimization for Goodwin Creek experimental watershed in United States concluded that the ability to find the global objective function minimum was an insufficient requirement to attain a hydrologically acceptable model. The author pointed out some limitations associated with the existing HEC-HMS automatic parameter optimization capabilities and proposed certain improvements. As potential improvements to existing HEC-HMS automatic parameter optimization, Gauss-Marqardt-Levenberg (GML) method of computer based parameter estimation method was presented. The author recommended two algorithmic enhancements to the GML method that retains its strengths, but overcomes its weaknesses in the face of local optima.

2.4 Antecedent Moisture Condition

Antecedent Moisture condition is the preceding relative moisture of the pervious surfaces prior to the rainfall event. This is also referred to as Antecedent Runoff Condition (ARC). Antecedent Moisture is considered to be low when there has been little preceding rainfall and high when there has been considerable preceding rainfall prior to the modelled rainfall event. In the event that the soil is fully saturated, the whole amount of rainfall will directly convert to runoff without infiltration losses and if the soil is fully dry, it is possible that the whole rainfall amount is absorbed by the soil, leading to no surface runoff. Thus, the antecedent moisture condition affects the process rainfall-runoff significantly (Mishra & Singh, 2003).

There are three concepts commonly used in hydrologic literature to recognize the antecedent moisture condition (AMC) of the soil and they are Antecedent precipitation index (API), Antecedent baseflow index (ABFI) and the Soil moisture index (SMI). The API is based on the amount of antecedent rainfall. The term antecedent varies from previous 5 days to 30 days. However, there exists no explicit guideline for varying the soil moisture with the antecedent rainfall of certain duration. Mockus et al. (1972) in the National Engineering Handbook uses the antecedent 5-d rainfall as API for AMC as shown in Table 2-2 and it is usually practiced.

The AMC is considered into three levels, AMC I, AMC II, and AMC III. The AMC I refers to the dry condition of the soil, AMC II to the normal or average, and AMC III to the wet condition of the watershed. Thus, the CN corresponding to AMC I refers to the dry CN or the lowest runoff potential, the CN corresponding to AMC III refers to the wet CN or the highest runoff potential, and the CN corresponding to AMC II stands for the average CN or the average runoff potential. In other words, higher the antecedent moisture or rainfall amount, higher the CN and higher the runoff potential of the watershed and vice versa (Mishra & Singh, 2003). The advantage of API approach is simple, easy to grasp and easy to apply in the field.

Table 2-2 Antecedent soil moisture condition (AMC)

AMC	**Total 5-day antecedent rainfall (cm)**	
	Dormant season	Growing season
I	Less than 1.3	Less than 3.6
II	1.3 to 2.8	3.6 to 5.3
III	More than 2.8	More than 5.3

Source: (Hydrologic Design Division, National Institute of Hydrology, Uttaranchal, India)

The concept of ABFI is based on the amount of antecedent baseflow which is infrequently used in practice. It appears to be a better index than API for it eliminates the problem of the selection of the antecedent duration but since baseflows are largely governed by the groundwater flow, there exists a problem of separating baseflows from total runoff. The concept of SMI is generally used for long-term hydrologic simulations, where soil moisture needs to be accounted for water balance reasons. Such simulations utilize evapotranspiration and thus incorporate other climate factors, such as daily temperature, solar radiation, etc.

Conferring to SCS-CN Methodology, Curve Number that should be used in forested and urban watershed according to (Mishra & Singh, 2003) are elaborated in the figures below.

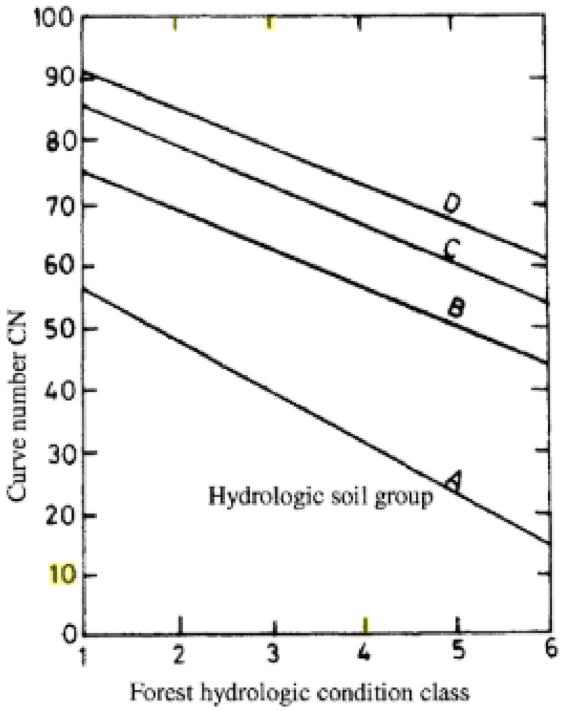

Figure 2-1 Curve numbers by hydrologic soil group and forest hydrologic condition classes.
Source: (Hydrologic Design Division, National Institute of Hydrology, Uttaranchal, India)

For urban watersheds, the composite CN should be computed using Figure 2-2 which is based on the percent (%) impervious area of the urban watershed. Figure 2-2 should be used to calculate composite CNs for design of temporary measures during grading and construction. In such cases, the percent impervious area refers to the degree of development.

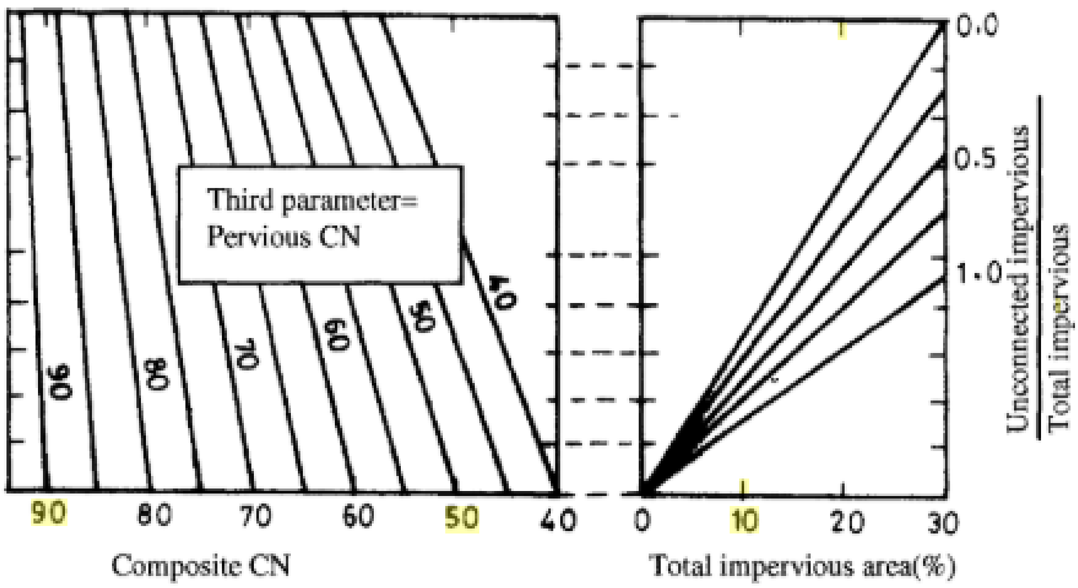

Figure 2-2 Composite CN as a function of total impervious area (%), ratio of unconnected impervious area to total impervious area and previous area CN.

Source: (Hydrologic Design Division, National Institute of Hydrology, Uttaranchal, India)

2.4.1 Importance of soil moisture on rainfall-runoff models

Soil water content in the upper soil layer prior to a rain event can be an important factor affecting the relationship between rainfall and runoff (Zhang et. al., 2011). Soil moisture plays a major role in the hydrological behaviour of a catchment, particularly for operational flood modelling. Several studies have observed that surface runoff is a threshold process controlled by catchment wetness conditions, where runoff coefficients increase when soil moisture thresholds are exceeded. In many instances, the condition of soil moisture stores in rainfall–runoff models is the principal factor in determining whether incident rainfall infiltrates into the soil, or becomes surface runoff. Better initialization of soil moisture variables is expected to lead to better partitioning of rainfall between infiltration and surface runoff and as a result more accurate simulation of flood events. The runoff coefficient is low on hill slopes, due to high infiltration losses, where topographic properties have a considerable influence on the hydrological processes. Depending on the storm intensity and duration, when the soil reaches a condition that precipitation intensity exceeds the infiltration capacity of the soil, infiltration excess runoff is generated. When the hill slope area switches to this wet condition, the lateral hydraulic conductivity increases substantially and subsurface lateral flow becomes dominant (Walker et. al., 2018).

Western et al. (1998) analysed relationships between watershed average soil moisture derived from point measurements and daily runoff coefficient for days with rainfall greater than 5 mm for the 10.5 ha semi-humid Tarrawarra watershed characterized by a silt loam soil type. Their results showed that the surface runoff was strongly controlled by soil moisture, with a threshold value of the volumetric water content varying from 41 % to 46 %, below which no runoff occurred. Similarly, another study conducted by Brocca et al. (2004, 2005) on a semi-humid watershed (12.9 km^2) with sandy loam soils in central Italy indicated that only when antecedent volumetric soil moisture content above approximately 36 % were the runoff coefficients generally greater than zero.

According to the study carried out by (Zhang, Wei, & Nearing, 2011), the sensitivity analysis of the model displayed an average of 0.05 mm change in runoff generation for each 1% change in soil moisture, indicating an approximate 0.15 mm average variation in runoff accounted by the 3 % standard deviation of measured antecedent soil moisture. This compared to a standard deviation of 4.7 mm in the runoff depths for all the measured events taken together. Thus, the low variability of soil moisture in this environment accounts for the relative lack of importance of storm antecedent soil moisture for modelling the runoff. Runoff characteristics simulated with a nine years average of antecedent soil moisture were statistically identical to those simulated with measured antecedent soil moisture, indicating that long term average antecedent soil moisture could be used as a substitute for measured antecedent soil moisture for runoff modelling of these watersheds.

2.4.2 CN variability with antecedent moisture condition

Curve numbers differ with storm occasions as indicated by SCS (1972). Conversion of CN of AMC II to CNs of AMC I and AMC III by SCS-CN Methodology by (Mishra & Singh, 2003) is listed in Table 2-3.

Table 2-3 Curve Numbers for three antecedent moisture conditions

AMC II	**AMC I**	**AMC III**	**AMC II**	**AMC I**	**AMC III**
100	100	100	61	41	78
99	97	100	60	40	78
98	94	99	59	39	77
97	91	99	58	38	76
96	89	99	57	37	75
95	87	98	56	36	75
94	85	98	55	35	74
93	83	98	54	34	73
92	81	97	53	33	72
91	80	97	52	32	71
90	78	96	51	31	70
89	76	96	50	31	70
88	75	95	49	30	69
87	73	95	48	29	68
86	72	94	47	28	67
85	70	94	46	27	66
84	68	93	45	26	65
83	67	93	44	25	64
82	66	92	43	25	63
81	64	92	42	24	62
80	63	91	41	23	61
79	62	91	40	22	60
78	60	90	39	21	59
77	59	89	38	21	58
76	58	89	37	20	57
75	57	88	36	19	56
74	55	88	35	18	55
73	54	87	34	18	54
72	53	86	33	17	53
71	52	86	32	16	52
70	51	85	31	16	51
69	50	84	30	15	50
68	48	84			
67	47	83	25	12	43
66	46	82	50	9	37
65	45	82	15	6	30
64	44	81	10	4	22
63	43	80	5	2	13
62	42	79	0	0	0

Source: *Soil Conservation Service (SCS-CN) Methodology by Mishra & Singh (2003)*

The popular AMC-Dependent CN-conversion formulae given by different researchers are listed in Table 2-4 below:

Table 2-4: Different formulae to convert AMC II to AMC I and AMC III

Method	AMCI	AMCII
Sobhani (1975)	$CN_I = \frac{CN_{II}}{2.334 - 0.01334CN_{II}}$	$CN_I = \frac{CN_{II}}{0.4036 + 0.005964CN_{II}}$
Hawkins et al. (1985)	$CN_I = \frac{CN_{II}}{2.281 - 0.01281CN_{II}}$	$CN_I = \frac{CN_{II}}{0.427 + 0.00573CN_{II}}$
Chow et al. (1988)	$CN_I = \frac{4.2CN_{II}}{10 - 0.058CN_{II}}$	$CN_I = \frac{23CN_{II}}{10 + 0.13CN_{II}}$
Neitsch et al. (2002)	$CN_I = CN_{II} - \frac{20(100 - CN_{II})}{\{100 - CN_{II} + exp[2.533 - 0.0636(100 - CN_{II})]\}}$	$CN_I = \frac{CN_{II}}{0.4036 + 0.005964CN_{II}}$

Mishra et al. (2008) evaluated these AMC conversion formulae and concluded that the Sobhani formula was found to perform the best in CN I conversion, and the Hawkins et al. (1985) formula in CN III conversion.

The Sobhani (1975) formulae found the existence of linear relationships between the potential retention, *S* for AMC II and for AMC I or AMC III. These equations are reportedly applicable in the CN-range (55 - 95), which encompasses the most estimated or experienced range of CN variation.

2.4.3 Advantages and limitations of the SCS – CN method

The Soil Conservation Service-Curve Number method has several advantages over the other methods. It is a simple conceptual method for estimation of the direct runoff amount from a storm rainfall amount, and it is well supported by the empirical data. The method relies on only one parameter that is the curve number which is a function of the major runoff-producing watershed characteristics. It is fairly well documented for its inputs (soil, land use/treatment, surface condition, and antecedent moisture condition), its features are readily grasped, well established and accepted for use in the United States and other countries (SCS, 1986).

Mishra & Singh (2003) pointed out several problems associated with the SCS-CN method. For example, it does not contain any expression for time and ignores the impact of rainfall intensity and its temporal distribution. As mentioned by Singh & Frevert (2002), Cowan (1957) demonstrated that time was not incorporated in the method because sufficient data were not available to describe infiltration rates for a wide range of soil, vegetation and land use complexes and there was no reliable method available for distributing rainfall in time.

There is a lack of clear guidance on how to vary antecedent condition, especially for lower CN and rainfall amounts, for the CN exhibits sensitivity to the antecedent condition (Hawkins, 1993). Ponce and Hawkins (1996), however, cautioned against the use of the method to watersheds larger than 20 km^2.

2.5 Methods of Areal Averaging Rainfall

Rainfall being one of the most important input in a hydrological model, it is of utmost importance to select a suitable areal averaging method to compute the input or application rainfall by considering all the rain gauging stations of the catchment area (Zeiger & Hubbart, 2017). Some of the most commonly used methods are Thiessen polygon, Arithmetic mean, and Isohyetal method, because of their simplicity

Arithmetic Mean Method - This is the simplest method of computing the average rainfall over a basin. The resultant rainfall is obtained by the division of the sum of rain depths recorded at different rain gauge stations of the basin by the number of the stations.

$$P_{av} = \frac{P_1+P_2+\cdots+P_n}{n} \qquad 1$$

where P_{av} is average rainfall, P_i is the station rainfall and n is the total number of stations.

Thiessen Polygon Method - The amount of rain recorded at any station should represent the amount for only that region enclosed by a line midway between the station under consideration and surrounding stations (Thiessen & Alter, 1911).

$$Q = \frac{A_aR_a+A_bR_b+\cdots+A_nR_n}{A_a+A_b+\cdots+A_n} \qquad 2$$

where Q is the average rainfall, R_i is rainfall of a station and A_i is the area represented by corresponding rainfall station.

Isohyetal Method - An isohyetal is a line joining places where the rainfall amounts are equal on a rainfall map of a basin. An isohyetal map showing contours of equal rainfall is more accurate picture of the rainfall over the basin. This method is suitable for hilly are, large basins with area over 5000 km^2 and rainfall station density is high.

$$P_{av} = \frac{A_1\frac{P_1+P_2}{2}+A_2\frac{P_2+P_3}{2}+\cdots+A_{n-1}\frac{P_{n-1}+P_n}{2}}{A_1+A_2+\cdots+A_n} \qquad 3$$

where P_i is the value of isohyet lines, A_i is the area between the pair of isohyet lines and P_{av} is the areal averaged rainfall.

2.6 Runoff Simulation Models

2.6.1 Based on SCS-CN method

Soil Conservation Service- Curve Number (SCS-CN) model has been widely used for surface runoff computations when streamflow data were not available at desired location or when the records contain missing streamflow data attributing to various reasons (Singh & Frevert, 2006).

Yu (1998) provided a theoretical framework in which the SCS method can be tested. They showed that the proportionality between retention and runoff and the SCS equation would follow if the temporal distribution of rainfall intensity and the spatial distribution of the maximum rate of infiltration are independent and described by exponential probability distributions. In particular, they showed that the maximum retention S could be seen as the product of the spatially averaged maximum rate of infiltration and the effective storm duration.

Mishra and Singh (1999) modified the existing SCS-CN method by taking 0.5(P - I_a) in place of (P - I_a). The existing SCS-CN method and the proposed modification are compared and the modified version is found to be more accurate than the current version. Mishra et al. (2004) modified the existing SCS-CN method, which is based on the Soil Conservation Service Curve Number (SCS-CN) methodology but incorporates the antecedent moisture in direct surface runoff computations and named it as MS model. They evaluated the modified version and by comparing with the existing SCS-CN method they found that the modified MS model performs far better than the existing SCS-CN model. In 2005, they applied the MS model with its eight variants at field using a large set of rainfall-runoff events and revealed that the performance of the existing version of the SCS-CN method was significantly poorer than that of all the model variants.

Jain, Mishra & Singh (2006) evaluated the I_a-S relationship and proposed another non-direct relationship that consolidated tempest precipitation. Ponce and Hawkins (1996) recommended that the fixed initial abstraction ratio of 0.20 may not be the most proper number and that it ought to be deciphered as a local parameter.

Mishra et al. (2006) employed a large dataset from 84 small watersheds (0.17– 71.99 ha in area) in the USA to investigate a number of I_a-S relationships that incorporated antecedent moisture as a function of antecedent precipitation.

Mishra et al. (2008) presented a rain duration-dependent procedure based on the popular SCS-CN methodology for computation of direct surface runoff from long duration rains. Curve numbers were derived from long-term daily rainfall-runoff data, and antecedent moisture condition (AMC) related with antecedent duration. The derived runoff curve numbers exhibited a strong dependency on the storm duration and the reasonable match of the observed runoff with those due to the proposed approach was better than those from the original SCS-CN method.

To overcome the slope limitation of the SCS-CN method, Gupta et al. (2012) modified the SCS-CN method to correct it for steep slopes. They incorporated antecedent moisture using Mishra et al. (2005a) approach. Furthermore, a hydrological model for runoff modelling should have two essential components such as generation of runoff and routing of runoff. The SCS-CN method is a static model and does not take into account routing phase of the runoff.

Tedela et al. (2012) compared SCS-CN tabulated curve numbers with watershed curve numbers determined by five procedures using gauged rainfall and runoff for forested watersheds of the mountainous eastern United States. These procedures included the median, geometric mean, arithmetic mean, nonlinear, least squares fit, and standard asymptotic fit. They found substantial uncertainties in using the curve number method for estimating runoff from un-gauged watersheds. They concluded that runoff estimates using tabulated curve numbers are unreliable and that curve number selection requires independent calibration to watersheds representative of regional landscape and hydrologic characteristics. In un-gauged watersheds presenting forested land covers with very permeable soils, the runoff coefficient can be accurately estimated using land cover and soil survey using remote sensing and GIS, as well as a numerical soil water flow model (Soulis et al., 2009).

.

2.7 Objective Function

Objective functions are indicators that are used to determine how good the solution is for serving a particular objective. It is a statistical indicator to calculate the efficiency of a model (Mata-Lima, 2011).

Sum of squared deviations (R^2) - The most commonly used objective function for hydrologic simulation models is the sum of squared deviations (Diskin & Simon, 1977).

$$R^2 = \Sigma(q_o - q_s)^2 \quad (4)$$

where q_o and q_s are the observed and simulated streamflow values.

Nash-Sutcliff Efficiency (NSE) - Nash & Sutcliff (1970) proposed NSE which is a normalized statistic that determines the relative magnitude of residual variance to that of measured variance

$$NSE = 1 - \frac{\Sigma(Y_{obs} - Y_{sim})^2}{\Sigma(Y_{obs} - Y_{mean})^2} \quad (5)$$

where Y_{mean} is the mean of observed data, Y_{obs} is the observed value and Y_{sim} is the simulated value. The NSE ranges from negative infinity to 1 where optimum value is 1.

The NSE is the error from the initial variance which is dependent on the mean of the observed data, therefore a comparison between two different catchments cannot be performed.

Mean Ratio of Absolute Error (MRAE) - Wijesekera & Perera, (2010) and Wijesekera & Ghanapala, (2003) used MRAE which is one of the efficiency indicators used by World Meteorological Organization (WMO, 1975) for parameter optimization and to determine the degree of accuracy by comparing observed and simulated streamflow values.

$$MRAE = \frac{1}{n} \Sigma \frac{|Q_C - Q_o|}{Q_o} \quad (6)$$

where Q_o is the observed streamflow and Q_c is the calculated streamflow and n is the number of observations used for calculation.

In a study of two-low lying urban watersheds in greater Colombo area for drainage and environment by Wijesekera & Ghanapala, (2003) compared the simulated streamflow with observed streamflow using the MRAE as the objective function to determine the degree of accuracy.

MRAE provides a mean average indicator for matching at each and every point of the two hydrographs relative to the observed value at that point based on the order of magnitude.

Mean Absolute Percentage Error (MAPE) - It is the mean or average of the absolute percentage errors of forecasts. Error is defined as actual or observed value minus the forecasted value. Percentage errors are summed without regard to sign to compute MAPE. This measure is easy to understand because it provides the error in terms of percentages. MAPE is a measure commonly used in forecasting (Swanidass, 2000) .

$$MAPE = \frac{100}{n} \Sigma \frac{|Q_C - Q_O|}{Q_O} \tag{7}$$

where Q_o is the observed streamflow and Q_c is the calculated streamflow and n is the number of observations used for calculation.

Root Mean Square Error (RMSE) – It measures how much error there is between two data set. It is also one of the most commonly used error index and it is considered an excellent general-purpose error metric for numerical predictions (Simon & Hashemi, 2018).

$$RMSE = \sqrt{\frac{\Sigma (Y_O - Y_S)^2}{n}} \tag{8}$$

where Y_o is the observed streamflow and Y_s is the simulated streamflow and n is the number of observations used for calculation.

Patry & Marino (1983) evaluated the performance of a nonlinear functional runoff model adopted the root-mean-square error as a criterion for comparison of hydrographs.

2.8 Model Calibration and Verification

The model is always an interpretation of reality and is a valid tool only if it represents the reality correctly. The model calibration is, therefore, an essential step after its development. Calibration is performed by comparing the model output with the corresponding measured values. The verification is a further step for a more general evaluation of the model and requires a different set of measured data for testing the model performance. Combined steps of calibration and verification make up the model validation (Benedini & Tsakiris, 2013).

Calibration uses observed hydro meteorological data in a systematic search for parameters that yield the best fit of the computed results to the observed runoff (USACE, 2000). The model calibration can be either done manually or auto-calibrated in HEC-HMS. In manual calibration, parameter values should be changed manually based on your judgment or knowledge of what parameter values may produce the best match between the model and the observed hydrographs whereas auto-calibration is possible through the optimization trial option in the compute menu (Merwade, 2016).

Model verification is in reality an extension of the calibration process. The purpose of verification is to assure that the calibrated model adequately assesses the range of variables and conditions that are expected within the simulation. Although there are several methods for verification, the most effective method is to use different data set of the available record of observed values. Once the calibration parameters are developed, simulation is performed for the remaining period of observed data and the goodness of fit is reassessed (Alagmand et al., 2010).

Giang and Phuong (2010) mentioned that the objective of calibration is to select model parameters. The model simulates the hydrological behaviour as closely as possible and verification is achieved by selecting new set of observed data and the parameters which have been calibrated. Authors further indicated that although there are many discussions on calibration and verification, there is no consensus on a particular methodology.

Cunderlik and Simonovic (2004) found that the continuous model systematically underestimates the total streamflow volume by 10 – 15% after carrying out the calibration and verification of the event for continuous models in Upper Thames River Basin. Hence, they suggested a correction factor for this.

Sudheer et al. (2006) mentioned that a general assessment of the model performance just based on goodness of fit statistics may mislead the modeller on the behaviour of model simulations. Authors proposed that the watershed model calibrations should be completed on a daily time step in order to preserve the hydrological behaviour of the watershed accurately and to enlighten the scope for improving/ developing effective auto calibration procedures.

3 MATERIALS AND METHODS

The details on study area, methodology opted for the study, process of rainfall event selections, curve number determination, soil moisture condition and data checking using visual and graphical methods are discussed under this chapter. With the data from Survey Department, Sri Lanka, the landuse and soil type map are extracted for Kelani river basin.

3.1 Study Area

The Kelani River originates from the Western face of the central highlands located in the Horton Plains National Park and Peak Wilderness Sanctuary. It drains approximately 2,292 km^2 of land area (Survey Department, 2007). It is the second largest river basin and fourth longest river in Sri Lanka. It includes parts of three provinces in the country and they are Western Province, Central Province and Sabaragamuwa Province. Kelani River flows through Nuwara Eliya, Kandy, Ratnapura, Kegalle, Kalutara, Colombo and Gampaha Districts comprising of 37 Divisional Secretariat areas. The study area is till Hanwella and it covers 1825 km^2. The study are map of sub-watershed up to Hanwella stream gauging station in Kelani basin is shown in Figure 3-1.

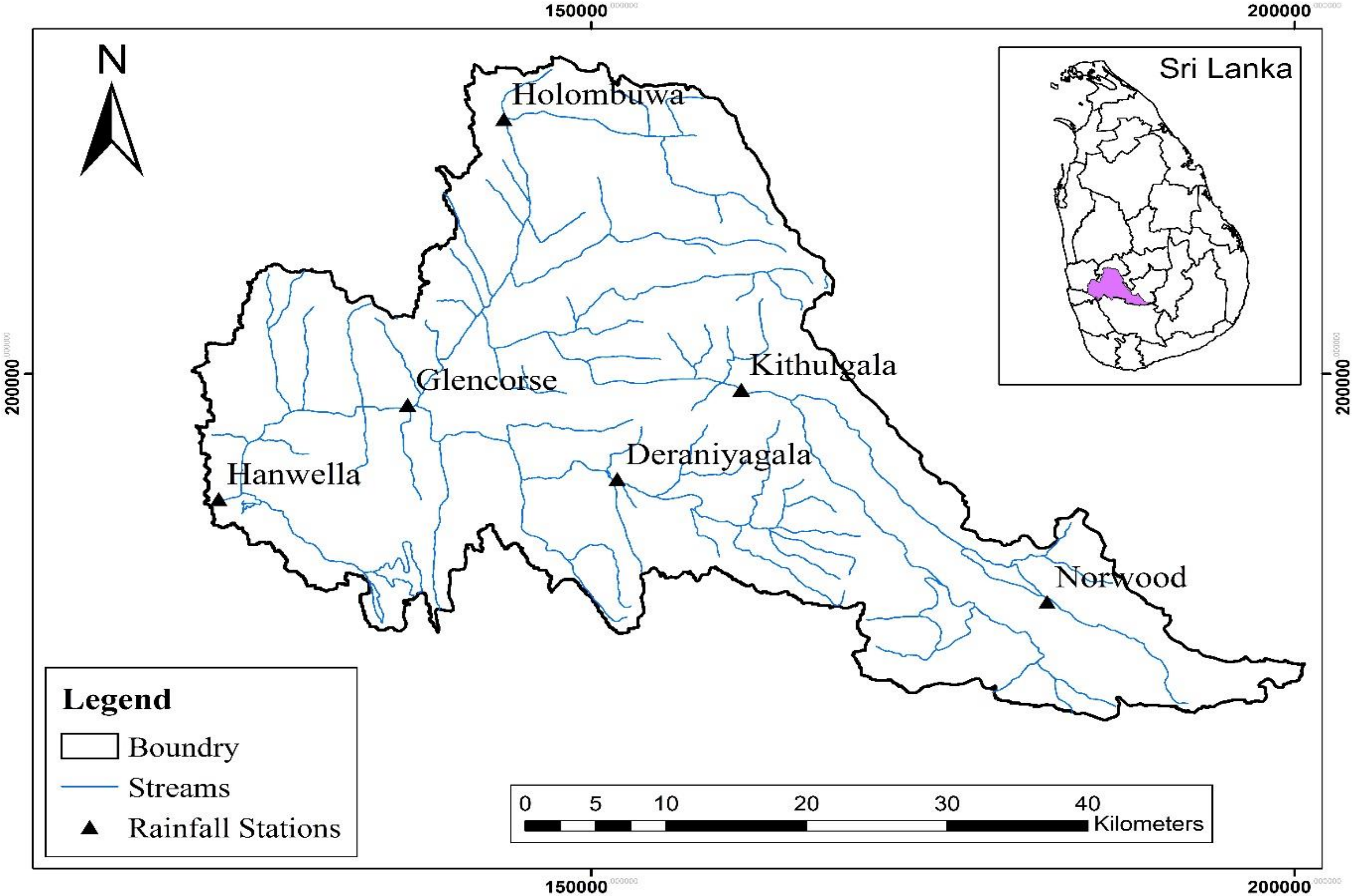

Figure 3-1 Study area map

3.2 Methodology

The problem in the study area is recognised and the objectives are identified. To be able to fulfil the study objective, the activities are broken down into several steps known as specific objectives. Literature review, data collection and checking were carried out simultaneously. Three different types of data such as observed rainfall and streamflow from six different gauging stations and evaporation from Colombo station for ten consecutive water years from 2007-2017 are used. Event separation was carried out from the data set and HEC-HMS model was developed. The first half events were used for model calibration and the second half for model verification. The parameters are manually calibrated and the calibrated parameters are used for model verification. Few random events were selected and different antecedent moisture conditions were applied to check the model performance. The detail methodology chart is shown in Figure 3-2.

3.3 Event Selection

3.3.1 Minimum inter event time

The literature review gave a perspective on the different types of MIT concepts and based on the frequency of the use by researchers, the N-Day concept of Linsley (1975) recession method was used. The event selection was done considering four (4) days of rainless period.

3.3.2 Rainfall event selection

Using the Minimum Inter event Time (MIT) method by taking four (4) days of rainless period before the event as discussed above, events were selected from daily Thiessen rainfall data from 2007-2017 water years. For the selection of streamflow, observation was made to the rainfall pulses. The N days concept on Linsley (1975) was used to conclude the event. The *N* days in this case was four (4) days.

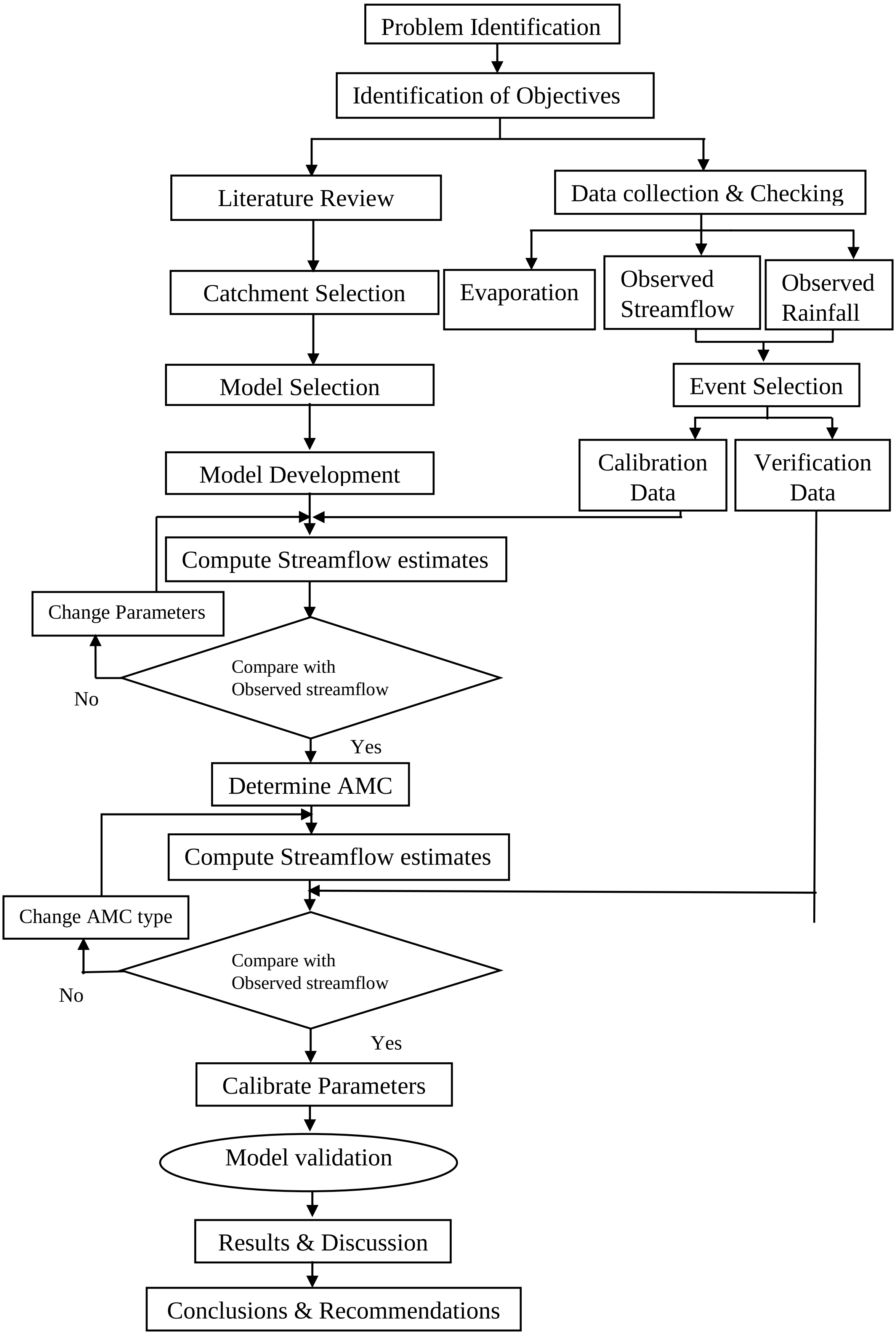

Figure 3-2 Methodology Flowchart

3.4 Curve Number from Catchment Properties

The curve number varies with antecedent moisture conditions. Curve number is an important parameter in this study and therefore to incorporate CN, the SCS-CN method was chosen in the loss model in HEC-HMS. To determine accurate CN, several methods were used to compare the results.

3.5 Curve Number From Field Data

Curve Number was determined for each investigated watershed, using the recorded rainfall-runoff (*P*-*Q*) episodes. To this end, *S*, the retention volume for each *P*-*Q* pair was calculated using the equation.

$$S = 5[(P + 2Q) - \sqrt{Q(4Q + 5P)} \qquad (1)$$

where *S* was transformed to CN scale using the following empirical relation;

$$CN = \frac{25{,}400}{S + 254} \qquad (2)$$

Initial abstraction, I_a was calculated by using the following formula for each individual events;

$$Ia = 0.2 * S \qquad (3)$$

where *S* and I_a is in mm and *P* and *Q* are cumulative values of the event both in mm. Using this procedure the CN was derived for individual events.

3.6 AMC Conversion

Four popular methods were available to calculated different types of AMC, namely, Sobhani (1975), Hawkins et al. (1988), Chow et al. (1988) and Neitsch at al. (2002) methods. The AMC I and AMC III were calculated using all four methods and compared. Chow et al. (1988) method was used in this study to calculate three different types of AMCs.

3.7 Data and Data Sources

The data used are observed rainfall and streamflow data, evaporation data, land use and soil maps. The details on data are presented in Section 3.71 and 3.7.2.

3.7.1 Data sources and data resolution

The details of the data such as resolution, source and station names and data period are listed in Table 3-1.

Table 3-1 Data Details of Kelani river basin

Data Type	Spatial Resolution	Station Name	Data Period	Source
Rainfall	Daily	Norwood	2007-2017	Department of Irrigation
		Holombuwa		
		Deraniyagala		
		Kithulgala		
		Glencorse		
		Hanwella		
Streamflow	Daily	Hanwella	2007-2017	Department of Irrigation
Evaporation	Daily	Colombo	2007-2017	Department of Meteorology
Land Use Map	1: 50,000		2015	Department of Survey
Soil Type	1: 50,000		2015	Department of Survey
Topographic	1: 50,000		2015	Department of Survey

3.7.2 Rainfall and streamflow stations

Coordinates of the six rainfall gauging stations and one streamflow station at outlet are listed in Table 3-2.

Table 3-2 Rainfall Gauging Station Details of Kelani river basin

Rainfall Station	Coordinates	
	Longitude (° N)	Latitude (° E)
Norwood	80.61466667	6.835638889
Kithulgala	80.41777778	6.989166667
Holombuwa	79.87677778	6.959722222
Deraniyagala	80.33805556	6.924444444
Glencourse	80.20305556	6.978055556
Hanwella	6.909722222	80.08166667
Streamflow Station	**Longitude (° N)**	**Latitude (° N)**
Hanwella	6.909722222	80.08166667

Source: Department of Irrigation, Sri Lanka

3.8 Data Checking

Available data requires satisfactory checking before it is used in modelling. Inconsistencies and non-homogeneities in the hydrological and meteorological time series could be identified by incorporating statistical tests that detect trends and change points. Inconsistency which reflects systematic errors during recording and the non-homogeneity that arises from either natural or man-made changes to the gauging environment are both important for adequate time series analysis (Wijesekera & Perera, 2012).

3.8.1 Thiessen average rainfall

Thiessen polygon method was used to calculate the catchment average rainfall. The Thiessen polygon method is a commonly used methodology for computing the mean areal precipitation for a catchment from rain gauge observations.

In this study, the Theissen polygons for Kelani river basin up to Hanwella stream gauging station sub-watershed is developed in ArgGIS 10.3 (ESRI, USA). The total area of the watershed is 1825 km^2 and the spatial contribution of each station using Thiessen method is shown in Figure 3-3.

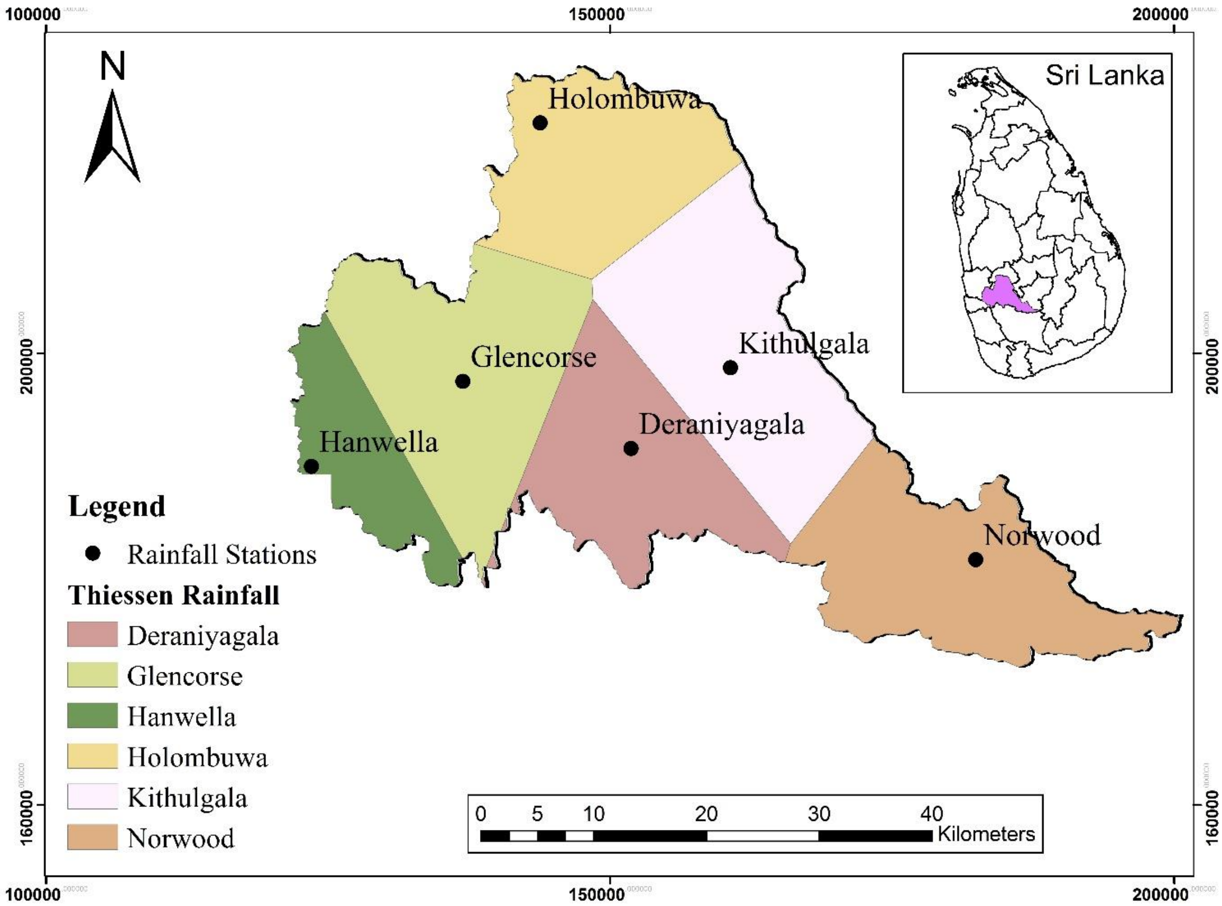

Figure 3-3 Theissen Polygon of Kelani river basin

The area covered by each rainfall gauging station with Thiessen weights are given in Table 3-3.

Table 3-3 Rainfall Thiessen Weights

Rainfall Station	Area (km^2)	Thiessen Weights
Norwood	350.8	0.192
Kitulgala	393.7	0.216
Holombuwa	280.8	0.154
Hanwella	146.1	0.080
Deraniyagala	281.8	0.154
Glencorse	372.5	0.204
Total Area	**1825.6**	**1.000**

The overall Thiessen rainfall and observed streamflow comparison for water year 2007-2017 are presented from Figure 3-4 to Figure 3-13. The streamflow response to rainfall for six gauging stations are plotted in normal graph and semi-log graph in APPENDIX A: STREAMFLOW RESPONSE WITH RAINFALL FOR INDIVIDUAL GAUGING STATIONS.

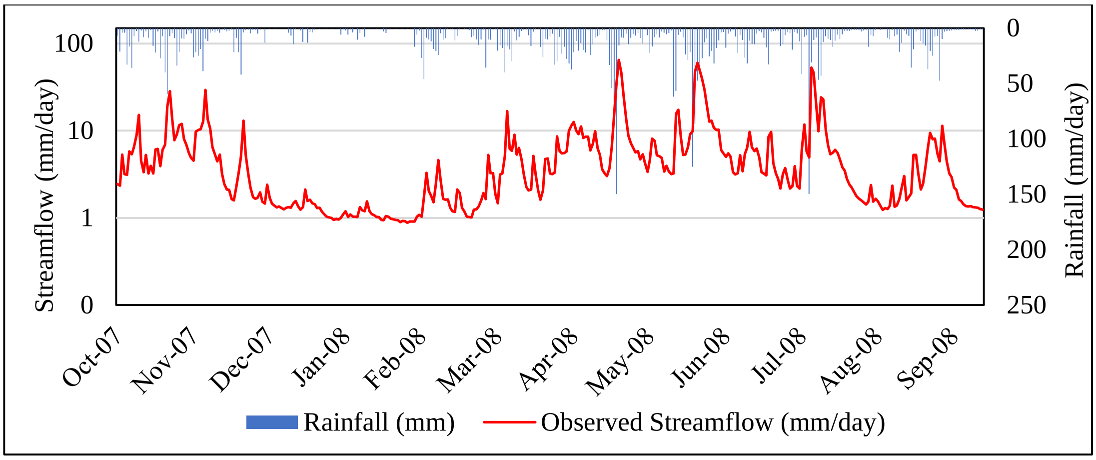

Figure 3-4 Thiessen Rainfall Vs Streamflow for Kelani River Basin for 2007-2008 Water Year

For the water year, 2008 – 2009, the Thiessen rainfall well responds and corresponds to the streamflow throughout the year. The highest rainfall was observed in between May-June, 2009 and in August, 2009 whereas the lowest rainfall was observed between January-March, 2009 as shown in Figure 3-5.

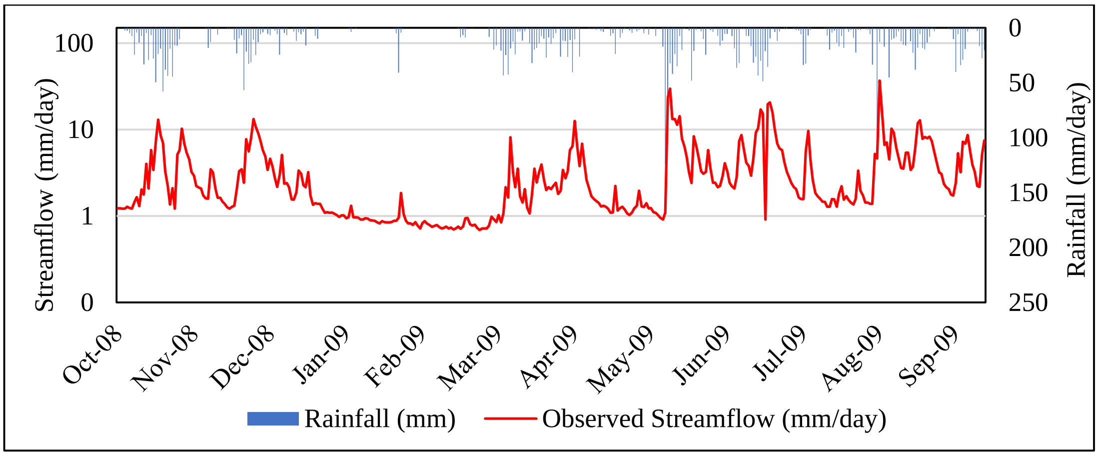

Figure 3-5 Thiessen Rainfall Vs Streamflow for Kelani River Basin for 2008-2009 Water Year

A sudden decrease in streamflow has been observed between February-March, 2010. Although dry days has been recorded during this period but the streamflow do not corresponds to the Thiessen Rainfall.

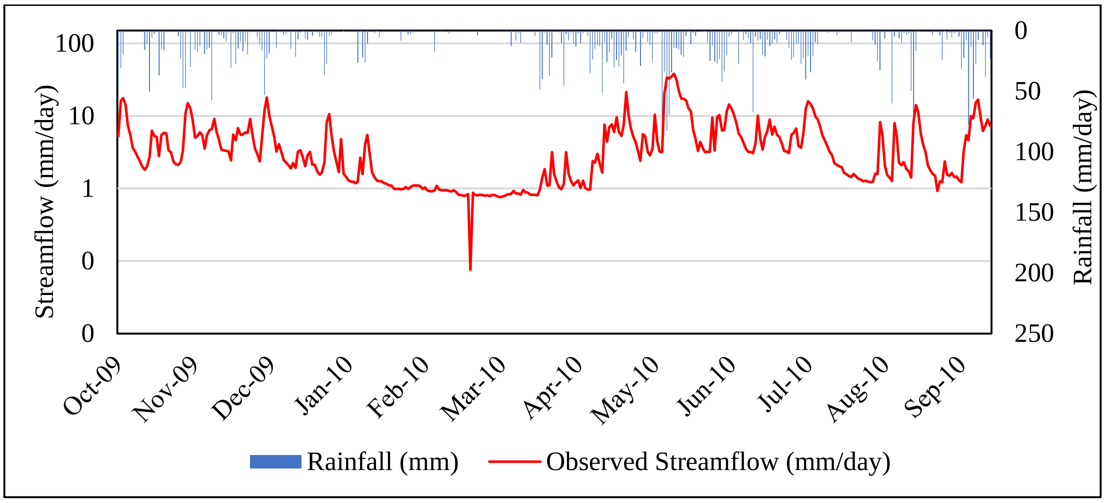

Figure 3-6 Thiessen Rainfall Vs Streamflow for Kelani River Basin for 2009-2010 Water Year

The water year 2010-2011 has received more rainfall compared to the previous water years. The streamflow corresponds fairly to the Thiessen rainfall and the highest rainfall received was in June, 2011. Unlike the previous water year, 2010-2011 water year has received good amount of rainfall from January-March, 2011.

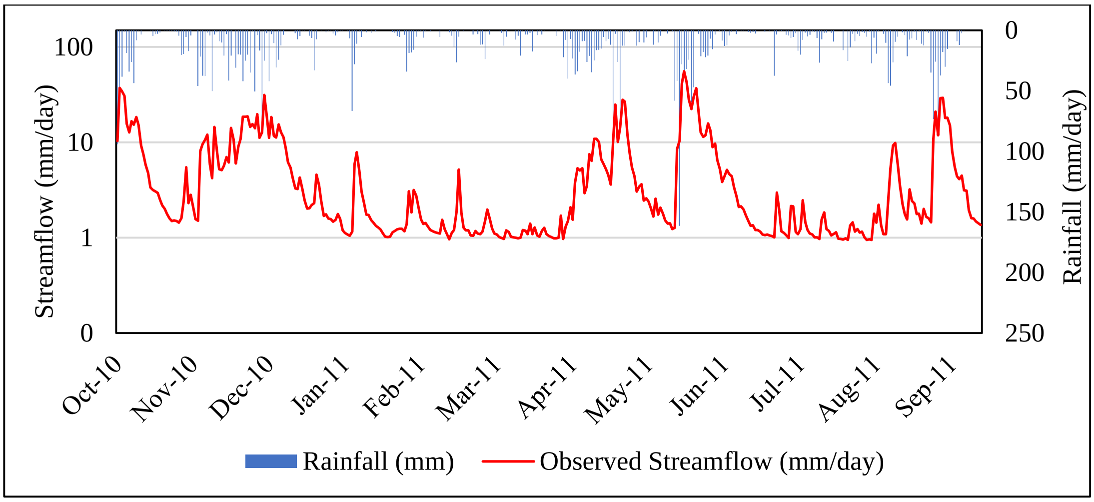

Figure 3-7 Thiessen Rainfall Vs Streamflow for Kelani River Basin for 2010-2011 Water Year

The total rainfall received in the water year, 2011-2012 has been decreased compared to the previous year. A shift in peak flow has also been observed. The highest flow observed in 2011-2012 water year was in July 2012 as shown in Figure 3-9.

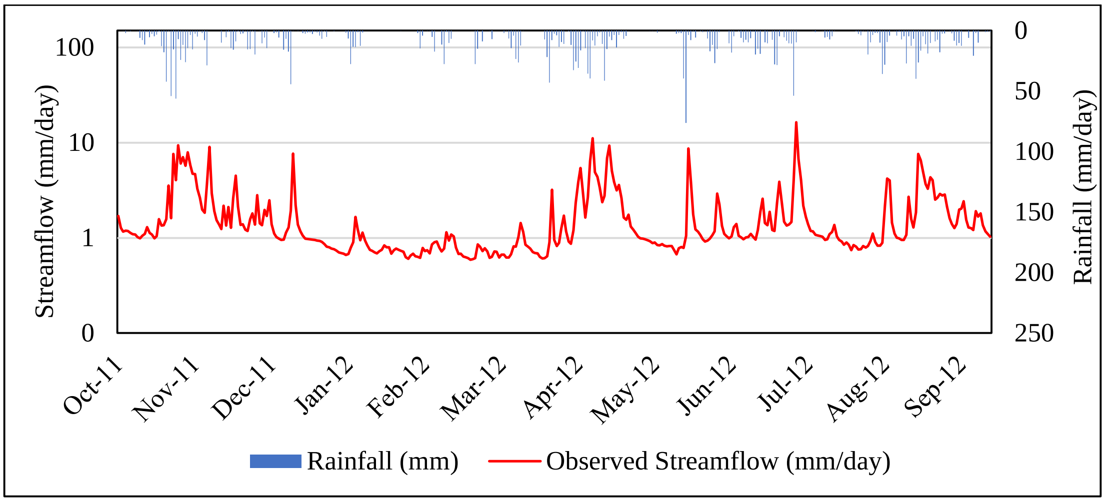

Figure 3-8 Thiessen Rainfall Vs Streamflow for Kelani River Basin for 2011-2012 Water Year

The streamflow corresponds to the Thiessen rainfall of Kelani river basin for the 2012-2013 water year. The highest streamflow was observed in November, 2012 while the lowest streamflow was observed in March, 2013.

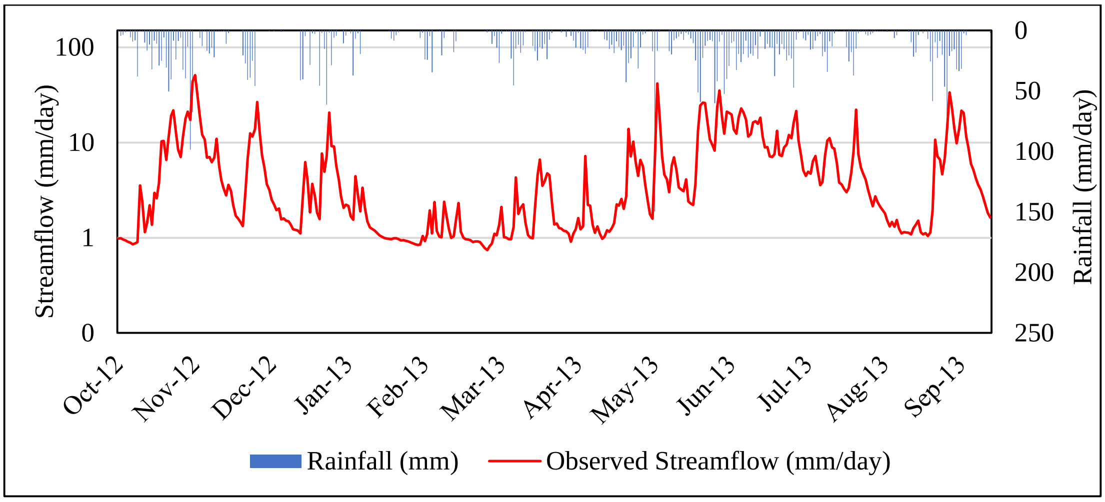

Figure 3-9 Thiessen Rainfall Vs Streamflow for Kelani River Basin for 2012-2013 Water Year

The amount of rainfall from December, 2013 – April, 2014 has been declined in the 2013-2014 water year compared to the previous water year. The month of June in the year 2014 has the highest observed streamflow followed by the August month of the same year.

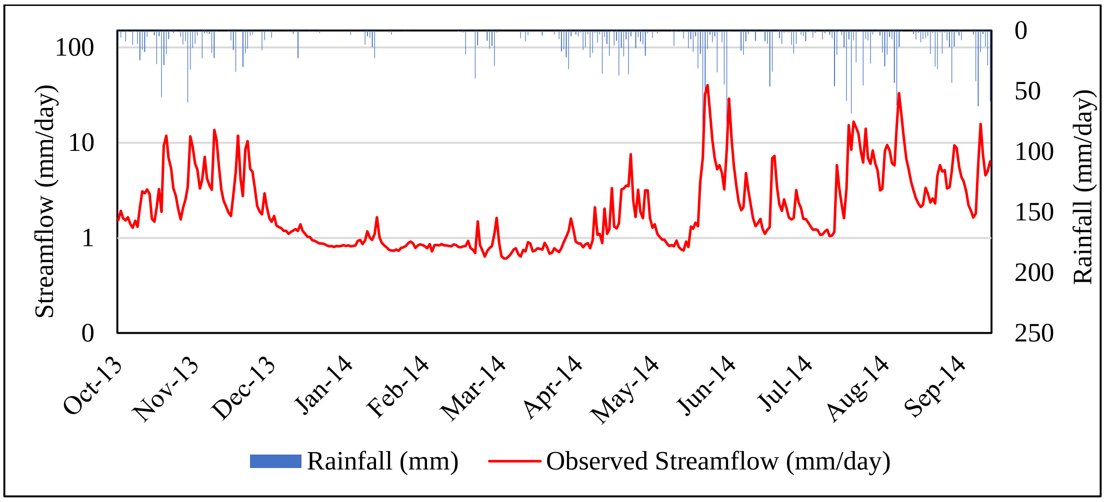

Figure 3-10 Thiessen Rainfall Vs Streamflow for Kelani River Basin for 2013-2014 Water Year

Strangely the highest observed streamflow in the 2014-2015 water year was in January, 2015. The streamflow corresponds to the Theissen rainfall and this indicates that in Kelani river basin, the peak flow can vary throughout the water year.

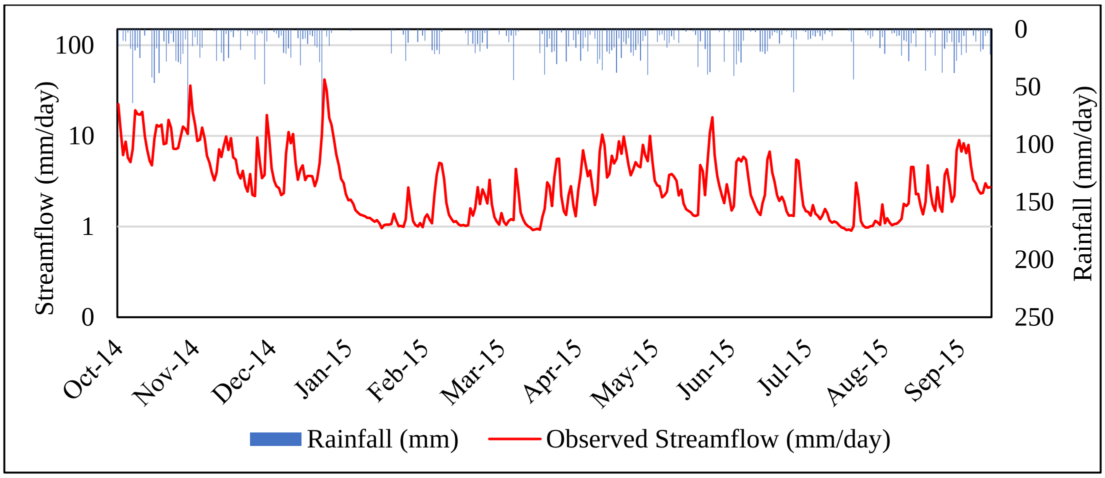

Figure 3-11 Thiessen Rainfall Vs Streamflow for Kelani River Basin for 2014-2015 Water Year

Extreme rainfall and streamflow was recorded in May, 2016. Kelani river basin was flooded causing serious damages especially in the western region including Colombo Metropolitan area (JICA, 2017). Beginning on 14 May 2016, a low pressure area over the Bay of Bengal caused torrential rain to fall across Sri Lanka. Some locations saw over 350 mm (13.77 inches) of rain fall in 24 hours. Floods and landslides have caused havoc in as many as 19 districts of the country, including around Colombo, causing floods and landslides which affected half a million people with causality reported over 100 and estimated huge economic losses (Alahacoon et al., 2016).

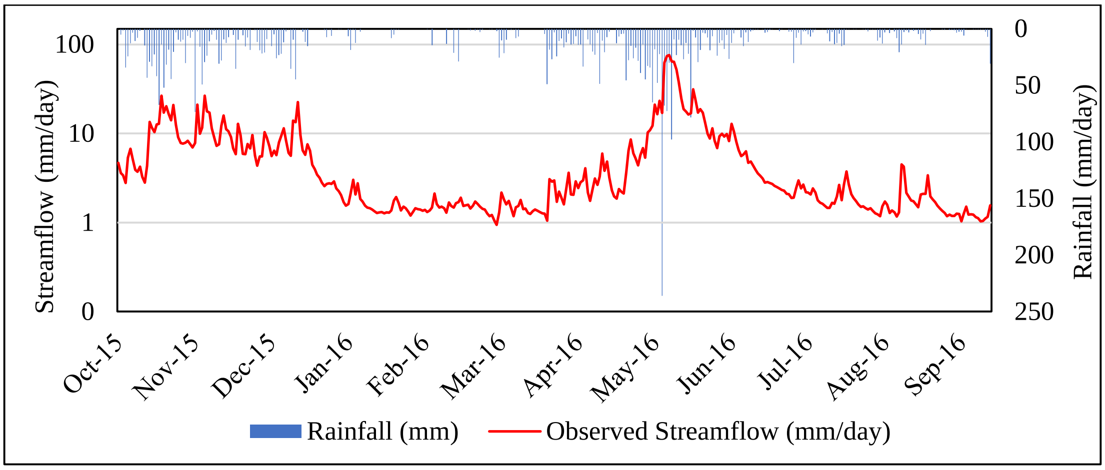

Figure 3-12 Thiessen Rainfall Vs Streamflow for Kelani River Basin for 2015-2016 Water Year

In the following water year, the highest streamflow has been observed in the same month but the intensity of the rainfall was lesser than the previous year. The lowest streamflow in the 2016-2017 water year has been observed in February, 2017.

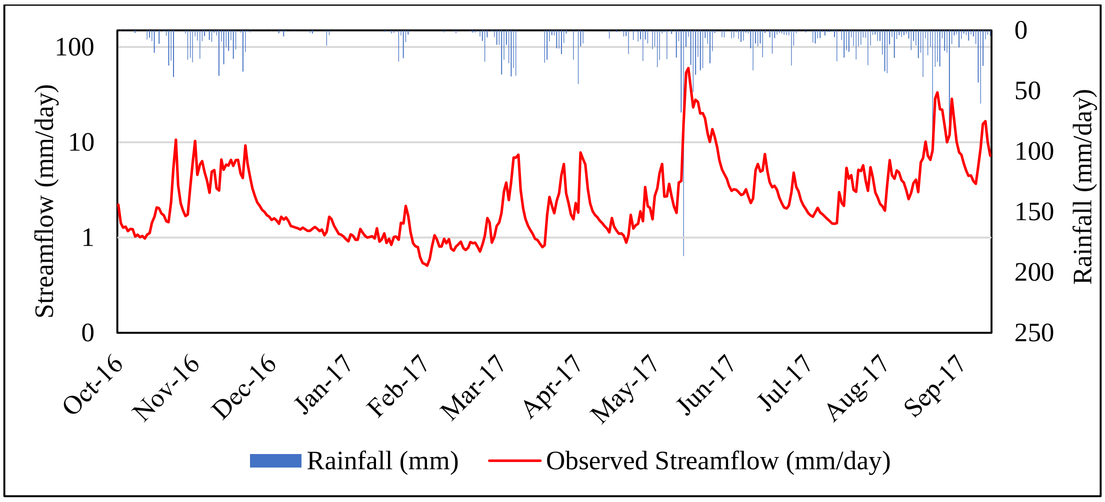

Figure 3-13 Thiessen Rainfall Vs Streamflow for Kelani River Basin for 2016-2017 Water Year

3.8.2 Visual data checking

Visual data checking was carried out to find whether there are inconsistencies or any outliers present in the data. Streamflow responses to rainfall were plotted for each rain gauging station and for each water year. Each rainfall gauging station is compared with the same station observed streamflow data and the graphs plotted are in APPENDIX A: STREAMFLOW RESPONSE WITH RAINFALL FOR INDIVIDUAL GAUGING STATIONS. The time where the streamflow does not match or respond to the rainfall is marked with a circle.

3.8.3 Monthly data checking

Monthly variation of Thiessen rainfall representing catchment rainfall for each month in a water year is shown in Figure 3-14. Two seasonal rainfall patterns in Sri Lanka corresponding to North East Monsoon (October to March) and South West Monsoon (April to September) shows two peak behavior in a water year. The graph below shows that the May month in the year 2016 received the highest rainfall in ten years.

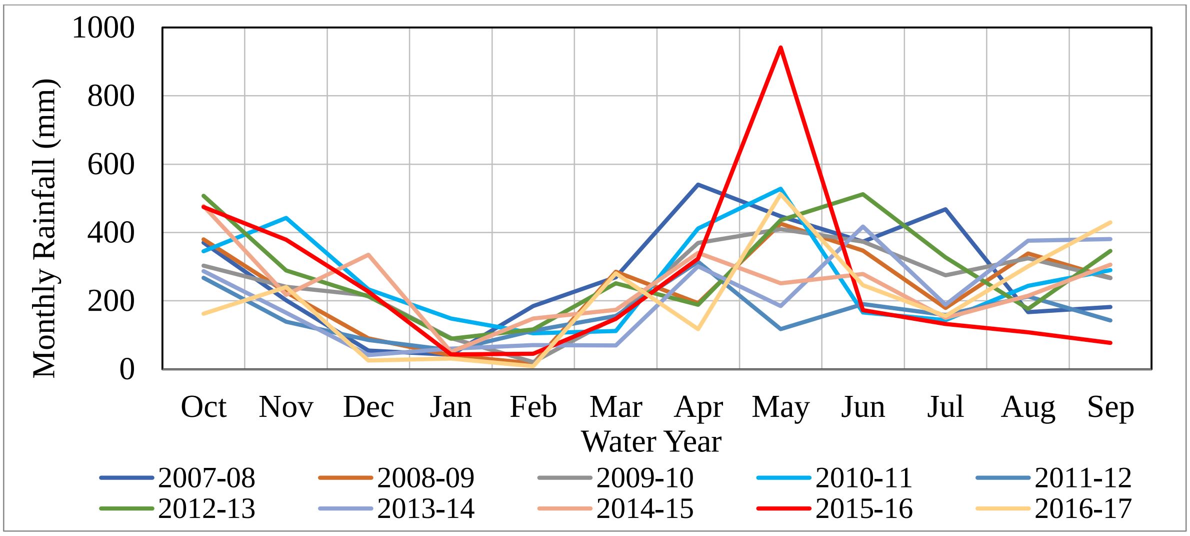

Figure 3-14 Monthly Thiessen Rainfall Pattern - Kelani River Basin

Monthly data checking for six rainfall gauging stations with respect to six streamflow gauging stations was also done in order to check the two peak behavior representing two monsoonal rainfall pattern in Sri Lanka. Deraniyagala rainfall gauging station received the highest rainfall recorded as 355.5 mm as per the record maintained by Irrigation Department. It is presented in APPENDIX B: MONTHLY RAINFALL COMPARISON FOR EACH GAUGING STATIONS.

3.8.4 Double mass curve

Double mass curve is used to check the consistency of many hydrologic data by comparing data for a single station with that of a pattern composed of the data from several other stations in the area. Double mass curves of cumulative rainfall data of one rainfall station with cumulative average of five nearby stations in the catchment were plotted to check the consistency of rainfall data. This graph is a straight line so that the relation between rainfalls is a fixed ratio. Breaks or inflections in the graph are caused by changes in data collection or changes in the rainfall station etc. Double mass curve plots for all gauging stations are in APPENDIX D: DOUBLE MASS CURVE. It was observed that there is no significant inconsistency in rainfall data.

3.8.5 Annual water balance

Water balance can be used to describe the flow of water in and out if a system having only one outlet. Annual water balance check is done to check the overall error with respect to annual total observed rainfall, streamflow and evaporation. Annual water balance for Kelani river basin from water year 2007-2017 has been carried out and the details are shown in Table 3-4.

Table 3-4 Annual Water Balance - Kelani River Basin

Year	Thiessen Averaged Rainfall (mm)	Observed Streamflow (mm)	Pan Evaporation (mm)	Annual Water Balance (mm)	Runoff Coefficient
2007/08	3299.85	2098.12	1187.04	1202	0.64
2008/09	2788.04	1280.92	1267.52	1507	0.46
2009/10	3038.80	1681.41	1205.61	1357	0.55
2010/11	3167.48	1984.17	1171.05	1183	0.63
2011/12	1951.36	638.68	1269.82	1313	0.33
2012/13	3451.40	2159.37	1207.24	1292	0.63
2013/14	2540.15	1168.14	1317.94	1372	0.46
2014/15	2942.41	1541.82	1198.95	1401	0.52
2015/16	3071.13	2194.51	1393.59	877	0.71
2016/17	2507.84	1507.26	1217.23	1001	0.60

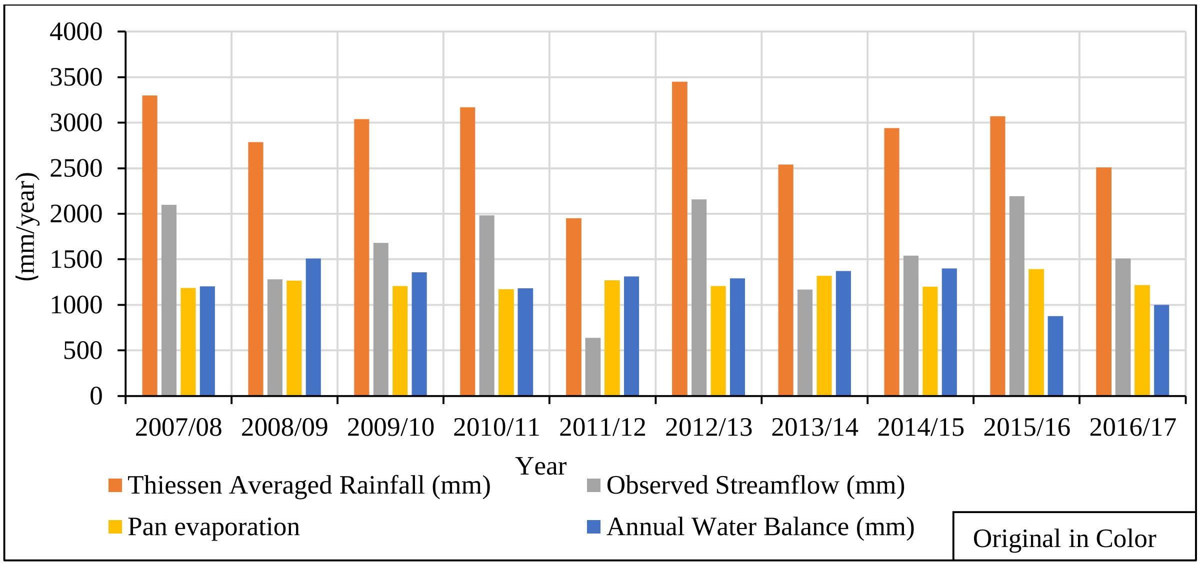

Figure 3-15 Annual Water Balance for Kelani Rive rbasin

3.9 Landuse Pattern

Using the land use data from Survey Department, Sri Lanka, there are fourteen different types of land use classification covering Kelani river basin up to Hanwella stream gauging station sub-watershed and it is shown in the map below in Figure 3-16.

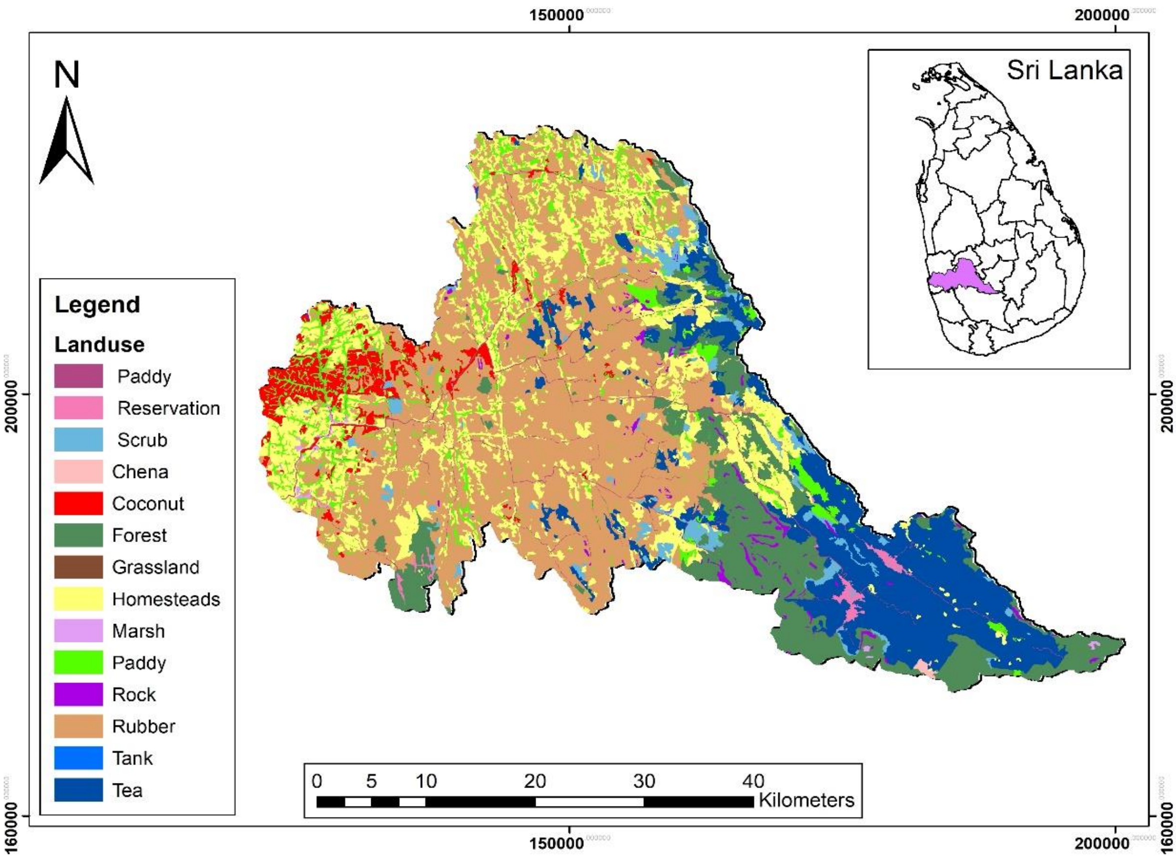

Figure 3-16 Land use map of Kelani river basin

Source: Survey Department, Sri Lanka.

The land use types are reclassified and presented in Table 3-5. Coconut, rubber and tea are reclassified as plantationa and it dominates over other land use types covering 54.23% followed by homestead covering 17.43% of Kelani river basin. Grassland covers only around 0.17 km^2.

Table 3-5 Landuse Reclassification Details

S/No	Landuse Classification	Reclassification	Area (km^2)	Area (%)
1	Paddy	Agriculture	136.3	7.4678
2	Chena			
3	Coconut	Plantation	989.8	54.2303
4	Rubber			
5	Tea			
6	Forest	Forest	295.5	16.1902
7	Reservation			
8	Grassland	Grassland	0.17	0.0090
9	Homestead	Homestead	318.2	17.4339
10	Marsh	Marsh	4.3	0.2356
11	Scrub	Scrub	63.6	3.4846
12	Rock	Buildup area	17.3	0.9479
13	Tank	Water bodies	0.015	0.0008

The reclassified landuse map of Kelani river basin is shown below in the Figure 3-17.

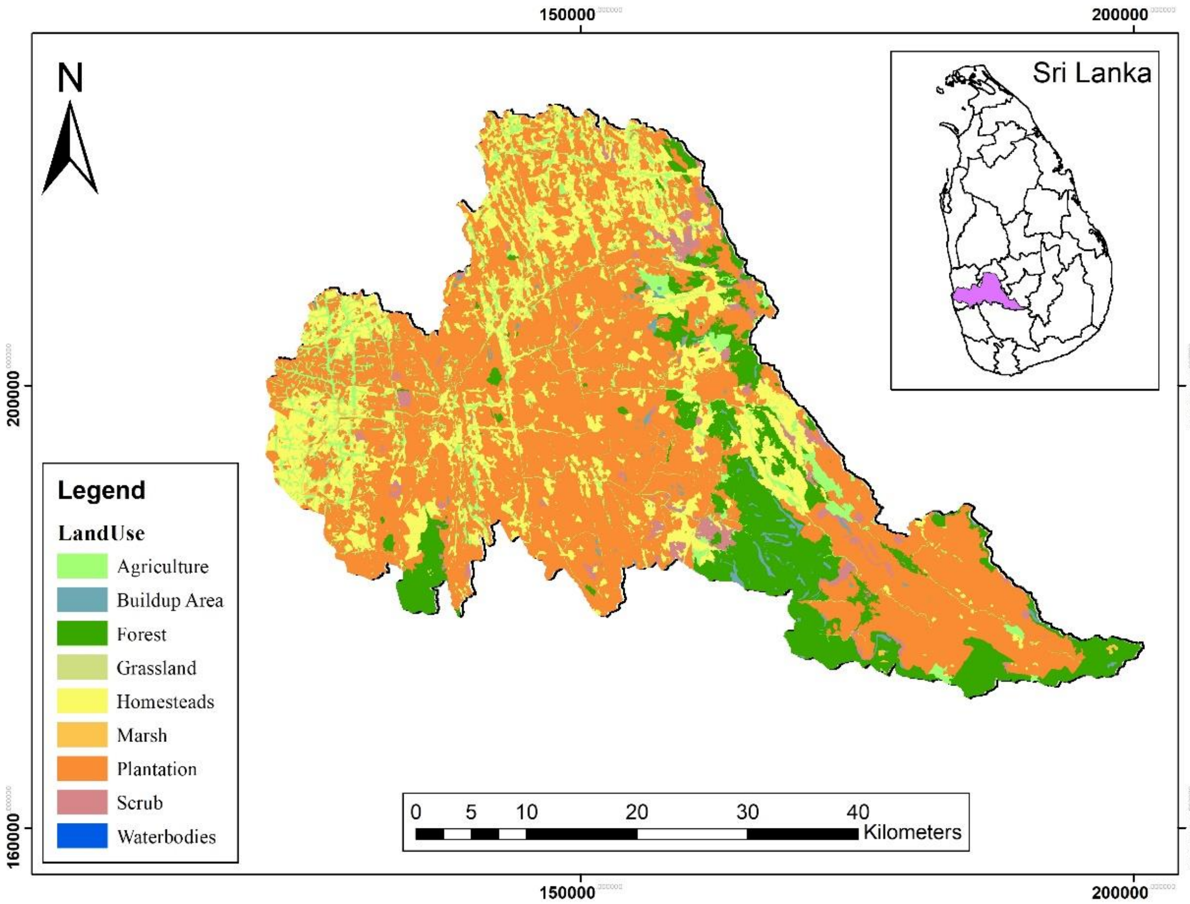

Figure 3-17 Reclassified landuse map of Kelani river basin

3.10 Soil Type

The predominant soil type in the study area is red-yellow podzolic soil which falls under Group C in hydrological soil classification of the NRCS Classification (1986). Red-Yellow podzolic soils covers 90.75 percent of the study area. The details of soil types and area percent coverage is shown in Table 3-6.

Table 3-6 Different types of soil coverage in Kelani river basin

S/No	Soil Type	Area (km^2)	Percentage (%)
1	Reddish brown letosolic soils	58.27	3.19
2	Red-Yellow podzolic soils	1655.90	90.75
3	Alluvial soils	23.93	1.31
4	Steep rock land	86.50	4.74

The soil classification map of Kelani river basin is shown in Figure 3-18.

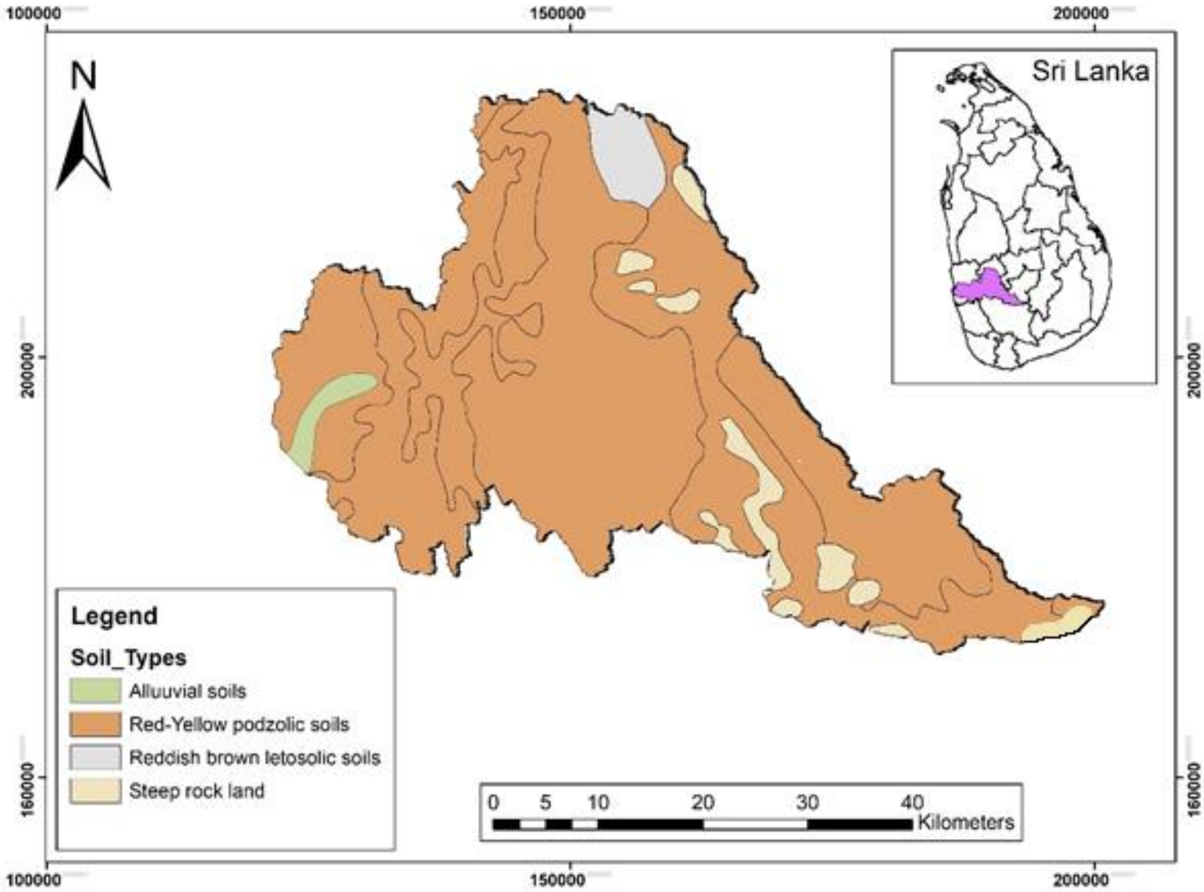

Figure 3-18 Soil Classification of Kelani river basin

4 RESULTS & ANALYSIS

This chapter contains detail information on method used to select events from data sets, HEC-HMS model development, model calibration and verification, parameter optimization and incorporation of antecedent moisture consideration to check model performances.

4.1 Selection of Events

4.1.1 Minimum inter-event time

A minimum inter-event time (MIT) of 96 hours between two consecutive events of rainfall was considered based on the literature specified by Linsley (1985) on the *N* value concept for event separation.

4.1.2 Rainfall and streamflow event selection

The rainfall-streamflow data from 2007-2017 water years were used to select rainfall events. The MIT values for rainfall-streamflow were considered while selecting events. Starting point of a streamflow event was selected when the streamflow starts to respond to event rainfall and the end was taken when hydrograph recession reaches either the point of inflections or reaches *N* value recommended by Linsley (1985). A total of 36 events were selected based on MIT value. Out of 30 events, 18 each were taken for calibration and validation. Considering the data resolution, a minimum rainless period of 4 days based on Linsley (1975) was taken. The duration of the events for calibration and validation are in Table 4-1.

Table 4-1 Event Selection

Purpose	Data Period	No. of events
Calibration	01/10/2007 - 25/10/2013	18
Validation	26/10/2013 - 01/10/2017	18

The total rainfall and streamflow, peak flow and total number of rainfall duration in all events are shown in Table 4-2. The total rainfall in all events and rainless days before event are presented in Figure 4-1 and Figure 4-2. Peak flow in all events and event streamflow and rainfall distribution are shown in Figure 4-3 and Figure 4-4. Event 14 has the highest total rainfall of 469.11 mm. Event 4 has the highest number of rainless days before the event. Event 21 has the highest peak flow of 250.7 m^3/s. The number of wet days in events vary according to Linsley (1975).

Table 4-2 Event Details

Event ID	Total Rainfall (mm)	Rainfall Duration (days)	Total Streamflow (mm)	Peak flow (m^3/s)
1	38.04	5	16.73	73.75
2	4.76	4	7.94	20.50
3	49.84	4	8.15	39.00
4	24.38	5	7.21	20.10
5	132.98	19	31.51	71.25
6	155.21	9	51.92	122.67
7	89.35	9	23.39	116.12
8	18.18	3	6.72	24.00
9	78.38	21	52.07	96.75
10	3.21	4	7.86	25.19
11	78.39	8	11.24	34.98
12	101.37	15	15.49	24.14
13	148.19	21	18.70	30.31
14	469.11	35	113.35	234.98
15	2.26	4	7.70	18.88
16	25.13	9	14.65	28.87
17	136.33	17	24.19	88.98
18	21.47	5	6.78	20.95
19	150.65	14	19.88	50.38
20	86.99	10	12.78	44.51
21	260.18	26	79.38	250.70
22	62.72	10	15.56	34.75
23	140.50	11	18.51	34.15
24	111.34	12	11.58	33.65
25	137.04	11	72.62	208.10
26	123.52	12	27.21	69.41
27	229.12	12	30.94	118.97
28	15.54	6	22.05	61.14
29	14.81	4	21.93	40.94
30	448.41	28	83.35	102.53
31	3.22	4	6.24	28.72
32	57.95	7	14.36	43.76
33	10.89	8	16.23	35.00
34	74.25	11	17.22	45.41
35	288.63	19	57.94	156.22
36	155.82	12	34.23	125.11

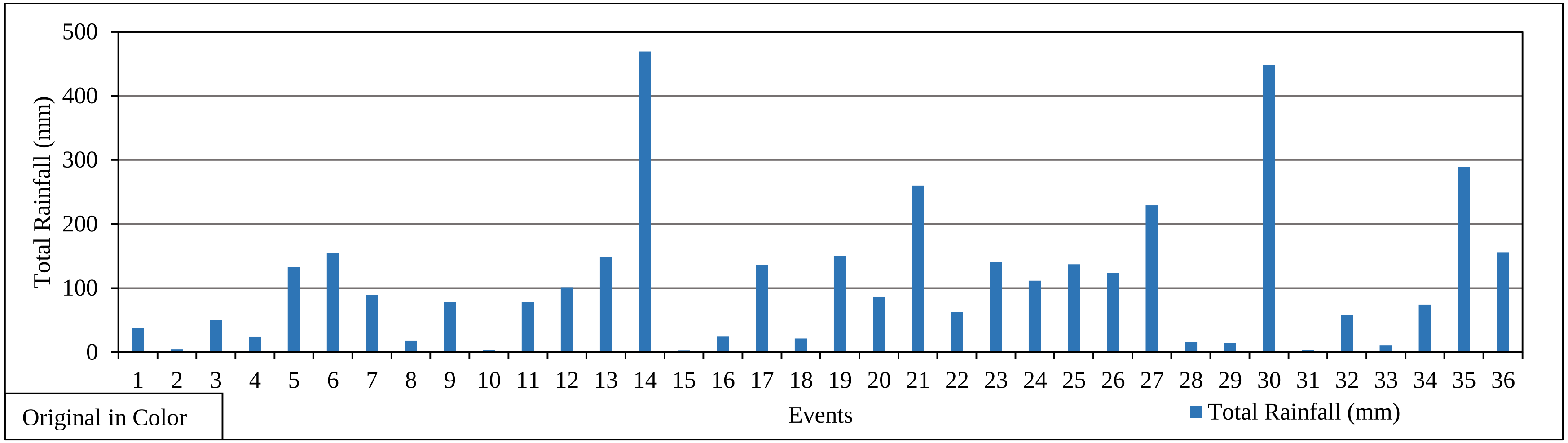

Figure 4-1 Total Rainfall of all 36 events

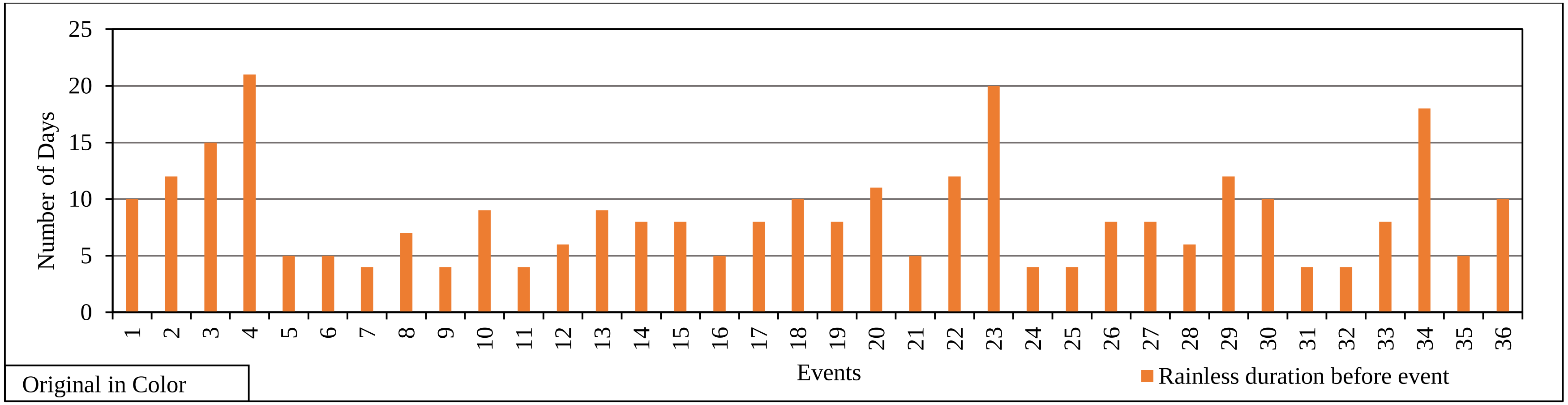

Figure 4-2 Rainless days before all 36 events

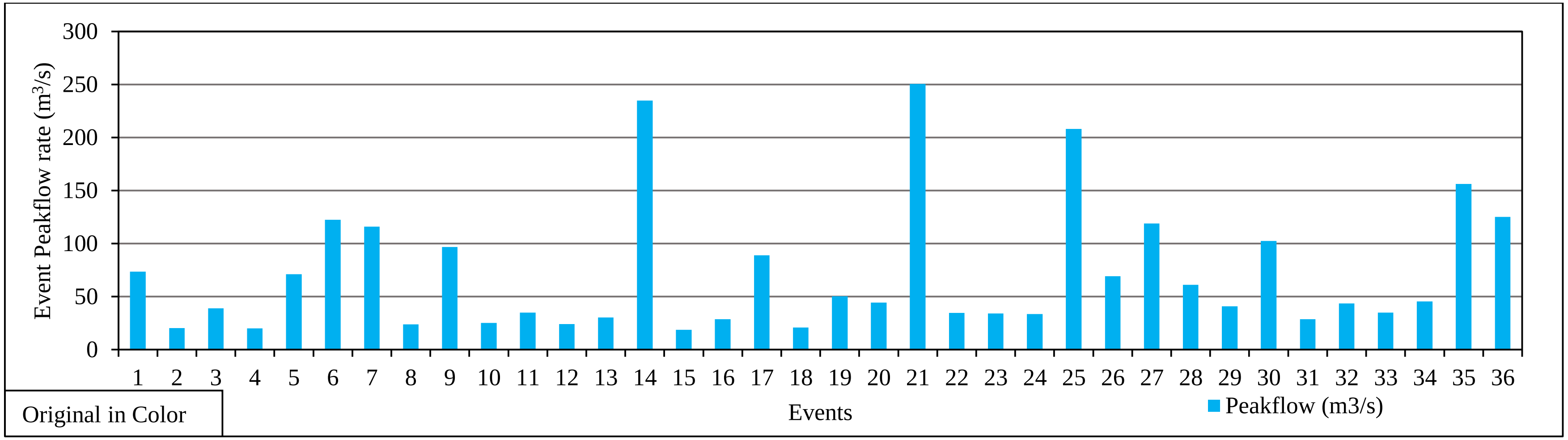

Figure 4-3 Event Peakflow for all 36 events

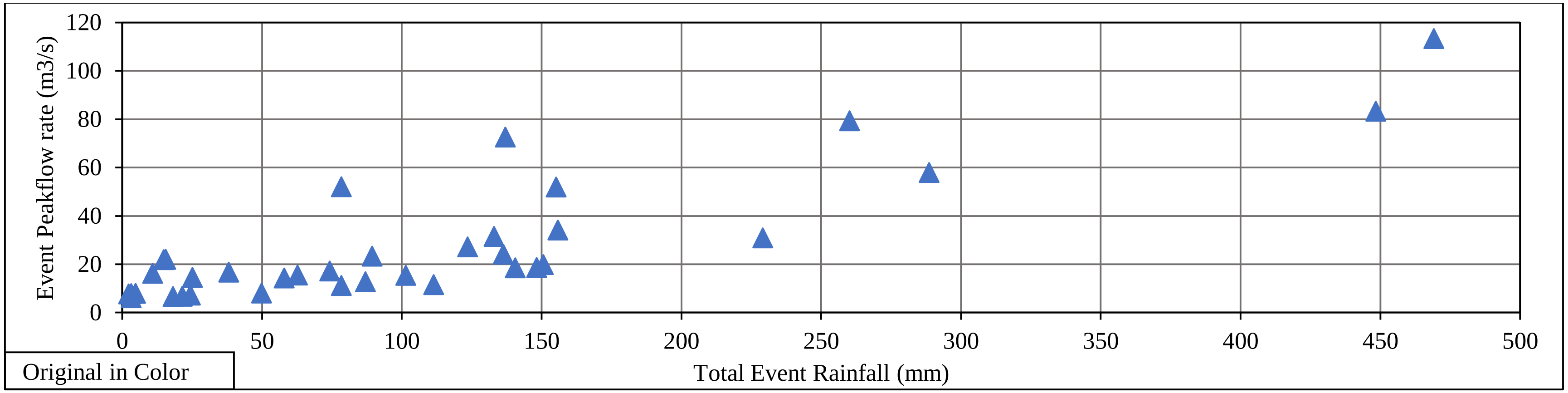

Figure 4-4 Event Rainfall and Streamflow Distribution

4.2 HEC HMS Model Development

The Hydrologic Modelling System (HEC-HMS) was selected for developing hydrological model for Kelani river basin as it is designed to be applicable in a wide range of geographic areas for solving the widest possible range of problems and accepted worldwide. The software is also freely available online (public domain).

4.3 Development of the basin model

There are number of properties for basin model such as gridded sub-basins, local flow, flow ratios, missing flow, unit system, sediment and water quality. Sub-basins that use the ModClark gridded transform method are considered gridded sub-basins. The loss rate and the surface transform calculations were carried out on a grid cell basis and properties of the grid cells are specified in a special grid cell file.

Local flow is defined as the sum of all sub-basin and source outflows entering a junction. Flow ratio can only be applied to sub-basin and source element and it is used to increase or decrease the computed flow by a fixed ratio. According to the HEC-HMS manual, ratio 1.0 is used for Kelani basin.

The rainfall and streamflow data checking was done manually, therefore the missing inflow data for an element was set to zero. The basin model is set in system international units (also called as metric units). The movement of the sediment in the watershed can be included as part of the hydrology of the basin model but in this study, sediment is disabled, no sediment processing took place in the basin model. The nutrient water quality (nitrogen and phosphorus) was also disabled.

4.4 Development of the precipitation loss model

Out of eleven methods available for estimation of precipitation loss given in HEC-HMS model, SCS Curve Number method was chosen in order to fulfil the objective of the study. The curve number varies depending on the type of soil moisture conditions and initial abstraction. The curve number is the most important parameter in the study. To incorporate curve number and initial abstraction in the model SCS Curve Number method has been selected as precipitation loss method.

The curve numbers were assigned by Chow (2010) and SCS (1986) method. Based on the catchment characteristics such as hydrologic soil group and land use types, curve number for different land use are identified as shown in Table 4-3. The average CN for the whole basin is 79.

Table 4-3 Weighted Curve Number Calculation for whole catchment

Soil Group: C					
Land Use	Area (km^2)	Area (%)	Individual CN	Weighted CN	CN
Agriculture	136.28	7.47	85	634.66	**79**
Buildup Area	17.30	0.95	78	73.92	
Forest	295.53	16.19	77	1246.79	
Grassland	0.17	0.01	74	0.67	
Homesteads	318.16	17.43	78	1359.70	
Marsh	4.27	0.23	98	22.95	
Plantation	989.84	54.23	79	4284.40	
Scrub	63.60	3.48	77	268.31	
Water bodies	0.02	0.001	79	0.07	
Total Area	**1825.2**	**100**		**7891.47**	

The maximum potential retention, S was calculated using the equation given in Chow et al. (2010) and it was 2.66 mm. The initial abstraction according to (SCS, 1972);

$I_a = 0.2 * S$, therefore the initial abstraction, I_a =0.53 mm.

4.4.1 Curve Number for events

Using the asymptotic curve number determination, curve number for individual events are determined. Each event has its own curve number and it is displayed in Table 4-4.

Table 4-4 Curve Numbers (CN) for events

Events	CN	Events	CN
1	72.2	10	48.9
2	90.5	11	38.3
3	65.7	12	18.1
4	93.9	13	43.5
5	43.6	14	41.1
6	53.4	15	63.6
7	85.2	16	28.0
8	42.7	17	61.3
9	55.5	18	46.3

The curve number is further optimized for calibration and the optimized CN for all events are given in Table 4-5. The average of the CN is taken for the validation.

Table 4-5 Optimized Curve Numbers (CN)

Events	Optimized CN	Events	Optimized CN
E1	72.2	E10	35.2
E2	86.7	E11	37.4
E3	35.1	E12	15.1
E4	72.0	E13	30.2
E5	27.1	E14	35.3
E6	46.4	E15	63.0
E7	79.6	E16	36.46
E8	43.3	E17	60.0
E9	35.2	E18	43.1
		Average	**47.4**

4.4.2 Development of transform model

In transform model development, SCS unit hydrograph method was selected. Lag time is the only parameter in SCS unit hydrograph method and it is calculated using the Kirpich formula.

$$T_c=0.0078\ (L^{0.77}/S^{0.385}) \qquad (4)$$

where, L=Length of the longest water course (L) and T_c= Time of concentration

Lag time for the lumped model of Kelani river basin is 720. 5 minutes which is equal to 12 hours.

4.4.3 Development of baseflow model

Recession method was selected for baseflows model out of four other methods as it is intended primarily for event simulation. It automatically reset after each storm event (USACE, 2000). Initial flow which is the flow at the beginning of simulation was specified manually. The recession constant and threshold flow in between 0 and 1 was considered when optimizing these two parameters.

4.4.4 Development of precipitation model

Theissen average (gauge weight) method for precipitation was used in the precipitation model. Theissen polygon is created by using the Geographic Information System (GIS) tool and the details on rainfall Theissen weights are mentioned in Table 3-3.

4.4.5 Control specification

The start date of the events are used as the starting date and the end date of the events are used as end date for model calibration and model verification. Time interval was taken as 1 day.

4.4.6 Model calibration

Kelani lumped model was calibrated by matching with the observed flow at Hanwella river gauging station. Nash-Sutcliff coefficient is chosen as the objective function as the study is based on event modelling. Figure 4-5 shows the comparison of observed and simulated peak flow. The results are relatively good with average Nash-Sutcliff (NASH) value of 0.63. Researchers at USGS considers 0.5 and above NASH values as good fit for streamflow conditions. The average RMS error is 1.3. Four events calibration shows no/poor result. It has been observed that when the event rainfall remains constant or when there is no peak flow, the model performs poor. The simulated flow at the initial stage of the event is mostly lower than that of observed streamflow because of incorporation of losses such as initial abstraction in the model.

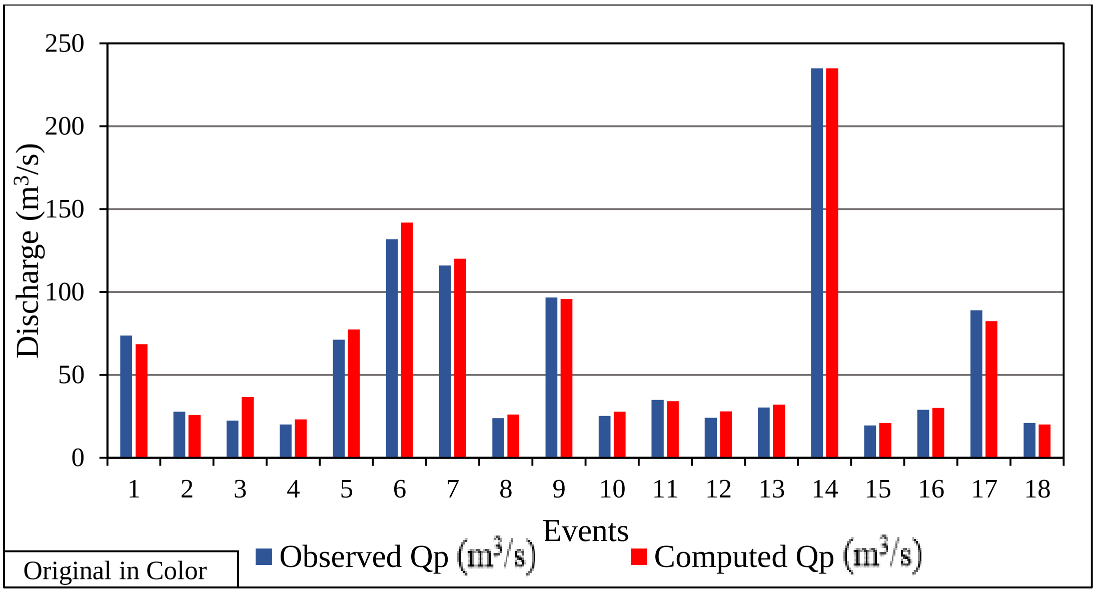

Figure 4-5 Comparison of Observed and Simulated Peak flow during Calibration

Figure 4-6 shows the difference in between observed total streamflow and computed total streamflow. The maximum total observed streamflow is 666.02 m^3/s while the maximum total computed streamflow is 673 m^3/s. The lowest total observed streamflow is 19 m^3/s while the lowest total computed streamflow is 20 m^3/s.

Table 4-6 Event Calibration Details

Event ID	**From**	**To**	**Total Rainfall (mm)**	**Observed QP (m3/s)**	**Computed QP (m^3/s)**	**Observed Total Streamflow (m^3/s)**	**Computed Total Streamflow (m^3/s)**	**Event NASH**	**RMS Error**
1	7-Nov-08	12-Nov-08	38.04	73.80	68.60	288.00	300.00	0.84	4.90
2	6-Jan-09	9-Jan-09	4.76	27.80	25.80	89.10	89.30	0.65	0.10
3	25-Jan-09	31-Jan-09	49.84	22.40	36.60	155.10	159.50	0.53	1.66
4	21-Feb-09	1-Mar-09	24.41	20.10	23.10	152.10	145.40	0.02	2.23
5	25-Jul-09	12-Aug-09	132.98	71.25	77.40	666.02	673.00	0.24	1.65
6	12-Oct-09	24-Oct-09	155.21	131.80	142.00	131.80	142.00	0.98	2.83
7	8-Jan-10	17-Jan-10	86.65	116.12	120.00	116.12	120.00	0.85	1.23
8	9-Feb-10	15-Feb-10	18.18	24.00	26.00	24.00	26.00	-	-
9	15-Dec-10	6-Jan-11	78.38	96.75	95.70	96.75	95.70	0.82	0.22
10	3-Oct-11	6-Oct-11	3.15	25.19	27.80	25.19	27.80	-	-
11	4-Jan-12	11-Jan-12	78.39	34.98	34.10	34.98	34.10	0.80	0.33
12	3-Feb-12	17-Feb-12	101.37	24.14	28.00	24.14	28.00	0.48	1.00
13	27-Feb-12	21-Mar-12	148.19	30.31	32.00	30.31	32.00	0.66	0.36
14	27-Mar-12	1-May-12	469.11	234.98	235.00	234.98	235.00	0.93	0.00
15	10-May-12	14-May-12	2.26	19.49	21.00	19.49	21.00	-	-
16	17-Jul-12	30-Jul-12	25.13	28.87	30.00	28.87	30.00	0.14	0.28
17	4-Aug-12	21-Aug-12	136.33	88.98	82.40	88.98	82.40	0.88	1.55
18	22-Jan-13	26-Jan-13	21.47	20.95	20.00	20.95	20.00	-	-
					Maximum	666.02	673.00	0.98	4.90
					Minimum	19.49	20.00	0.02	0.00
					Average	124.67	70.94	0.63	1.31

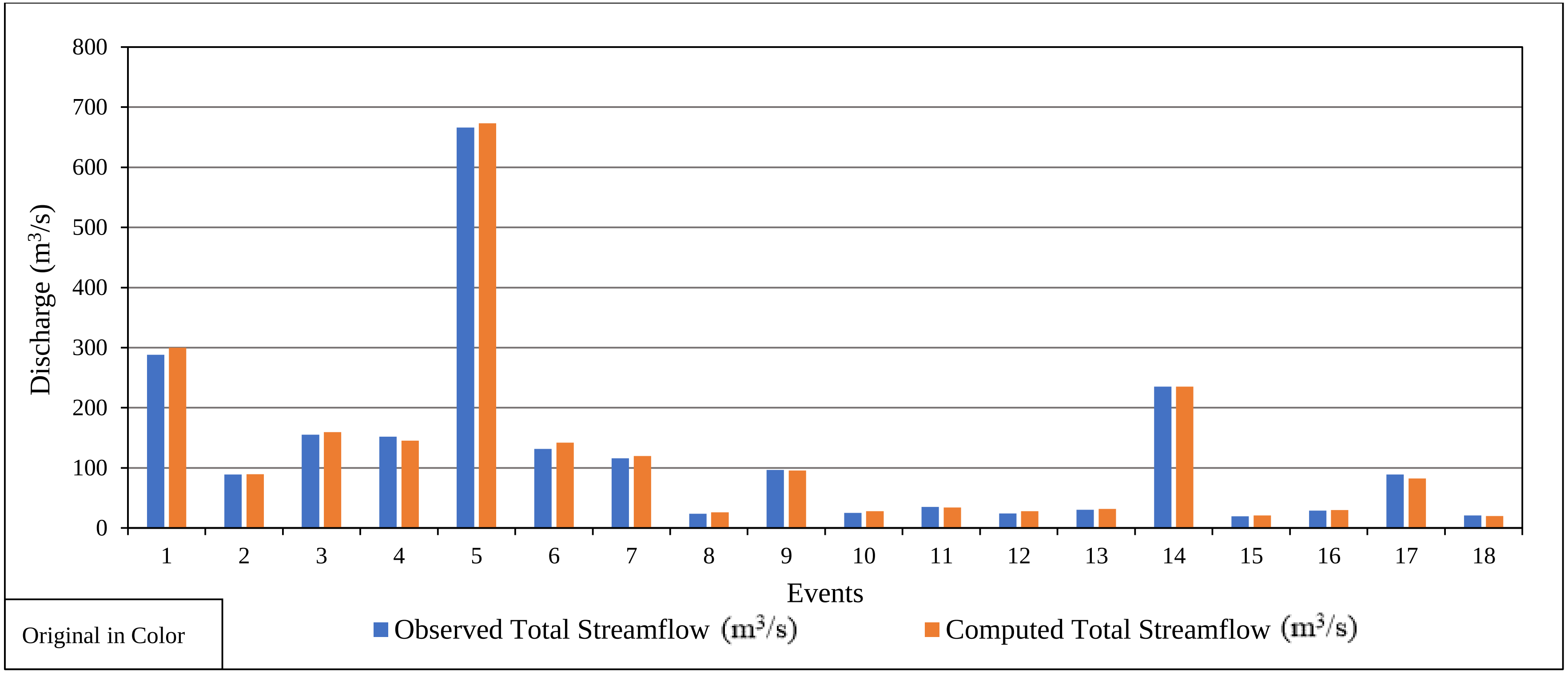

Figure 4-6 Comparison of Total Observed and Simulated Streamflow during Calibration

4.5 Model Verification

Sixteen events from January 2013 to September 2017 are used for model verification from the same data set. The average of Curve Number which is 47.4 is used in model verification. In baseflow model, there are two discharge types and they are discharge and discharge per area. Discharge is chosen for all the events and like in model calibration, the initial discharge is manually given from each event verification data set as the initial discharge for all 36 events are different.

The computed peak flow are slightly higher than that of the observed peak flow in model verification. The average of the initial abstraction from calibration is used in model verification whereas in model calibration, the precipitation loss was calculated for each event separately.

The average NASH value for verification data set is 0.62 and RMS error is 2.82. The maximum NASH value from model verification is 0.93 whereas the minimum NASH value is 0.17. The maximum RMS error is 5.21 while the minimum RMS error is 0.24.

The average NASH value for model calibration and verification are almost same but the RMS error are higher in model verification than in model calibration. The RMS error in the verification data set has been increased to an average of 2.82 from 1.31 from the model calibration. The model verification data set has more error than that of model calibration data set.

Figure 4-8 shows the difference in between observed total streamflow and computed total streamflow in model verification. The maximum total observed streamflow is 1677.3 m^3/s while the maximum total computed streamflow is 1753.5 m^3/s. The lowest total observed streamflow is 45 m^3/s while the lowest total computed streamflow is 48.0 m^3/s.

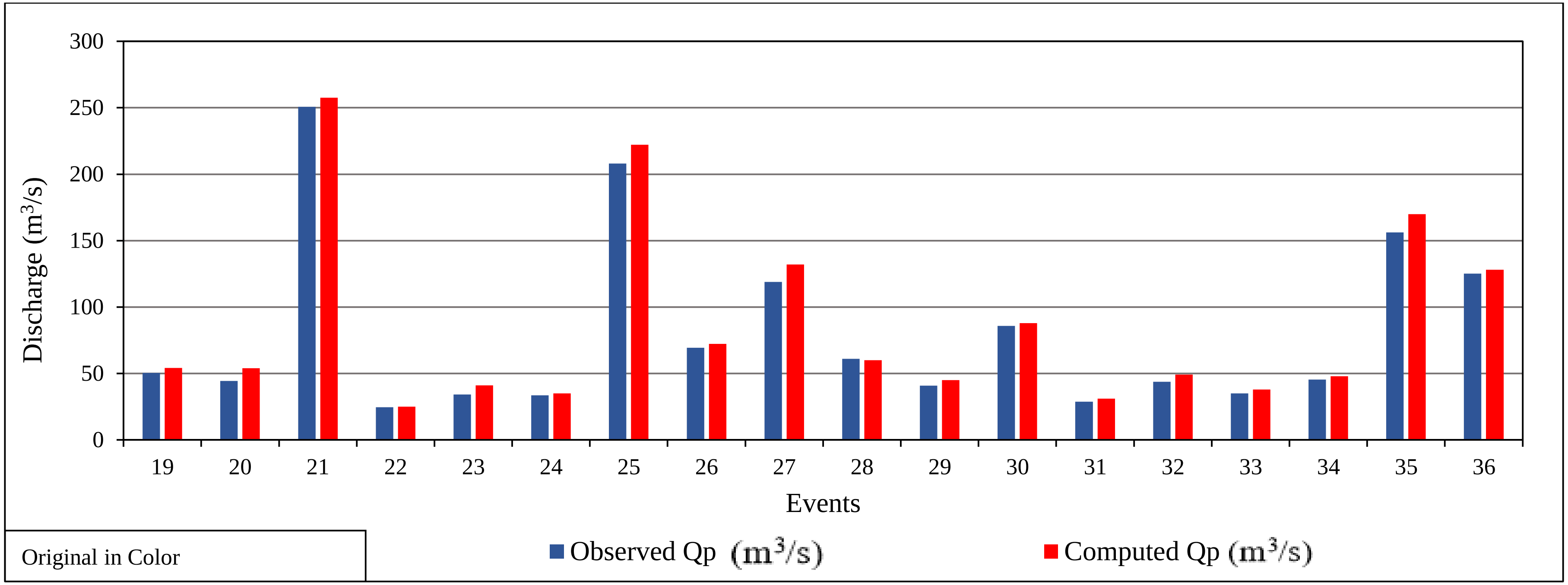

Figure 4-7 Comparison of Observed and Simulated Peak flow during Verification

Table 4-7 Event Verification Details

Event ID	**From**	**To**	**Total Rainfall (mm)**	**Observed QP(m3/s)**	**Computed QP(m^3/s)**	**Observed Total Streamflow (m^3/s)**	**Computed Total Streamflow (m^3/s)**	**Event NASH**	**RMS Error**
19	4-Feb-13	15-Feb-13	123.8	50.4	54.2	351.2	349.7	0.76	0.4
20	3-Mar-13	14-Mar-13	87.0	44.5	54.0	270.0	277.2	0.66	2.1
21	30-Sep-13	25-Oct-13	260.2	250.7	257.6	1677.3	1753.5	0.89	4.4
22	6-Jan-14	16-Jan-14	62.7	24.7	25.0	219.2	202.4	0.17	4.8
23	20-Feb-14	12-Mar-14	140.5	34.2	41.0	377.5	366.8	0.71	3.0
24	1-Apr-14	12-Apr-14	111.3	33.7	35.0	244.6	203.6	0.24	5.2
25	10-Nov-14	21-Nov-14	137.0	208.1	222.1	1534.5	1490.7	0.71	4.7
26	22-Feb-15	9-Mar-15	118.9	69.4	72.3	464.3	445.6	0.82	_
27	26-Mar-15	6-Apr-15	188.5	119.0	132.0	653.7	649.1	0.45	1.0
28	4-Jan-12	7-Jan-12	15.5	61.1	60.0	430.2	387.1	_	_
29	23-Jan-16	30-Jan-16	14.8	40.9	45.0	261.9	259.2	0.69	1.0
30	27-Mar-16	18-Apr-16	345.3	85.9	88.0	1185.9	1109.6	0.79	2.7
31	9-Sep-16	13-Sep-16	3.2	28.7	31.0	131.8	126.5	_	1.1
32	13-Oct-16	21-Oct-16	53.5	43.8	49.1	272.2	250.5	0.58	3.7
33	4-Dec-16	14-Dec-16	10.9	35.0	38.0	343.0	326.9	0.17	_
34	19-Jan-17	31-Jan-17	74.3	45.4	48.0	45.4	48.0	0.50	0.2
35	25-Feb-17	21-Mar-17	288.6	156.2	170.0	1224.2	1140.1	0.93	5.2
36	27-Mar-17	9-Apr-17	155.8	125.1	128.1	723.3	719.1	0.81	_
					Maximum	1677.3	1753.5	0.93	5.2
					Minimum	45.4	48	0.17	0.2
					Average	578.34	561.42	0.62	2.82

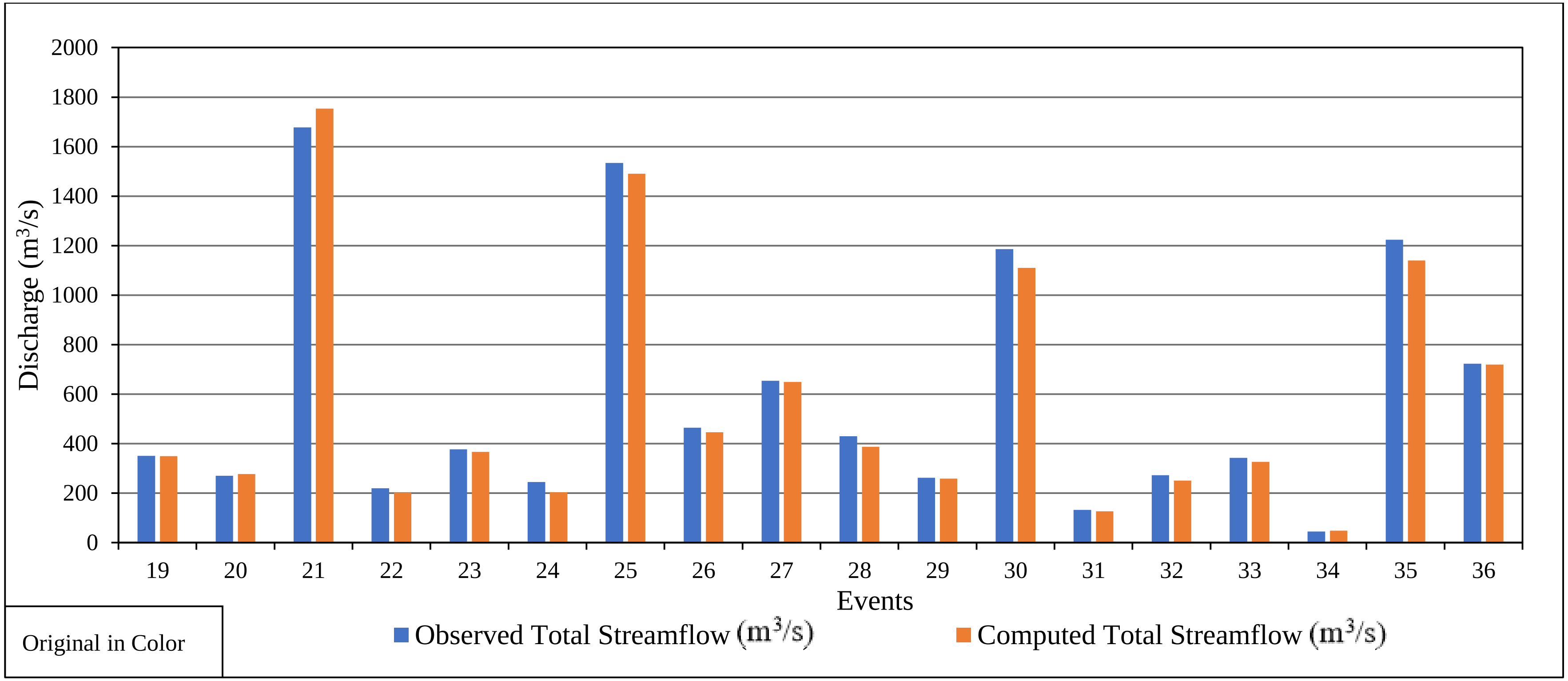

Figure 4-8 Comparison of Observed and Simulated Total Streamflow during Verification

4.6 Incorporation of Antecedent Moisture Condition in HEC-HMS Model Performance

Table 4-11 shows some of the popular formula to calculate AMC I and AMC II from AMC II condition. Among these formulas and the AMC conversion formula in SCS-CN Methodology, Chow et al., (1998) formula for conversion is chosen following the literature review.

Table 4-8 AMC I and AMC III Calculation using popular formulas

Event ID	AMC	Sonhani (1975)	Hawkins et al. (1988)	Chow et al. (1988)	Neitsch et al. (2002)
1	AMC I	52.7	53.3	52.2	18.6
	AMC II	72.2	72.2	72.2	72.2
	AMC III	86.6	85.9	85.7	87.1
3	AMC I	18.8	19.2	18.5	19.9
	AMC II	35.1	35.1	35.1	35.1
	AMC III	57.3	55.9	55.5	54.4
5	AMC I	13.7	14.0	13.5	20.0
	AMC II	27.1	27.1	27.1	27.1
	AMC III	47.9	46.5	46.1	44.2
13	AMC I	18.2	18.6	17.9	19.9
	AMC II	34.2	34.2	34.2	34.2
	AMC III	56.3	55.0	54.5	53.3
17	AMC I	34.9	35.4	34.4	19.7
	AMC II	55.6	55.6	55.6	55.6
	AMC III	75.6	74.6	74.2	74.9
19	AMC I	30.6	31.1	30.2	19.8
	AMC II	50.7	50.7	50.7	50.7
	AMC III	71.8	70.7	70.3	70.7
20	AMC I	30.6	31.1	30.2	19.8
	AMC II	50.7	50.7	50.7	50.7
	AMC III	71.8	70.7	70.3	70.7

4.6.1 Incorporation of AMC in event 1

When AMC III condition is applied in Event 1, the model performances increases. When AMC II, which is the average soil moisture condition was used, the NASH value generated was 0.84. The Nash value when AMC III condition used is 0.88. Event 1 performance increase when it is considered at wet soil moisture condition state.

Table 4-9 Event 1 and its curve number

Events	CN II	Optimized CN	CN III
E1	65.7	72.23	85.68

The performance of the model while using AMC III or CN III is shown in the normal and semi-log form graph in Figure 4-9.

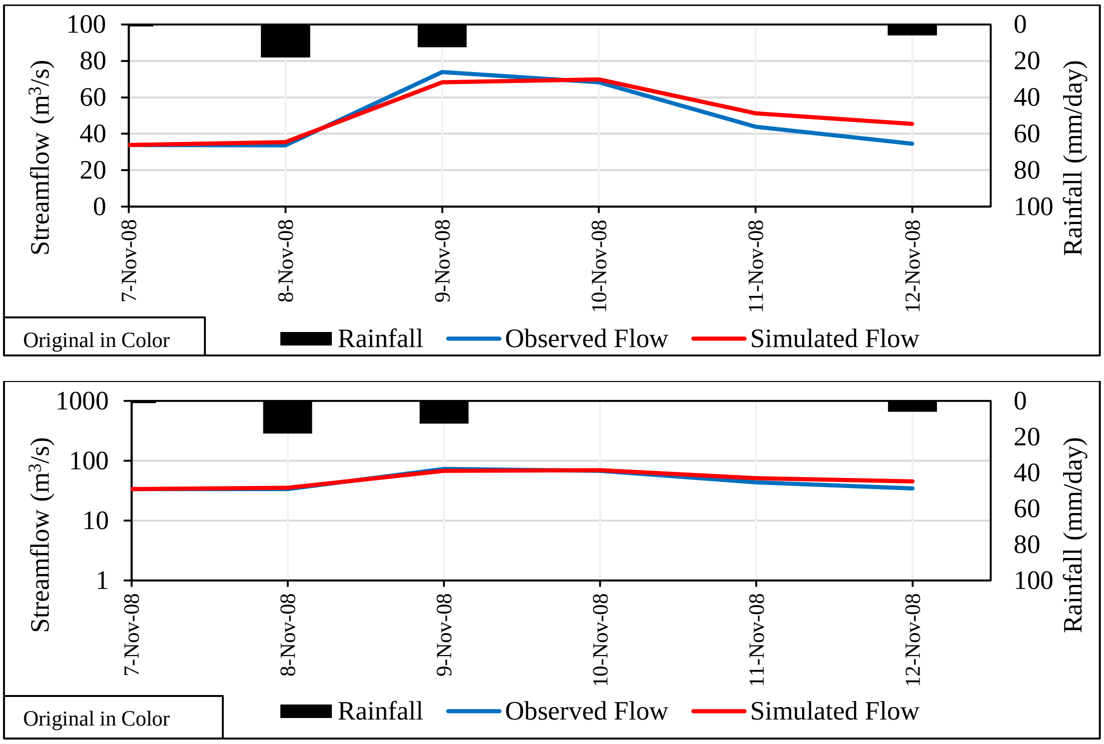

Figure 4-9 Model Performance of Event 1 when AMC III is incorporated

4.6.2 Incorporation of AMC in event 3

The NASH value for Event 3 increases to 0.73 when AMC III condition is applied. To verify, AMC III condition was applied to Event 5, 13, 19 and 20. It has been observed that the model performance increases when AMC III is applied when the events fall within in Maha season.

Table 4-10 Event 3 and its curve number

Events	CN II	Optimized CN	CN III
E3	72.23	35.122	55.459

The performance of the model while using AMC III or CN III is shown in the normal and semi-log form graph in Figure 4-910.

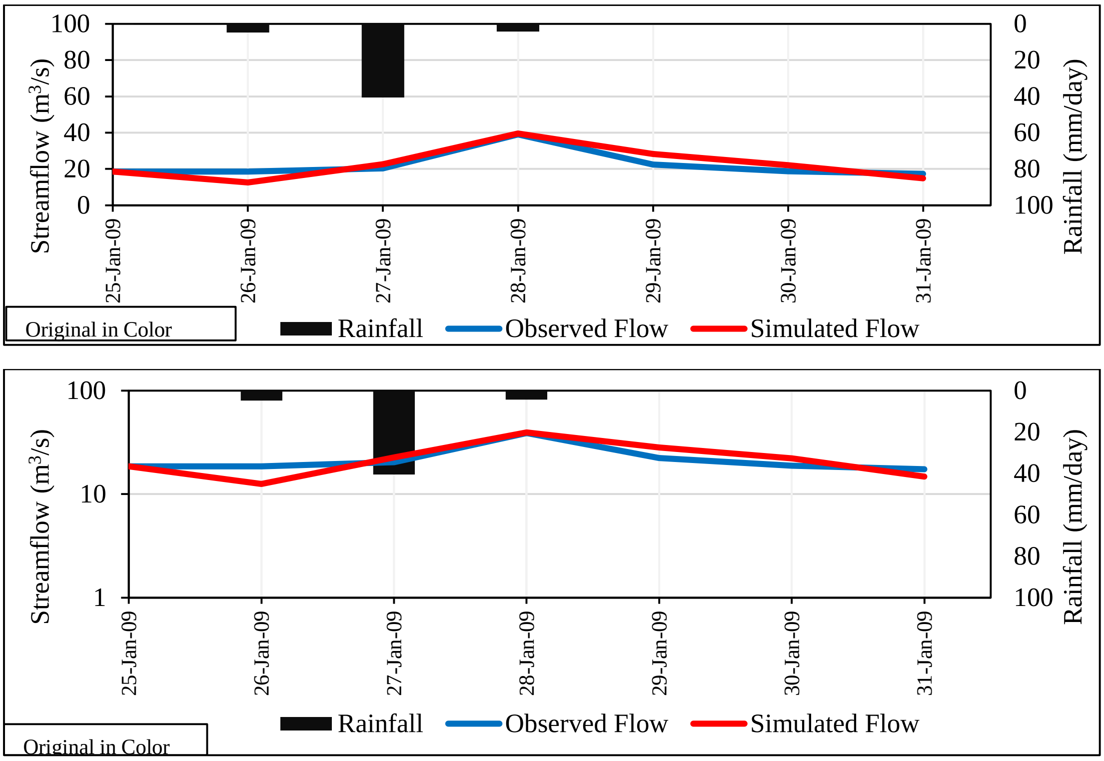

Figure 4-10 Model Performance of Event 3 when AMC III is incorporated

4.6.3 Incorporation of AMC in event 5 and event 17

When AMC III and AMC I conditions were applied in Event 5 and Event 17, the model performance neither improve nor deteriorate. The NASH value for Event 5 and Event 17 are 0.24 and 0.88, respectively, which is as same as in calibration. These events falls in Yala season. Although there is no significant model improvement when AMC conditions are applied in events that fall in Yala season but there is a slight improvement in total simulated streamflow.

Table 4-11 Event 5 and its curve number

Events	CN II	Optimized CN	CN III	CN I
E5	43.60	27.07	46.06	24.51

The performance of the model while using AMC III or CN III and AMC I or CN I conditions are shown in the normal and semi-log form graph, Figure 4-911.

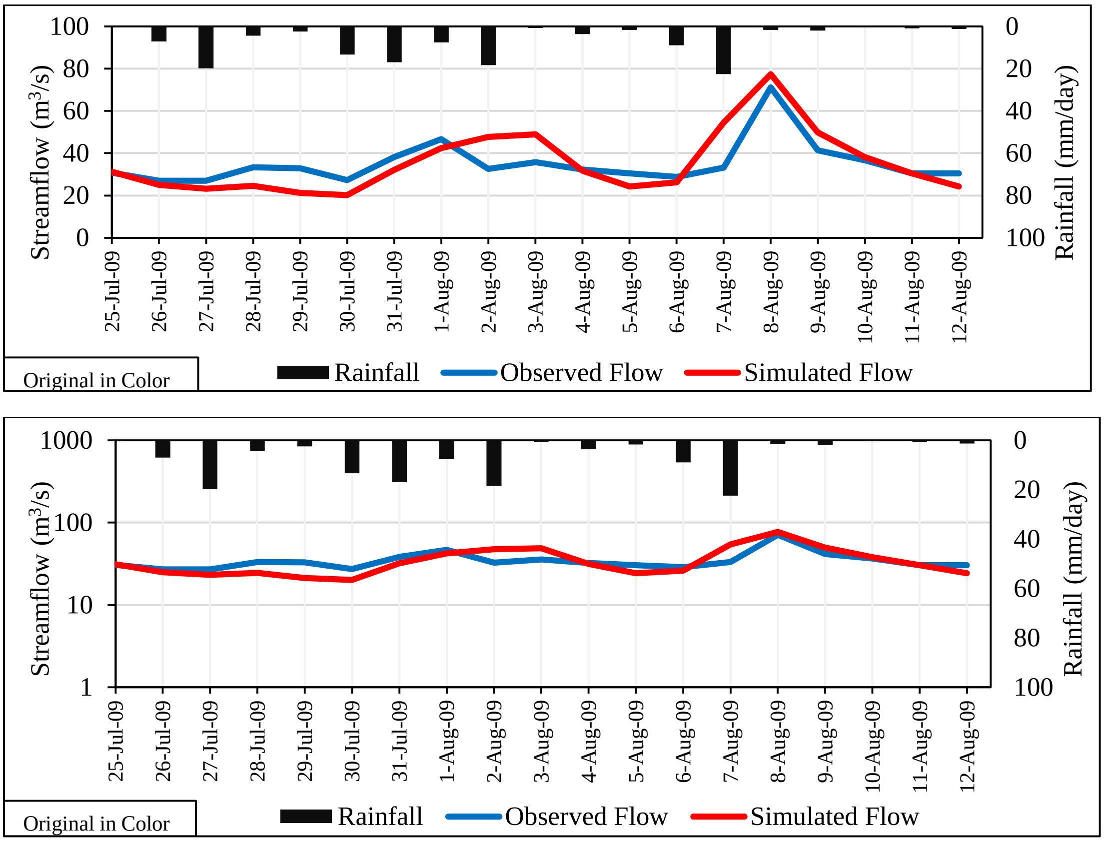

Figure 4-11 Model Performance of Event 5 when AMC is incorporated

The CN for event 17 is 43.5 when the soil moisture is considered at normal condition. When the soil moisture condition is considered wet the CN changes to 74.2 whereas it is 24.4 when soil moisture is considered dry.

Table 4-12 Event 17 and its curve number

Events	CN II	Optimized CN	CN III	CN I
E17	43.52	55.58	74.21	24.45

The performance of Event 17 while using AMC III or CN III and AMC I or CN I conditions are shown in the normal and semi-log graph in Figure 4-912.

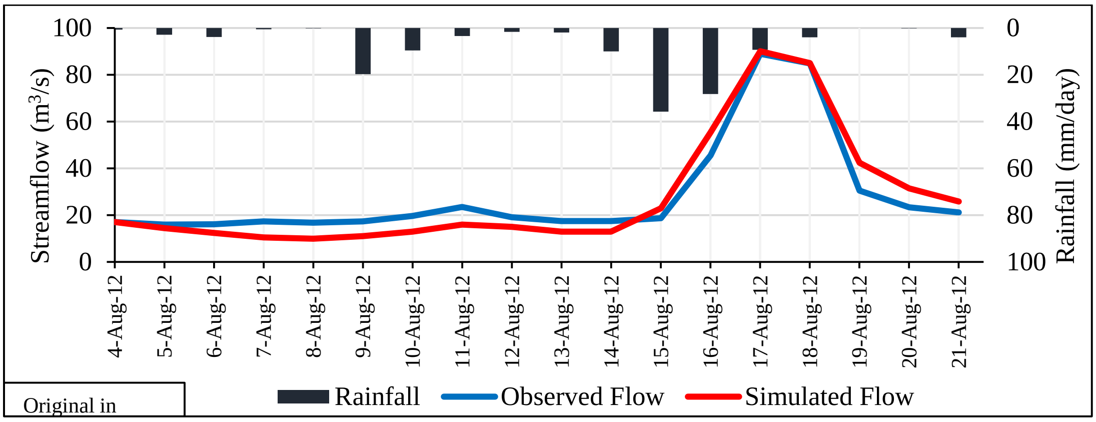

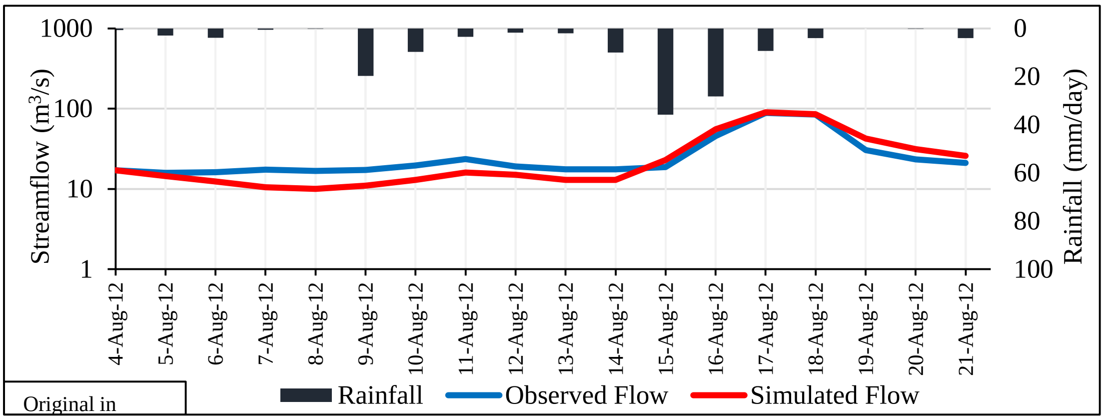

Figure 4-12 Model Performance of Event 17 when AMC is incorporated

4.6.4 Incorporation of AMC in event 19

Event 19 falls in the Maha season, considering AMC III condition in the event increases the model performances. The NASH values with AMC III condition is 0.82, an increase by 0.06.

Table 4-13 Event 19 and its curve number

Events	CN II	Optimized CN	CN III	CN I
E19	50.71	50.71	70.29	30.17

The performance of event 19 while using AMC III or CN III and AMC I or CN I conditions are shown in the normal and semi-log graph in Figure 4-913.

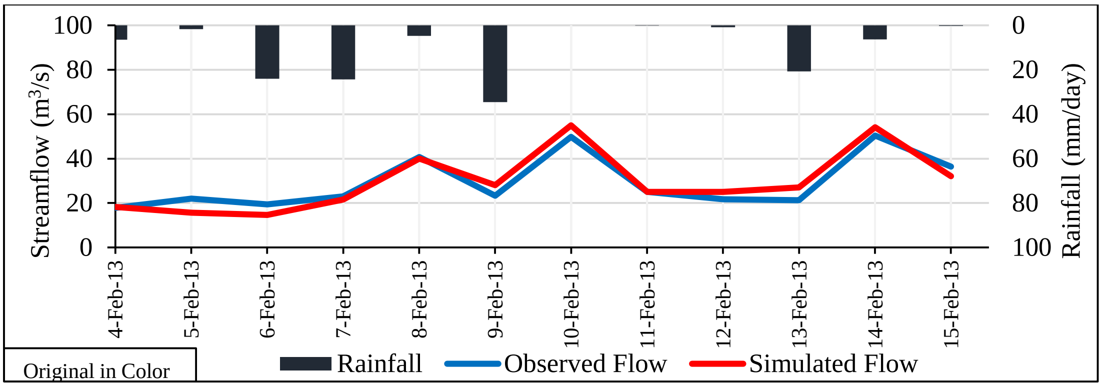

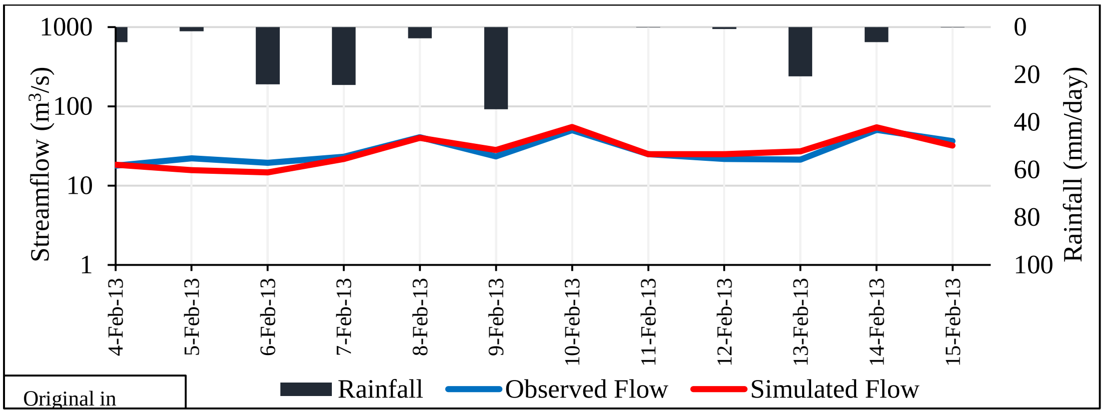

Figure 4-13 Model Performance of Event 19 when AMC is incorporated

4.6.5 Incorporation of AMC in event 20

Event 20 also falls in the Maha season. Considering AMC III in the event increases model performances whereas considering AMC I neither improves nor retrogress the model performances. When AMC II was considered, the NASH value was 0.66 whereas when AMC III condition was applied, the NASH value is 0.69. This shows that the model performances slightly increases when wet condition of the soil is considered.

Table 4-14 Event 20 and its curve number

Events	CN II	Optimized CN	CN III	CN I
E20	50.71	50.71	70.290	30.168

The performance of event 20 while using AMC III or CN III and AMC I or CN I conditions are shown in the normal and semi-log graph in Figure 4-914.

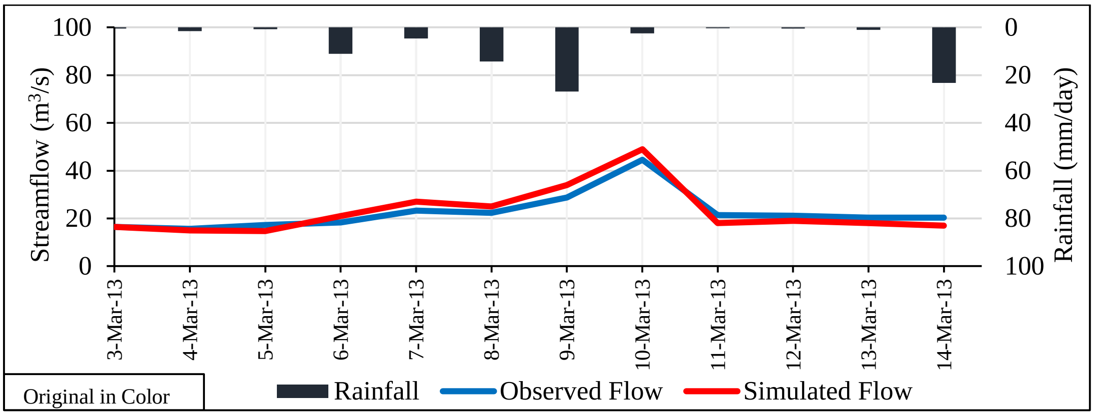

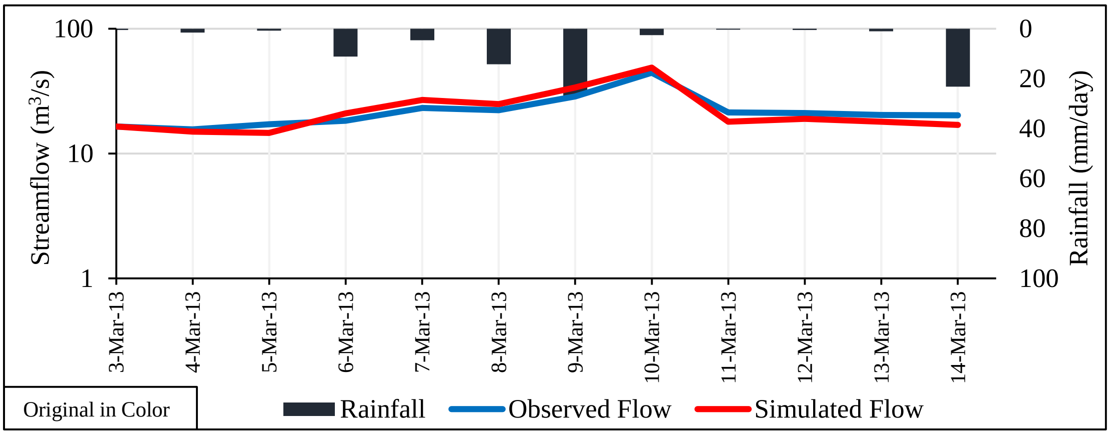

Figure 4-14 Model Performance of Event 20 when AMC is incorporated

5 DISCUSSION

5.1 Event Selection

Ten water years data starting from 2007 to 2017 was used for the study. Six rainfall and streamflow gauging stations maintained by Irrigation Department, Sri Lanka of Kelani river basin namely Norwood, Kithulgala, Holombuwa, Deraniyagala, Glencorse and Hanwella were used.

Based on the literature review, using MIT method, thirty six (36) events were selected from the ten years (10) data set. Minimum four (4) days of rainless periods were considered before all the events. The thirty six events are broken down into two parts equally for calibration and verification of the model. The calibration data set starts from October 2007 to August 2012 and the Verification data set starts from January 2013 to September 2017.

Six random events were chosen from Yala and Maha season to calculate antecedent moisture condition of the events by using popular formulas. The AMC calculated is incorporated in the HEC-HMS model to check the model performance.

The Minimum Inter event Time (MIT) value for the data was four (4) days. The starting point at which the observed streamflow hydrograph responds to rainfall event was considered as starting point of the event and the infliction point of the hydrograph was considered as the end point. However in some events, when it was not possible to clearly identify the infliction point, N value suggested by Linsley et al. (1975) was taken to determine the end point of the event.

5.2 Data Resolution

Hourly or finer data set would have yielded more effective result from the model. An hourly data of Kelani river basin would generate more accurate curve number and initial abstractions which would improve the overall model performance. Curve number do not just varies seasonally but it varies monthly or even weekly. In HEC-HMS loss model, potential maximum retention, S is calculated from the data set of the events. Curve Number as well as the initial abstraction depends on potential maximum retention value. Both Curve Number and initial abstractions are calculated using SCS-CN method.

The daily data resulted in mismatch of some observed rainfall and streamflow data. Out of 18 events used for calibration, three events (event 8, 10 and 15) could not be calibrated as some events consist of constant rainfall or no rainfall peak. Two events (event 28 and 31) from verification data set could not match. A major concern was the shift in the peak flow which could not be matched while in calibrating and verifying.

5.3 Curve Number

There are many methods to calculate curve number. In this research, curve number from the watershed characteristics was used initially in the model. Due to the poor model performance, curve number calculated from the field data for individual events were used. Curve number was found to be one of the most sensitive parameter.

5.4 Model Calibration

The model was manually calibrated as well as auto-calibrated through trial and error method in HEC-HMS model. Six parameters are auto calibrated while two parameters are manually calibrated. The two parameters which are manually calibrated are curve number and initial abstraction from the loss model. Time of concentration and storage coefficient from transform model and recession constant and threshold type from baseflow model are auto calibrated until the line of best fit is achieved between the observed and the simulated streamflow. There are two threshold types and they are ratio to peak and threshold discharge. Ratio to peak has been used in baseflow model.

Event number 8, 10 and 15 could not be calibrated. The observed streamflow in Event 8, 10 and 15 ranges from 19.4 m^3/s to 24 m^3/s, 23.84 m^3/s to 25.18 m^3/s and 17.60 m^3/s to 19.49 m^3/s, respectively, however, it was observed that these events fall under constant streamflow. It varied in a small scale and there was an absence of even a single peak event.

The SCS-CN method used in the loss model performs well when the event has one single peak event. Initial abstraction parameter used in the loss model affects or decreases the runoff at the initial stage.

The minimum NASH value and RMS error in calibration data are 0.02 and 0.0, respectively. The maximum NASH value and RMS error are 0.98 and 4.90, respectively. The average value for NASH and RMS error from 18 events are 0.63 and 1.31, respectively.

5.5 Model Verification

Eighteen events from January 2013 to September 2017 are used for model verification. The average of curve number from calibration was used while verifying the model. The average curve number used was 47.4. In baseflow model, the initial discharge was manually set referring to the initial discharge at the beginning of the event.

The average NASH value for verification data set is 0.62 and RMS error is 2.82. The maximum NASH value and RMS error are 0.93 and 5.21 and the minimum are 0.17 and 0.24, respectively.

The RMS error in the verification data set has been increased to an average of 2.82 from 1.31 from the model calibration. It was observed that the validation event errors were slightly higher than those obtained from event calibration. Hydrograph plots revealed that through the error indicators reflected acceptable values, the matching of shape was not encouraging. The hydrograph shape response reflected the need for significant improvement.

5.6 Incorporation of AMC to Check Model Performance

Four popular formulas by Sonhani (1975), Hawkins et al. (1988), Chow et al. (1988) and Neitsch et al. (2002) are used to calculate three different types of AMC, namely AMC I, AMC II and AMC III. The AMC II is the normal condition which is also considered and CN II. The average of optimized CN value is taken as AMC II in this study. The AMC I is the dry condition and AMC III is the wet condition. The calculated AMC using four above formulas are compared.

Neitsch et al. (2002) formula generates very low AMC I value or there is a sudden jump in AMC I compared to other three formulas therefore this particular method to find different AMC types is eliminated. The other three methods generates almost similar results for AMC I and AMC III conditions. In this study Chow et al. (1988) formula is opted to calculate different AMC types to be incorporated in HEC-HMS model performance.

Event 1 falls in Maha season and when AMC III is incorporated, the model performances increases slightly. The NASH value when AMC III was incorporated is 0.88 whereas it was only 0.84 in Event 1 calibration. Similarly the NASH value for Event 3 increases to 0.73 when AMC III condition is applied. To verify, AMC III condition was applied to Event 13, 19 and 20. It has been observed that the model performance increases when AMC III is applied when the events falls in Maha season.

When AMC III and AMC I conditions were applied in Event 5 and Event 17, the model performance neither improve nor deteriorate. The NASH value for Event 5 and Event 17 are 0.241 and 0.924, respectively which is as same as in calibration. These events falls in Yala season. Although there is no significant model improvement when AMC conditions are applied in events that falls in Yala season but there is a slight improvement in total simulated streamflow.

5.7 Summary Discussion

1. Using MIT method, thirty six events were selected from ten years data set. All events are broken down into two parts for calibration and verification of the model. The calibration data set starts from October 2007 to August 2012 and the verification data set starts from January 2013 to September 2017.

2. Some events could not be matched due to absence of peak flow or the rainfall remains constant throughout the event duration.

3. Curve number from the watershed characteristics was used in the loss model initially. However it resulted in poor model performances as CN was found to be the most sensitive parameter. Curve number calculated from field data gives better model performance.

4. In model calibration, the average NASH value and RMS error are 0.63 and 1.31, respectively whereas in model verification, the average NASH value is 0.62 and the average RMS error is 2.82.

5. Neitsch et al. (2002) formula generates very low AMC I value. The other three methods generates almost similar results for AMC I and AMC III conditions. In this study, Chow et al. (1988) formula is opted to calculate three different antecedent moisture conditions.

6. Random events were selected to incorporate different types of antecedent soil moisture. When events fall in Maha season, it has been noticed that the model performances increases when AMC III is applied whereas the model performance neither improves nor deteriorates when events fall in Yala season.

6 CONCLUSIONS

1. Curve numbers differ with storm occasions and it is the most sensitive parameter in precipitation loss model in HEC-HMS. Curve number determined for individual event using asymptotic curve number method gives better model performance then curve number determined from catchment characteristics.

2. The maximum potential retention of the soil is determined and then the initial abstraction for each events are calculated. In model calibration, losses at initial stage of the computed streamflow are observed compared to the observed streamflow due to initial abstraction incorporation in loss model.

3. Nash–Sutcliffe efficiency indicator was used to describe the predictive accuracy with the observed streamflow to compare the model results. The average NASH value in model calibration was 0.63 while the average NASH value in model verification was 0.62. The closer the model efficiency is to 1, the more accurate the model is. The aforementioned NASH value indicates a model of sufficient quality.

4. The average RMS error in model calibration was 1.3 whereas the average RMS error in model verification was 2.8. RMSE is used to check the absolute measure of fit and for good predictive model, RMSE values should be low. The RMSE value in model calibration has better fit compared to the RMSE value in model verification.

5. Three events from calibration and two events from verification data set failed to match or fit with the observed streamflow as the streamflow throughout the event remains constant without a single rainfall peak event.

6. The average soil moisture condition (AMC II or CN II) is generally used in hydrological modelling but the status of soil moisture plays a major role in the hydrological behaviour of a catchment, particularly for flood modelling. The curve number varies depending on the antecedent moisture condition of the soil. The use of AMC III (wet soil condition) increases the curve number and shows improvement in HEC-HMS model performance when the events fall in Mmaha season.

7. When AMC III is incorporated in Event 1, model performances increases by generating a NASH value of 0.88 where by it was 0.84 in Event 1 calibration. Similarly, the NASH value for Event 3 increases to 0.73 when AMC III condition was applied. To verify, AMC III condition was applied to Event 13, 19 and 20. It has been observed that the model performance increases when AMC III is applied when the events falls in Maha season.

8. When AMC I and AMC III are incorporated in events that falls in yala season (event 5 and event 17), the model performance neither improve nor deteriorate. The NASH value for Event 5 and event 17 are 0.241 and 0.924, respectively, which is the same as in model calibration.

9. Considering the results from the event based HEC-HMS modelling for Kelani river basin, it is suggested to incorporate antecedent moisture condition while determine curve number or take antecedent moisture condition into account while doing flood modelling in order to improve the model performance. This will help in recommending sustainable solutions for better flood management.

7 RECOMMENDATIONS

1. There are uncertainties in deriving curve number from the watershed characteristic such as land use and soil type, it is recommended to use the latest land use and soil type map from the reliable source.

2. Curve number is the most sensitive parameter in loss model in HEC-HMS therefore it is recommended to use many method to derive Curve Number and then compare to use the best one that gives the good fit between the observed and the simulated streamflow.

3. A data of finer resolution such as hourly or 6 hourly data is advised to use while performing event modelling in order to get best model performance.

4. A catchment that falls under small category is advised to use while modelling in HEC-HMS using SCS-CN method as the size of catchment affects the model performance.

5. Antecedent moisture conditions are recommended to take into account for event based modelling in order to improve model performances and give effective solutions for better flood management.

8 REFERENCES

Akhondi, E. (2001). Analyzing curve number model in estimating flood by using geographical information systems. *MA dissertation*. (T.-e.-M. U. The Faculty of Natural Resources and Maritime Sciences, Compiler)

Alaghamand, S., Abdullah, R. B., & Abustan, I. (2010). Selecting the best set value in calibration process for validation of hydrological modeling: A case study on Kayu Ara river basin, Malaysia.

Alahacoon, N., Pani, P., Matheswaran, K., Samansiri, S., & Amarnath, G. (2016). Rapid Emergency Response Mapping for the 2016 floods in Kelani River Basin, Sri Lanka . *International Eater management Institute (IWMI)*. Battaramulla, Sri Lanka.

Arduino, G., Reggiani, P., & Todini, E. (2005). Recent advances in floodforecasting and flood risk assessment. *Hydrology and Earth Sciences*, 115–123.doi:10.1061/(ASCE)1084-0699(2000)5:2(115).

Asadi, A., & Boostani, F. (2013, September). Application of HEC-HMS for Flood Forecasting in Kabkian Basin and Delibajak Sub-basin in Iran. *IOSR Journal of Engineering (IOSRJEN)*, e-ISSN: 2250-3021, p-ISSN: 2278-8719.

Benedini, M., & Tsakiris, G. (2013). Model Calibration and Verification. In: Water Quality Modelling for Rivers and Streams. *Springer*, 223-229.

Bogardi, J. (2004). *The news letter of the United Nations University and its international network of research and training centers/programmes*. Retrieved from https://www.researchgate.net/deref/http%3A%2F%2Fupdate.unu.edu%2Farchive%2Fissue32.htm

Brocca, L., Melone, F., & Moramarco, T. (2004). Soil water content monitoring in an experimental basin in central Italy, Proceedingsof International Conference ERB2004. *Euromediterranean Conference*, (pp. 18 - 21). Torino.

Brocca, L., Melone, F., & Moramarco, T. (2005). *Empirical and conceptual approaces for soil moisture estimation in view of event-based rainfall-runoff modeling.* UNESCO: Paris: Edited by: Maraga, F and Arattano, M., IHP-VI, Technical Documents in Hydrology, No. 77.

Central Environment Authority (CEA), International Union for the Conservation of Nature (IUCN) Sri Lanka office country and United Nations Children's Fund (UNICEF). (2016). *Natural resources Profile of the Kelani river basin*. Retrieved from file:///E:/MSc%20Sri%20Lanka/MSc/RESEARCH/LITERATURE/About%20K%20Basin/03_Natural_Resource_Profile_of_the_Kelani_River_Basin.pdf

Chow, V. T., Maidment, D. R., & Mays, L. w. (1988). *Applied Hydrology.* McGraw Hill, 572p.

Chow, V. T., Maidment, D. R., & Mays, L. W. (2010). *Applied Hydrology.* New Delhi, India: Tata MacGraw Hill.

Cunderlik, J., & Simonovic, S. P. (2004). *Calibration, verification and sensitivity analysis of the HEC-HMS hydrologic model.* CFCAS project: Assessment of Water Resources Risk and Vulnerability to Changing Climatic Conditions.

Daly, E., & Porporato, A. (2005). A Review of Soil Moisture Dynamics: From RainfallInfiltration to Ecosystem Response. *ENVIRONMENTAL ENGINEERING SCIENCE, 22*, 1.

Davis, C. (2000). *USACE, HEC-HMS hydrologic modeling system user's manual.* Hydrologic Engineering Center.

De Silva, M. G., Weerakoon, S. B., & Herath, S. (2014). Modeling of Event and Continuous Flow Hrdrographs with HEC-HMS: Case Study in the Kelani River Basin, Sri Lanka. *Journal of Hydrologic Engineering*, 800 - 806. doi:10.1061/(ASCE)HE.1943-5584.0000846

Devi, G. K., Ganasri, B. P., & Dwarakish, G. S. (2015). A review on hydrological models. *ELSEVIER*, 1001-1007.

Diskin, M. H., & Simon, E. (1977). The procedure for selection of objective functions for hydrologic simulation models. *Journal of Hydrology, 34(1),* 129-149.

Feldman, D. A. (2000). *Hydrologic Modeling System HEC-HMS Technical Reference Manual.* Davis, CA: USACE.

Giang, N. T., & Phuong, T. A. (2010). Calibration and verification of a hydrological model using event data. *Journal of Science, Earth Sciences, (26),* 64-74.

Gupta, P. P., S, P., S, S., & Parihar, J. S. (2012). Runoff Modeling in an Agro-Forested Watershed Using Remote Sensing and GIS. *Journal of Hydrologic Engineering*, 1255-1267.

Gyathri, K. D., Ganasri, B. P., & Dwarakish, G. S. (2015). A Review on Hydrological Models. *International Conference on Water Resources, Coastal and Ocean Engineering (ICWRCOW 2015)* (p. 1002). Karnataka, India: Department of Applied Mechanics and Hydraulics, National Institute of Technology.

Halwatura, D., & Najim, M. M. (2013). Application of the HEC-HMS model for runoff simulation in a tropical catchment . *Environmental Modelling and Software*, 155-162.

Hawkins, R. H. (1993). Asymptotic determination of curve numbers from data. *journal of Irrigation and Drainage Division- ASCE, 119(2)*, 334-345.

Hawkins, R. H., Hjelmfelt, J. T., & Zevenbergen, A. W. (1985). Runoff probability, storm depth and curve numbers. *Journal of Irrigation and Drainage Division*, 330-340.

International Centre for Water Hazard and Risk Managemnet (ICHARM) Report. (2009). *Gobal trends in water related disasters: an insight for policymakers.* Sukuba, Japan: International Cetre for Water Hazard and Risk Management (UNESCO). Retrieved from https://www.researchgate.net/deref/http%3A%2F%2Fwww.icharm.pwri.go.jp

Jain, M. K., Mishra, S. K., & Singh, V. P. (2006). Evaluation of AMC dependent SCS - CN based models using watershed characteristics. *Journal of Water Resources Management, 20(4)*, 531-555.

Jain, S. K., Mani, P., Jain, S. K., Prakash, P., Singh, V. P., & Tullos, D. (2018). A Brief review of flood forecasting techniques and their applications. *Taylor & Francis*. Retrieved from https://doi.org/10.1080/15715124.2017.1411920

JICA. (2017). *Data collection survey on disater risk reduction sector in Sri Lanka.* Earth System Science Co., Ltd & CTI Engineering International Co., Ltd.

Kabiri, R., Chan, A., & Ramani, B. (2013). Comparison of SCS and Green-Ampt Methods in Surface Runoff-Flooding Simulation for Klang Watershed in Malaysia. *Open Journal of Modern Hydrology, 3*, 102-114.

Kumar, A., & Rajput, P. S. (2013). Assessment of hydro-environmental loss as surface runoff using CN method of Pahuj River Basin Datia, India. *Proceedings of the International Academy of Ecology and Environmental Sciences, 3(4)*, 324-329.

Kumar, S. S., Venkateswaran, S., & Kannan, R. (2017, April). Rainfall–runoff estimation using SCS–CN and GIS approach in the Pappiredipatti watershed of the Vaniyar sub basin, South India. *Modeling Earth Systems and Environment, 3*, 1.

Li, Z.-J. (2010). Application of HEC-HMS for flood forcasting in Misai and Wan'an catchments in China. *Water Journal*, 14-22. doi:10.3882/j

Linsley, R. K. (1982). Rainfall-runoff models- an overview. *Proceedingd of the International Symposium on Rainfall-Runoff Modelling* (pp. 3-22). Water Resources Publications .

Linsley, R. K., Kohler, M. A., & Paulhus, J. H. (1975). *Hydrology for Engineers*.

Manchanayake, P., Sumanaweera, S., & Jayaratne, J. A. (1985). Preliminary Studies on Loss Rate of Few Sri Lankan Catchments . *Engineers, vol(XIII), No.02,* 7-12.

Mata, L. (2011). Evaluation of the objective functions to improve production histroy matching performance based on fluid flow behaviour in reservoirs. *Journal of Petroleum Science and Engineering, 78(1),* 42-53.

Merwade, V. (2016, October). HEC HMS: Model Calibration. Indiana, US: Purde University.

Ministry of Disaster Mangement, Sri Lanka. (2016). Retrieved from http://www.disastermin.gov.lk/web/

Mishra, K. S., & Singh, V. P. (1999). Another Look at SCS-CN Method. *Journal of Hudrologic Engineering,* Volume 4 issue 3.

Mishra, S. K., & Singh, V. P. (1999). Another look at SCS-CN method. *Journal of Hydrologic Engineering, ASCE, 4(3),* 257 - 264.

Mishra, S. K., & Singh, V. P. (2003). *Soil Conservation Service (SCS-CN) Methodology.* Baton Rouge, USA: Kluwer Academic Publisers.

Mishra, S. K., Babu, P. S., Venugopal, K., & Kaliappan, S. (2008). *Comparison of AMC - dependent CN - conversion Formulae.* Water Resources Management, 22(10), 1409 - 1420. DOI: 10.1007/s11269-007-9233-5.

Mishra, S. K., Jain, M. K., & Singh, V. P. (2004). Evaluation of the SCS-CN-Based Model Incorporating Antecedent Moisture. *Water Resources Management,* 567-589.

Mishra, S. K., Sahu, R. K., & Jain, M. K. (2006). An improved Ia - S Relation Incorporating Antecedent Moisture in SCS - CN Methodology. *Springer*, Water Resources Management 20: 634 - 660.

Mockus, V., McKeever, V., Owen, W., & Rallison, R. (1972). *National Engineering Handbook.*

Moore, R. J., Bell, V. A., & Jones, D. A. (2005). Forecasting for floodwarning. *Comptes Rendus Geosciences, 337 (1),* 203–217. doi:10.1016/j.crte.2004.10.017.

Nandalal, H. K., & Ratnayake, U. R. (2010). Event based modeling of a watershed using HEC-HMS. *Engineers, 43(2),* 271-279.

Nash, J. E., & Sutcliffe, J. V. (1970). River flow forcasting through conceptual models part I- A discussion of principles. *Journal of Hydrology, 10(3),* 282-290.

Neitsch, S. L., Arnold, J. G., Kiniry, J. R., Williams, J. R., & King, K. W. (2002). *Soil and Water Assessment Tool (SWAT): theoretical documentation.* Texas: Water Resources Institude, Sollege Station.

Nelder, J. A., & Mead, R. (1965). A simplex method for function minimization. *Computer Journal*, 308-313.

Nockus, V. (1965). *National engineering Handbook.*

Patry, G. G., & Marino, M. A. (1983). Nonlinear runoff modelling: parameter identification. *ASCE*, 865-880.

Ponce, V. M., & Hawkins, R. H. (1996). Runoff curve number: Has it reached maturity? *Journal of Hydrologic Engineering- ASCE 1(1)*, 11-19.

Ray, K. (1975). Hydrology for Engineers. *McGraw Hill Kogakusha*.

Razi, M. M., Ariffin, J., Tahir, W., & Arish, N. M. (2010). Flood Estimation Studies using Hydrologic Modeling System (HEC-HMS) for Johor River, Malaysia. *Journal of Applied Sciences, Volume 10 (11): 930-939, 2010*, 930-939. doi:DOI: 10.3923/jas.2010.930.939

Reshma, T. K., P, S. B., M.J, R., & Kumar, K. S. (2010). Simulation of Runoff in Watersheds using SCS-CN AND Muskinggum-Cunge Methods using Remote Sensing and Geographical Information Systems. *International Journal of Advanced Science and Technology*, 31-42.

Sardoii, R. E., Rostami, N., Sigaroudi, K. S., & Taheri, S. (2012). Calibration of loss estimation methods in HEC-HMS for simulation of surface runoff (Case Study: Amirkabir Dam Watershed, Iran) . *Advances in Environmental Biology*, 6(1): 343-348.

Simon, P. N., & Hashemi, M. R. (2018). Ocean Modelling for Resource Characterization. *Science Direct*.

Singh, V. P. (1989). Hydrologic Systems: Volume 2-Watershed modeling. *Pretice hall*.

Singh, V. P., & Frevert, D. K. (2002). *Mathematical Models for Small Watershed Hydrology and Applications.* Denver, Colorado, USA: Water Resources Publication, LLC.

Singh, V. P., & Frevert, D. K. (2006). Watershed Models. *CRC Press*.

Skahill, B. E. (2006). *Potential Improvements for HEC-HMS Automated Parameter Estimation* . Washington, DC: US Army Corps of Engineers, Enginner Research and development Center.

Sobhani, G. (1975). A review of selected small watersged design methods for possible adoption to Iranian conditions. *(unpublished mater's thesis)*. Utah State University, Logan, UT.

Soil Conservation Service . (1986). *Urban hydrology for small watersheds.* Washington D.C, United States : Department of Agriculture.

Sorooshian, S., & Moradkhani, H. (2008). *General review of rainfall-runoff modeling: model calibration, data assimilation, and uncertainty analysis. Hydrological modeling and the water cycle.* Springer. 291 p. ISBN 978-3-540-77842-4.

Soulis, K. X., Valiantzas, J. D., Dercas, N., & Londra, P. A. (2009). Analysis of the runoff generation mechanism for the investigation of the SCS-CN method applicability to a partial area experimental watershed. *Hydrology and Earth System Sciences Discussion*, 373-400.

Sudheer, K. P., Chaubey, I., Garg, V., & Migliaccio, K. W. (2006). Impact of time scale of the calibration objective function on the performance of watershed models. *Journal of Hydrological Processes*. doi:10.1002/hyp.6555

Survey Department of Sri Lanka. (2007). *Sri Lanka Survey Department*. Retrieved from https://www.survey.gov.lk/sdweb/home.php

Swanidass, P. M. (2000). Encyclopedia of Production and Manufacturing Management. *Springer*. doi:https://doi.org/10.1007/1-4020-0612-8

Tedela, N. M., S, C. R., T, C. H., R, H. S., Campbell, J. A., M, B. J., . . . Tollner, E. W. (2012). Runoff Curve Numbers for 10 Small Forested Watersheds in the Mountains of the Eastern United States. *Journal of Hydrologic Engineering, 17(11)*, 1188-1198.

Thiessen, A. H., & Alter, J. C. (1911). Climatological data for July, 1911: District No. 10, Great Basin. *Monthly weather review*, 1082-1089.

United States Army Corps of Engineers (USACE). (1998). *Hydrologic Modeling System HEC-HMS User's Manual.* U.S Army Corps of Engineers, Hydrologic Engineering Center. Retrieved from https://www.hec.usace.army.mil/software/hec-hms/documentation/HEC-HMS_Users_Manual_4.0.pdf

United States Army Corps of Engineers, Hydrologic Enginnering centre (USACE), technical Reference Manual. (2000). Davis, California: USACE.

USACE. (1992). *US Army Corps of Engineers*. Retrieved from Hydrologic Engineering Centre: https://www.hec.usace.army.mil

Vogel, R. M., Yaindl, C., & Walter, M. (2011). Nonstationarity: floodmagnification and recurrence reduction factors in the UnitedStates. *Journal of the American Water Resources Association, 47 (3)*, 464–474.

Walker, J. P., Wang, Q. J., Robertson, D. E., & Shahrban, M. (2018). On the importance of soil moisture in calibration of the rainfall-runoff models: tw case studies. *Hydrological Sciences Journal*, 1292 - 1312.

Western, A. W., Bloschl, G., & Grayson, R. B. (1998). The Tarrawarra data set: soil moisture patterns, soil characteristics, and hydrology flux measurements. *Water Resour. Res., 34*, 2765 - 2768.

Wheater, H., Sorooshian, S., & Sharma, K. D. (2007). *Hydrological Modelling in Arid and Semi-Arid Area*. New York: Cambridge University Press.

Wijesekera, N. S., & Ghnanapala, P. P. (2003). *Modelling of two low lying urban watersheds in the greater Colombo area for drainage and environment improvement*. Retrieved from http://dl.lib.mrt.ac.lk/handle/123/8582

Wijesekera, N. S., & Perera, K. J. (2010). Potential on the Use of GIS Watershed Modeling for River Basin Planning _ Case Study of Attanagalu Oya Basin, Sri Lanka. *ENGINEER*, 13-22.

Wijesekera, N. S., & Perera, L. H. (2012). Key issues of data and data checking for hydrological analysis- case study of rainfall data in the Attanagalu Oya basin of Sri Lanka. *Journal of the institude of engineers*, 1-12.

WMO. (September 2011). Workshop on Intercomparison of Flood Forecasting Models., (pp. 14 - 16). Koblenz, Germany.

Yu, B. (1998). Theoretical justification of SCS method for runoff estimation. *Journal of Irrigation and Drainage Engineering, 17(11)*, 234-238.

Zeiger, S., & Hubbart, J. (2017). An assessment of mean areal precipitation menthods on simulated stream flow: A SWAT model performance assessment). *Water*. doi:10.3390/w9070459

Zhang, Y., Wei, H., & Nearing, M. A. (2011). Effect of antecedent soil moisture on runoff modeling in small semiarid watersheds of southeastern Arizona. *Hydrology and Earth System Sciences*, 3172 - 3179.

APPENDIX A: STREAMFLOW RESPONSE WITH RAINFALL FOR INDIVIDUAL GAUGING STATIONS

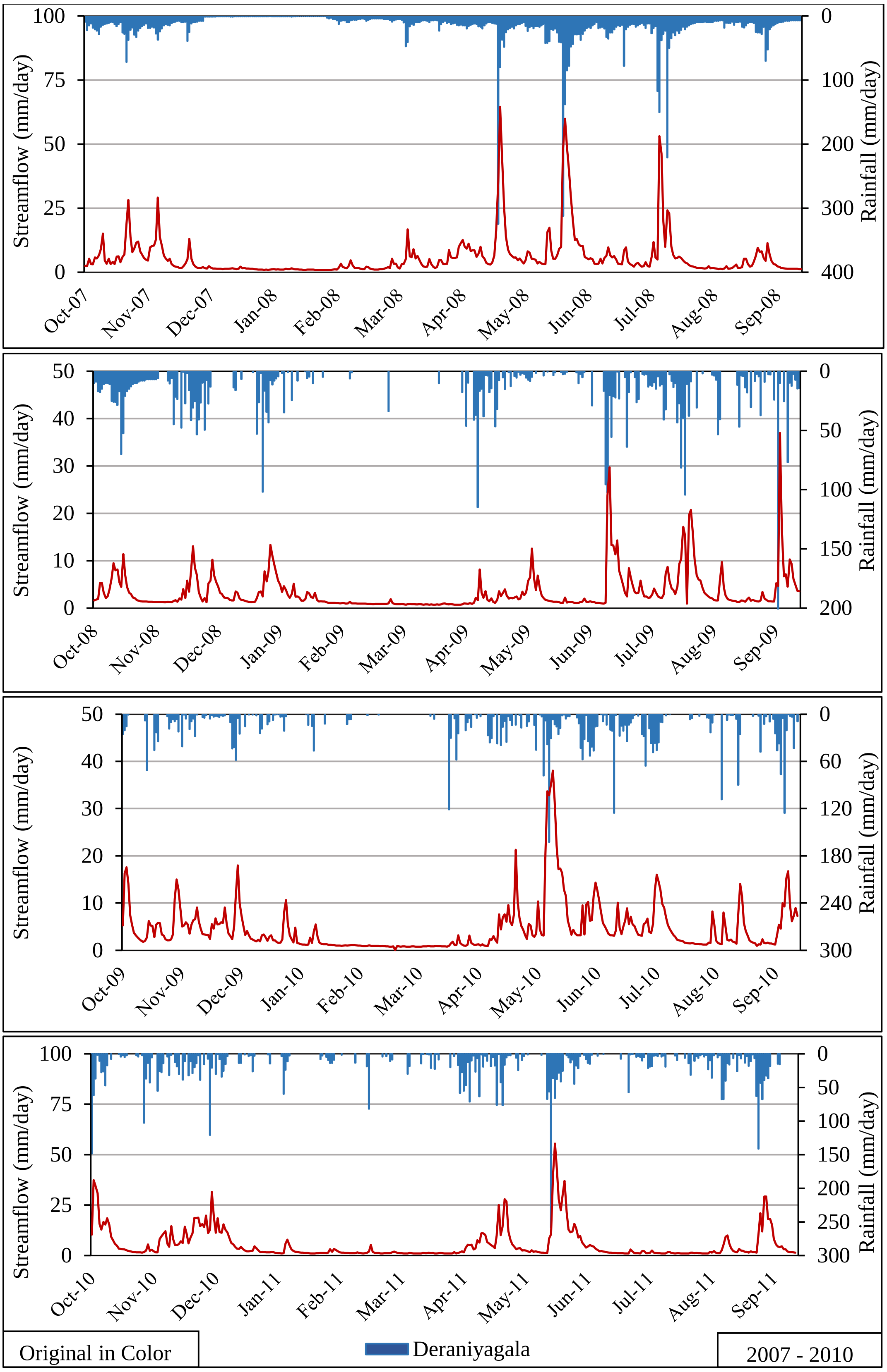

Figure A - 1 Streamflow with response to Rainfall for Deraniyagala Station for the Water Year 2007-2010 in Normal Hydrograph

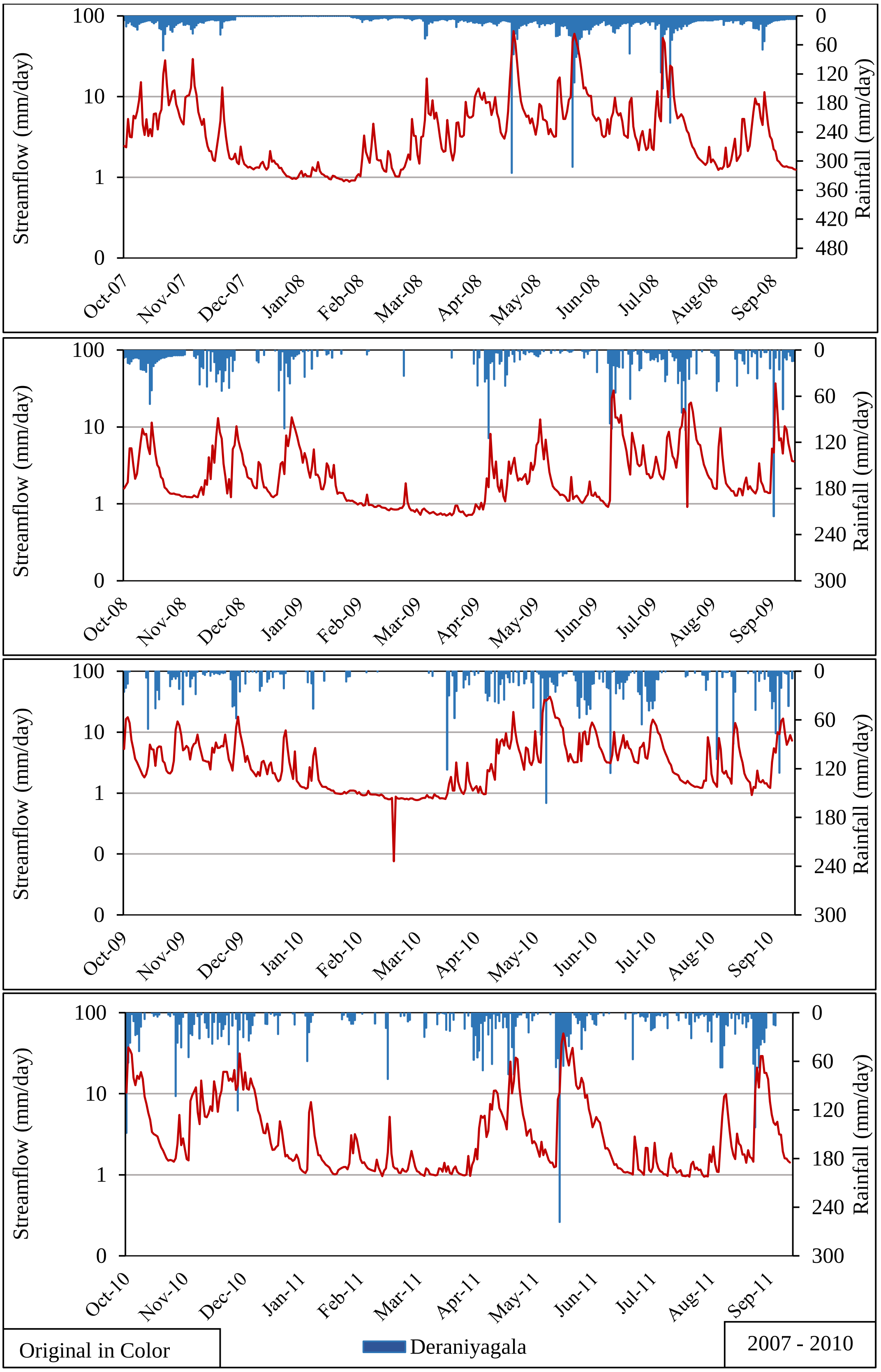

Figure A - 2 Streamflow with response to Rainfall for Deraniyagala Station for the Water Year 2007-2010 in Semi-log Hydrograph

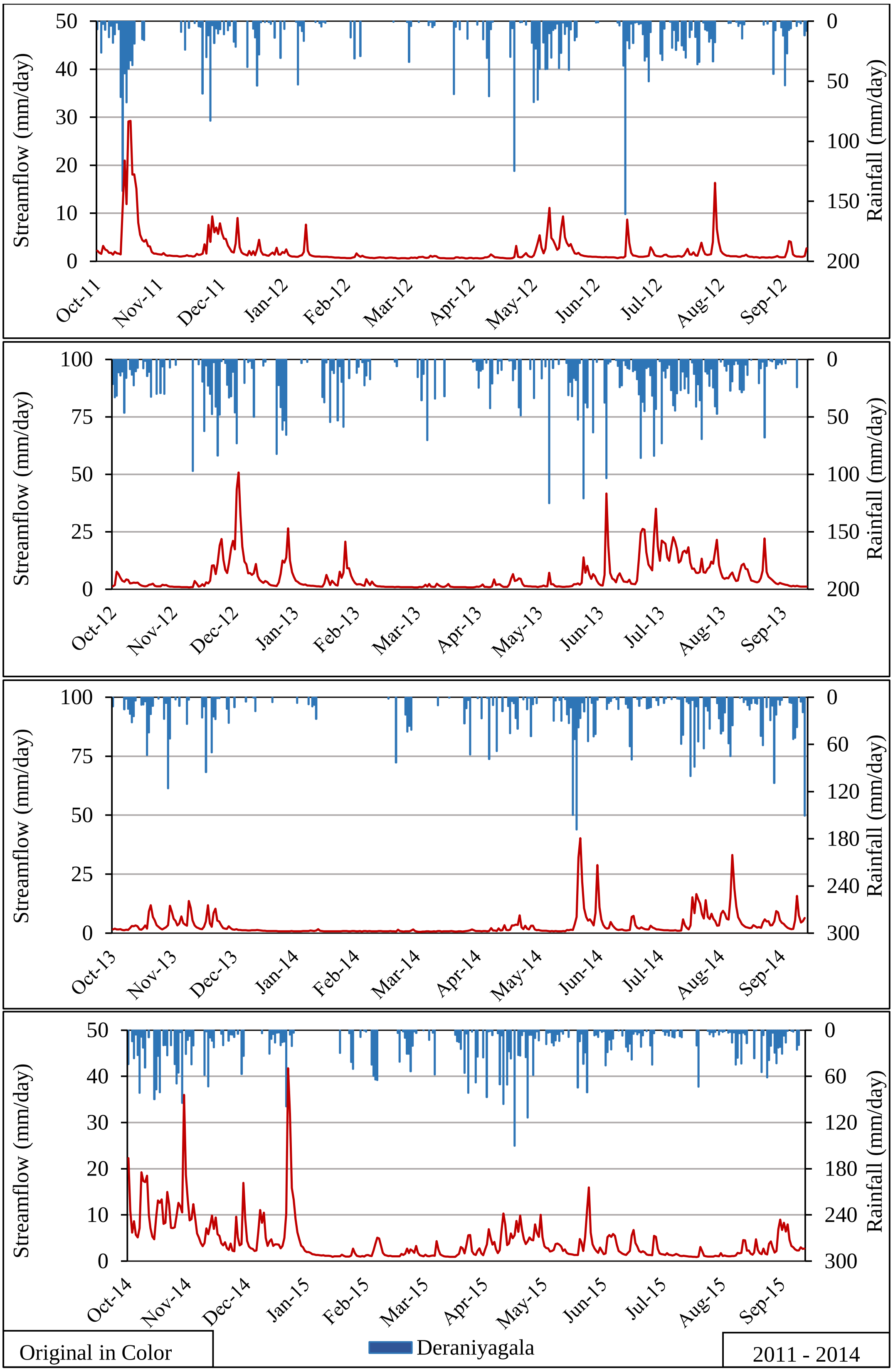

Figure A - 3 Streamflow with response to Rainfall for Deraniyagala Station for the Water Year 2011-2014 in Normal Hydrograph

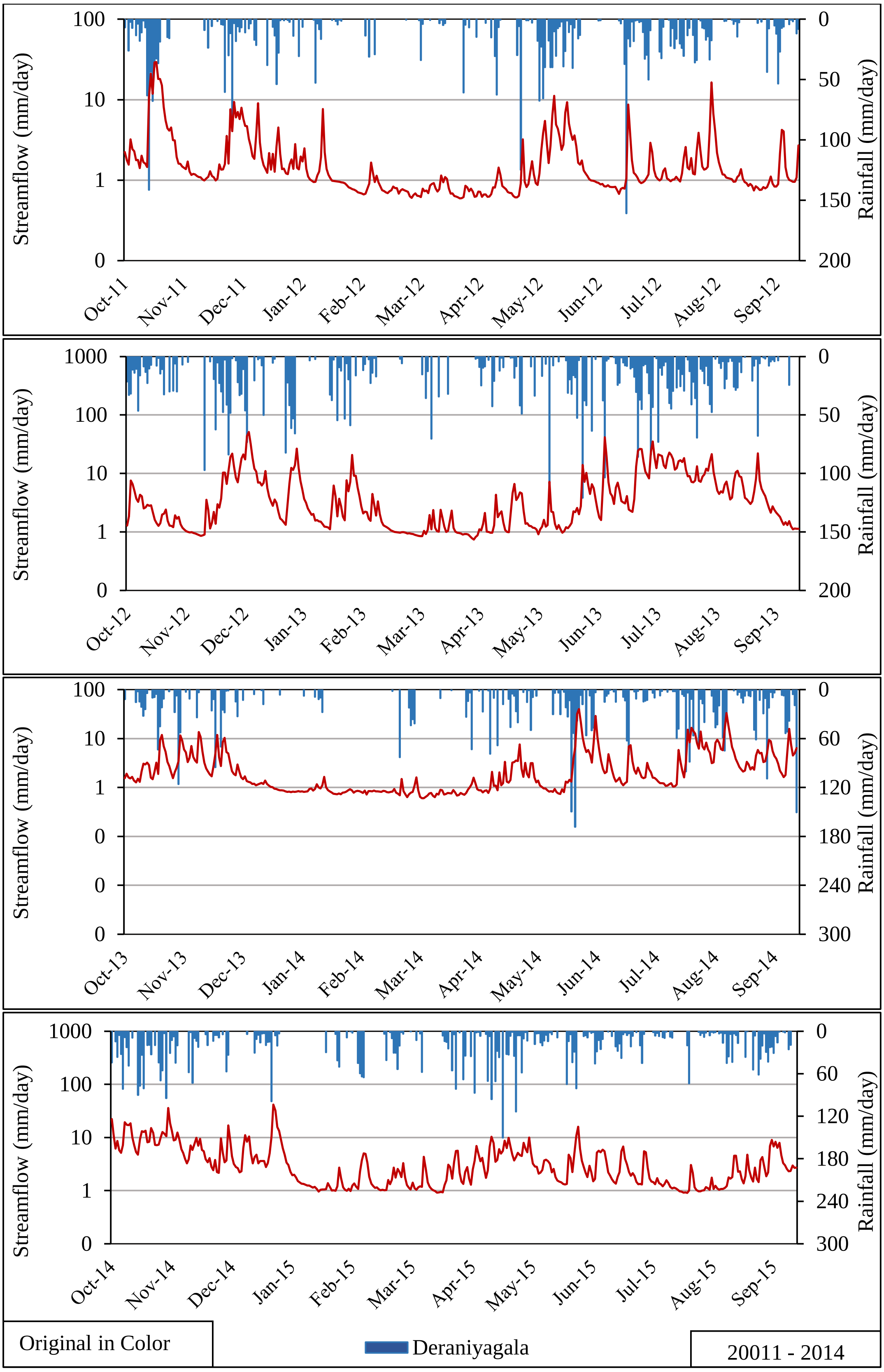

Figure A - 4 Streamflow with response to Rainfall for Deraniyagala Station for the Water Year 2011-2014 in Semi-log Hydrograph

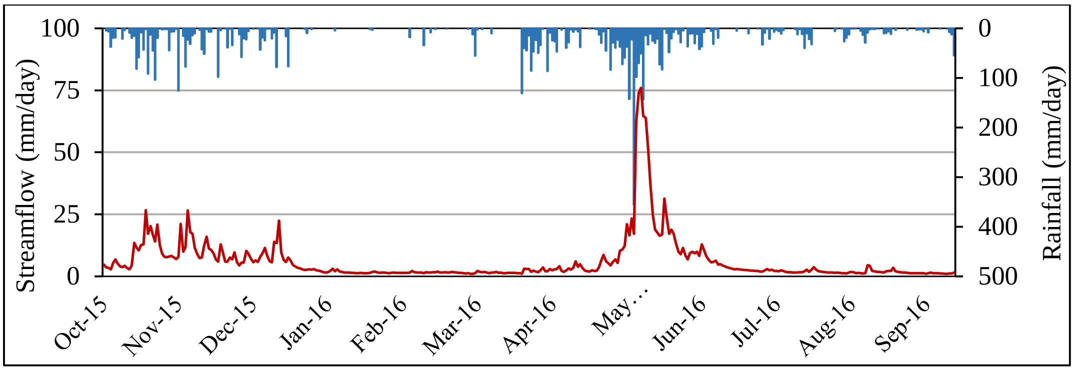

Figure A - 5 Streamflow with response to Rainfall for Deraniyagala Station for the Water Year 2015 - 2016 in Normal Hydrograph

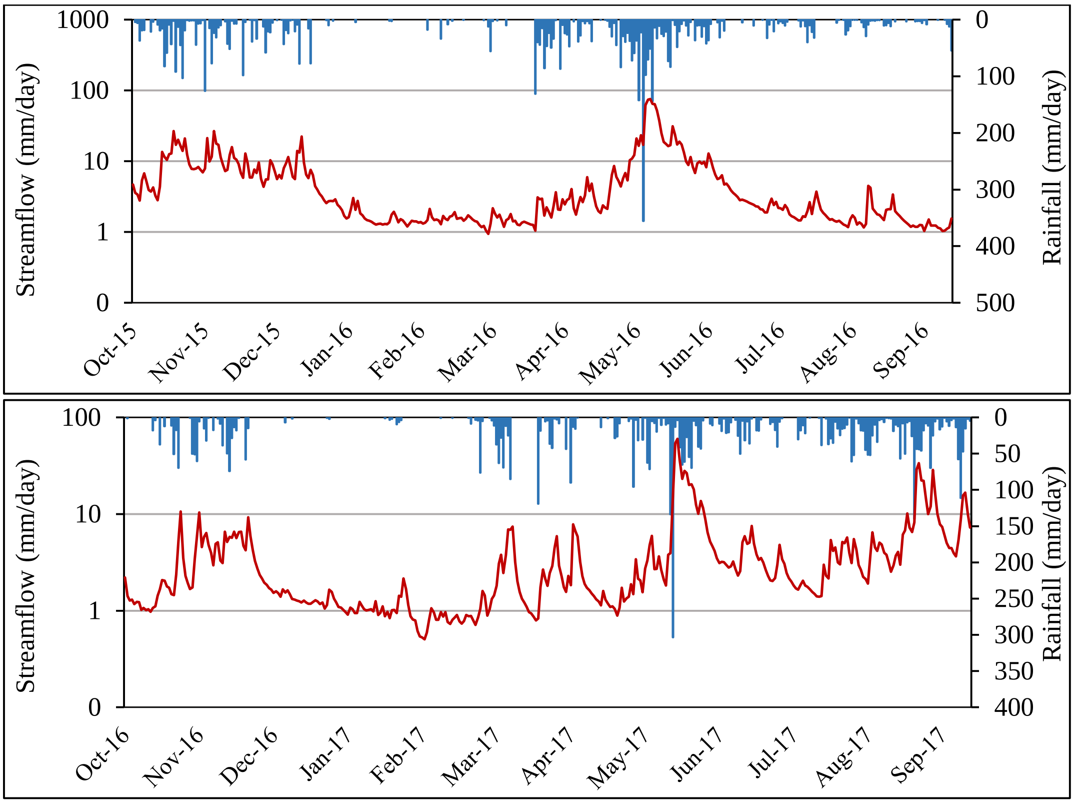

Figure A - 6 Streamflow with response to Rainfall for Deraniyagala Station for the Water Year 2015-2017 in Semi-log Hydrograph

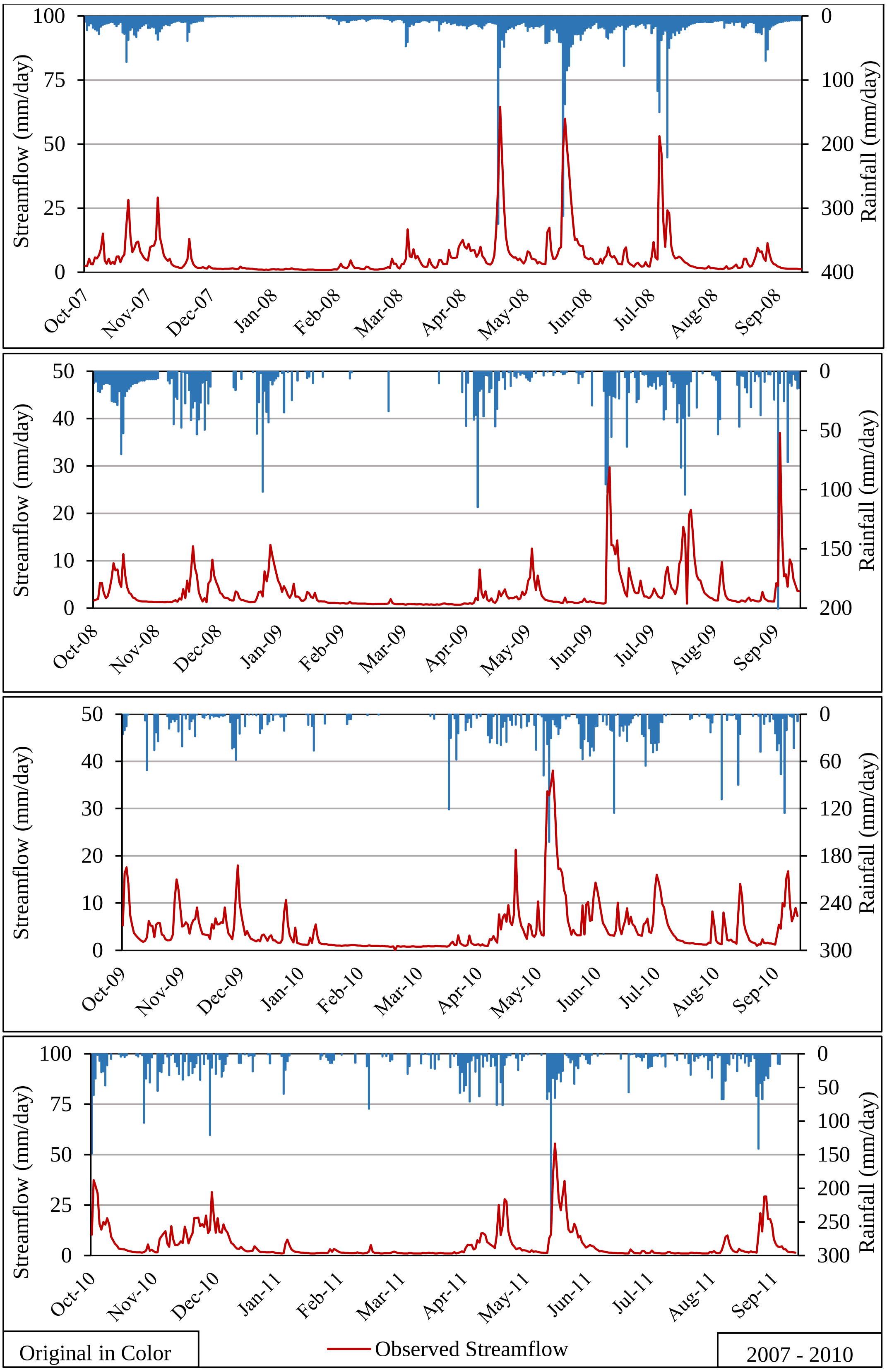

Figure A - 7 Streamflow with response to Rainfall for Norwood Station for the Water Year 2007-2010 in Normal Hydrograph

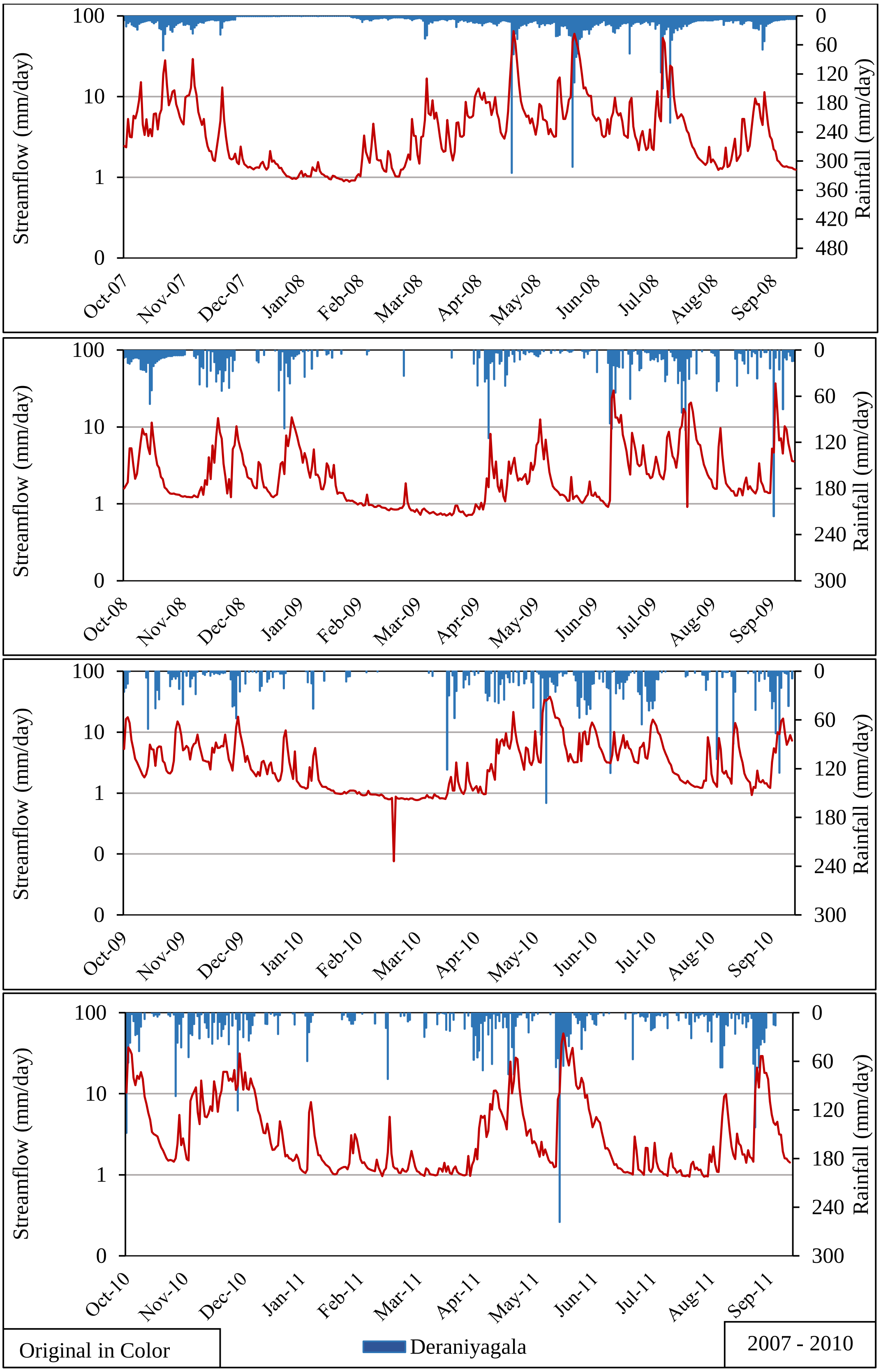

Figure A - 8 Streamflow with response to Rainfall for Norwood Station for the Water Year 2007-2010 in Semi-log Hydrograph

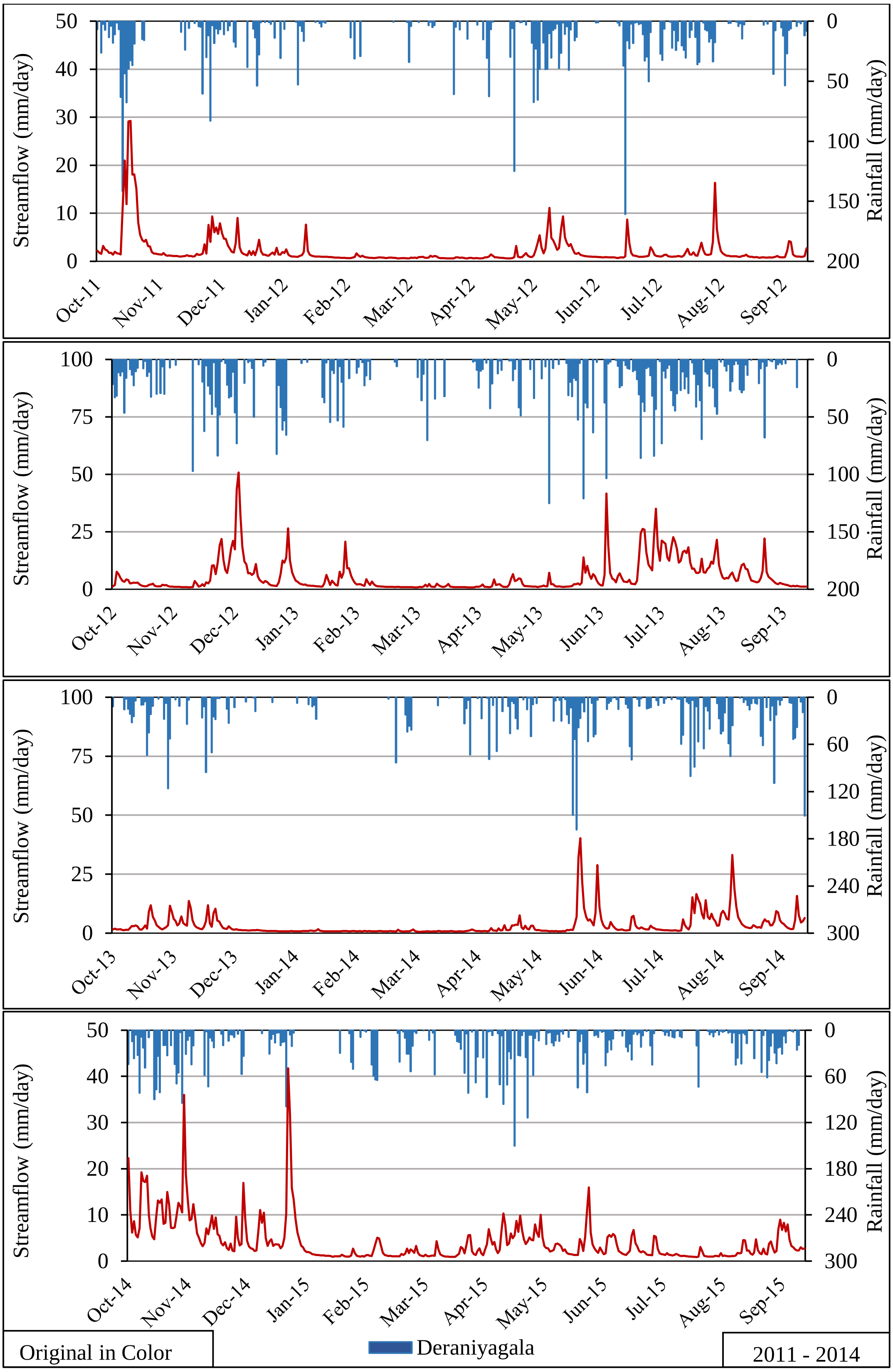

Figure A - 9 Streamflow with response to Rainfall for Norwood Station for the Water Year 20011-2015 in Normal Hydrograph

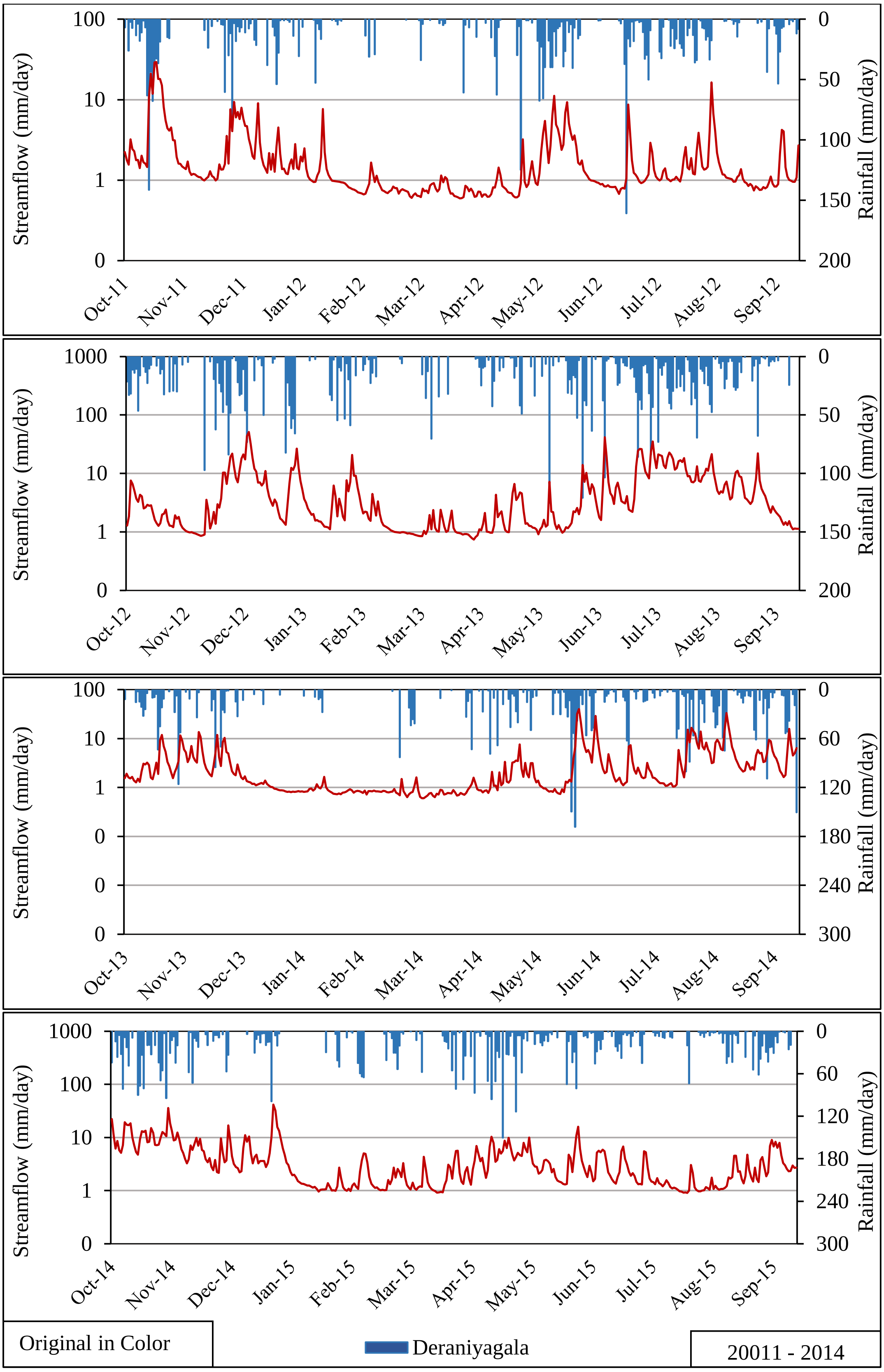

Figure A - 10 Streamflow with response to Rainfall for Norwood Station for the Water Year 2011-2015 in Semi-log Hydrograph

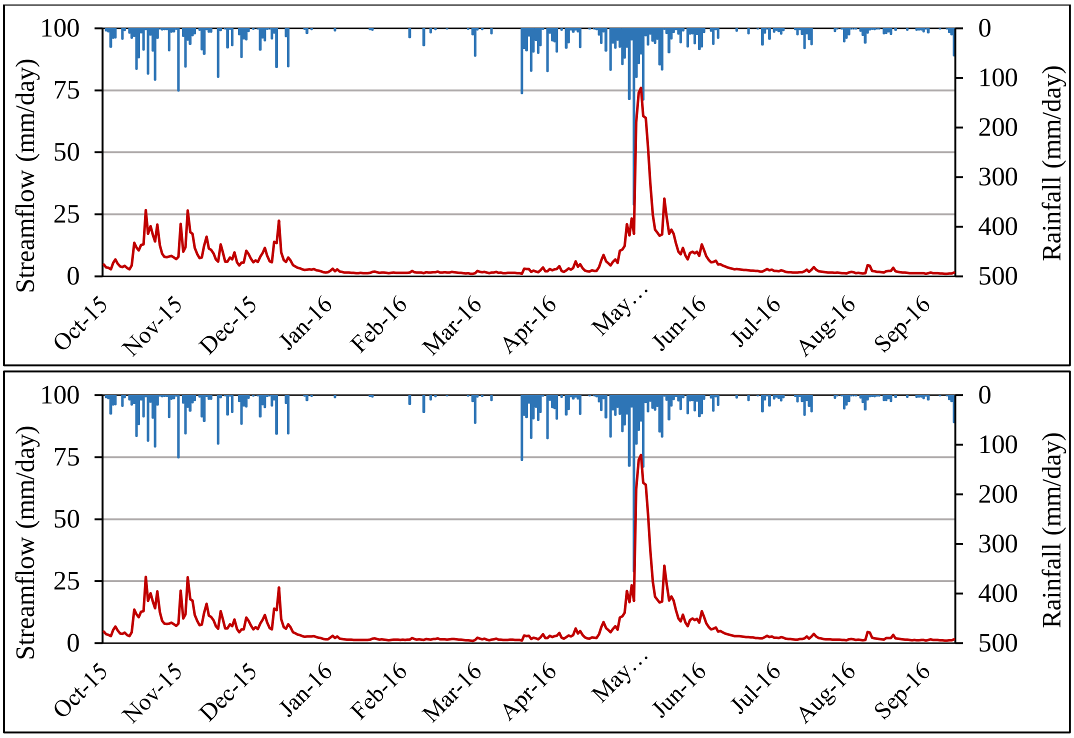

Figure A - 11 Streamflow with response to Rainfall for Norwood Station for the Water Year 2015 - 2017 in Normal Hydrograph

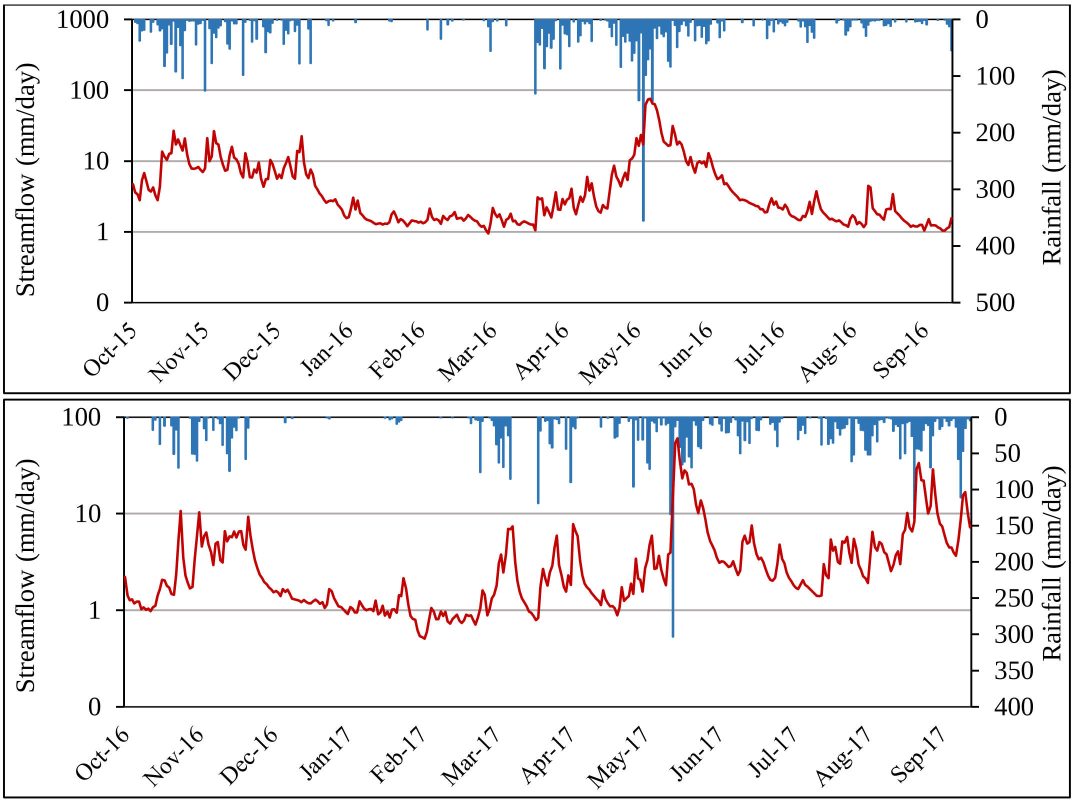

Figure A - 12 Streamflow with response to Rainfall for Norwood Station for the Water Year 2015-2017 in Semi-log Hydrograph

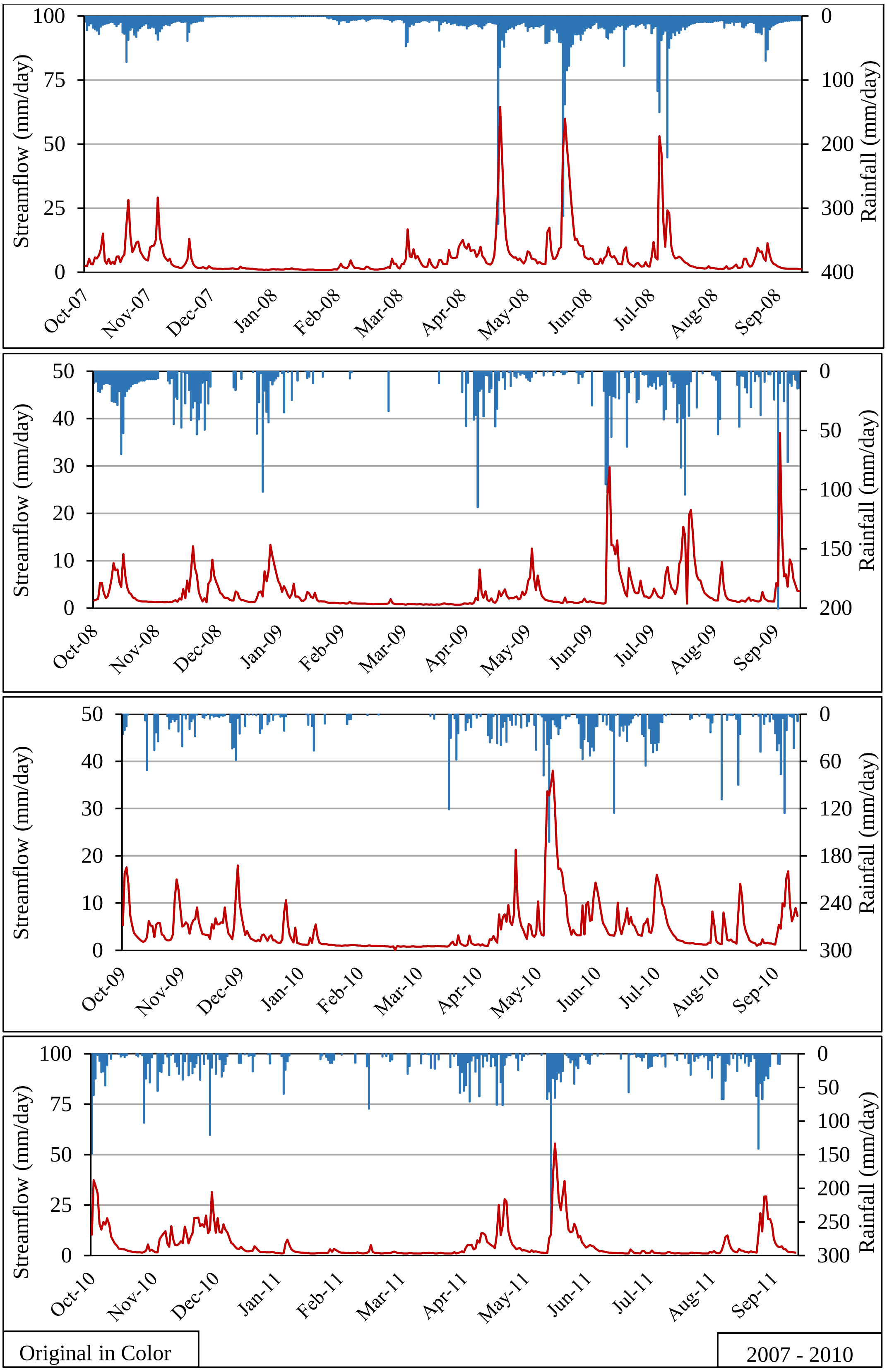

Figure A - 13 Streamflow with response to Rainfall for Kitulgala Station for the Water Year 2007-2010 in Normal Hydrograph

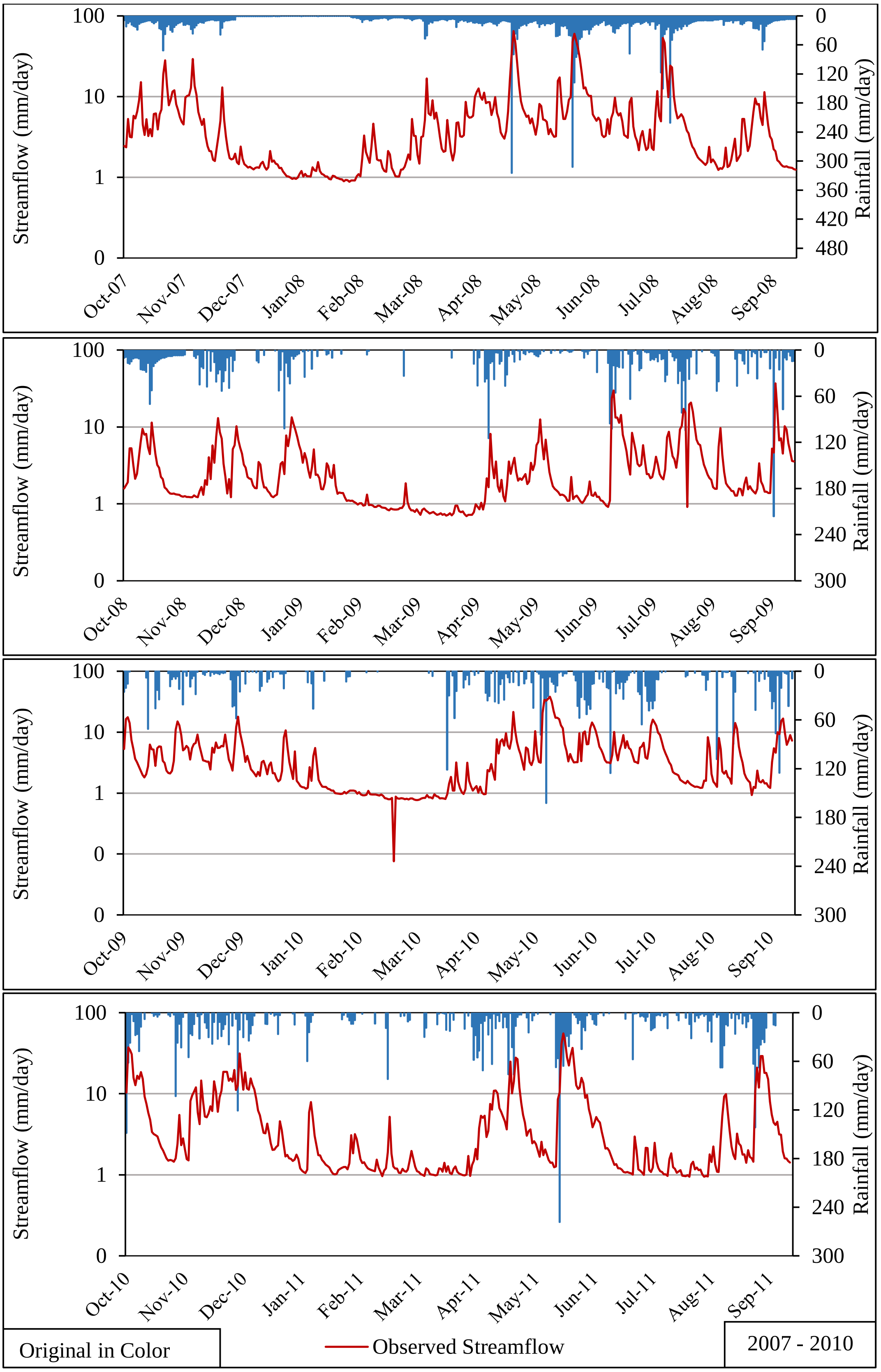

Figure A - 14 Streamflow with response to Rainfall for Kitulgala Station for the Water Year 2007-2010 in Semi-log Hydrograph

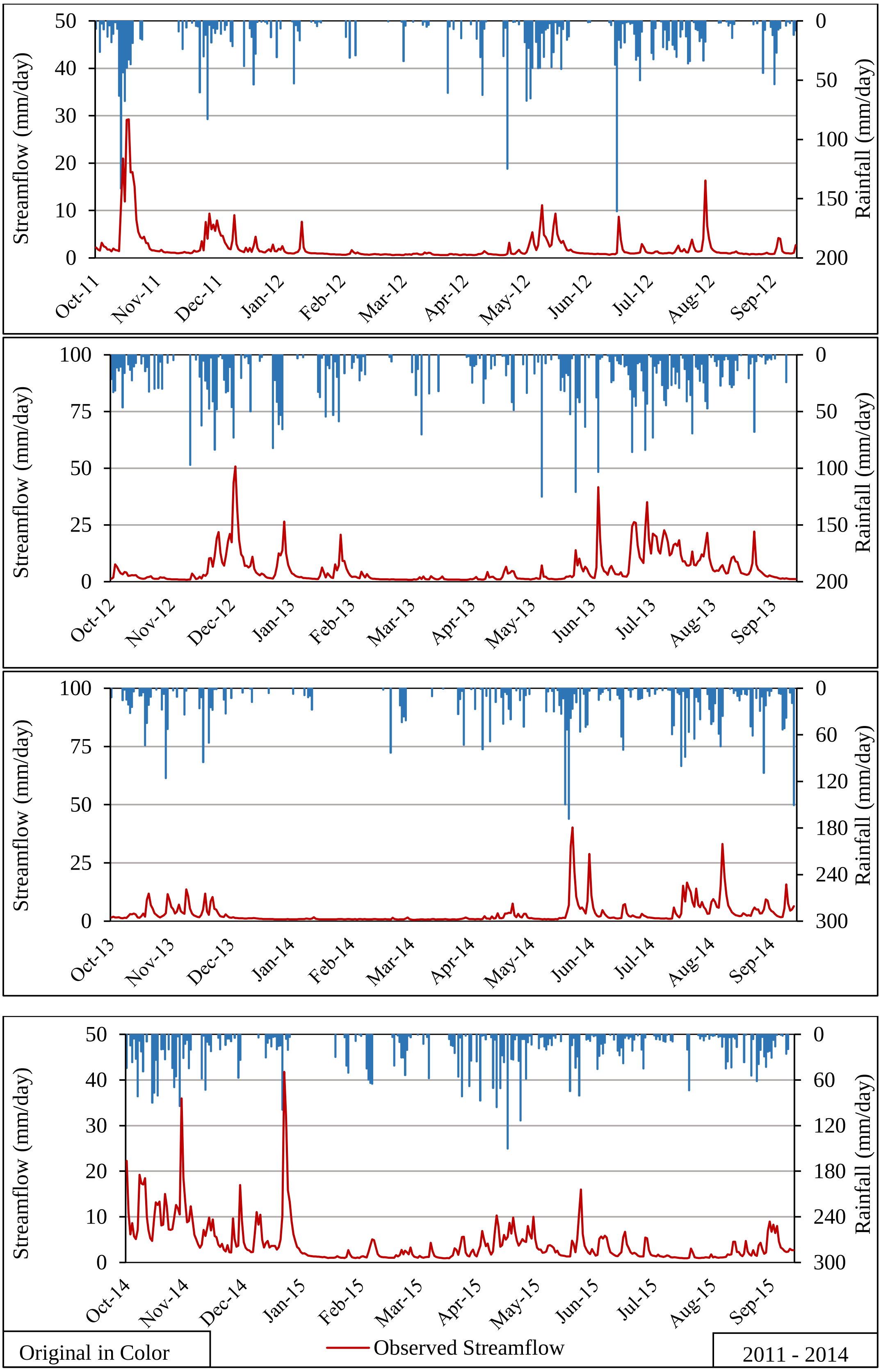

Figure A - 15 Streamflow with response to Rainfall for Kitulgala Station for the Water Year 2011-2014 in Normal Hydrograph

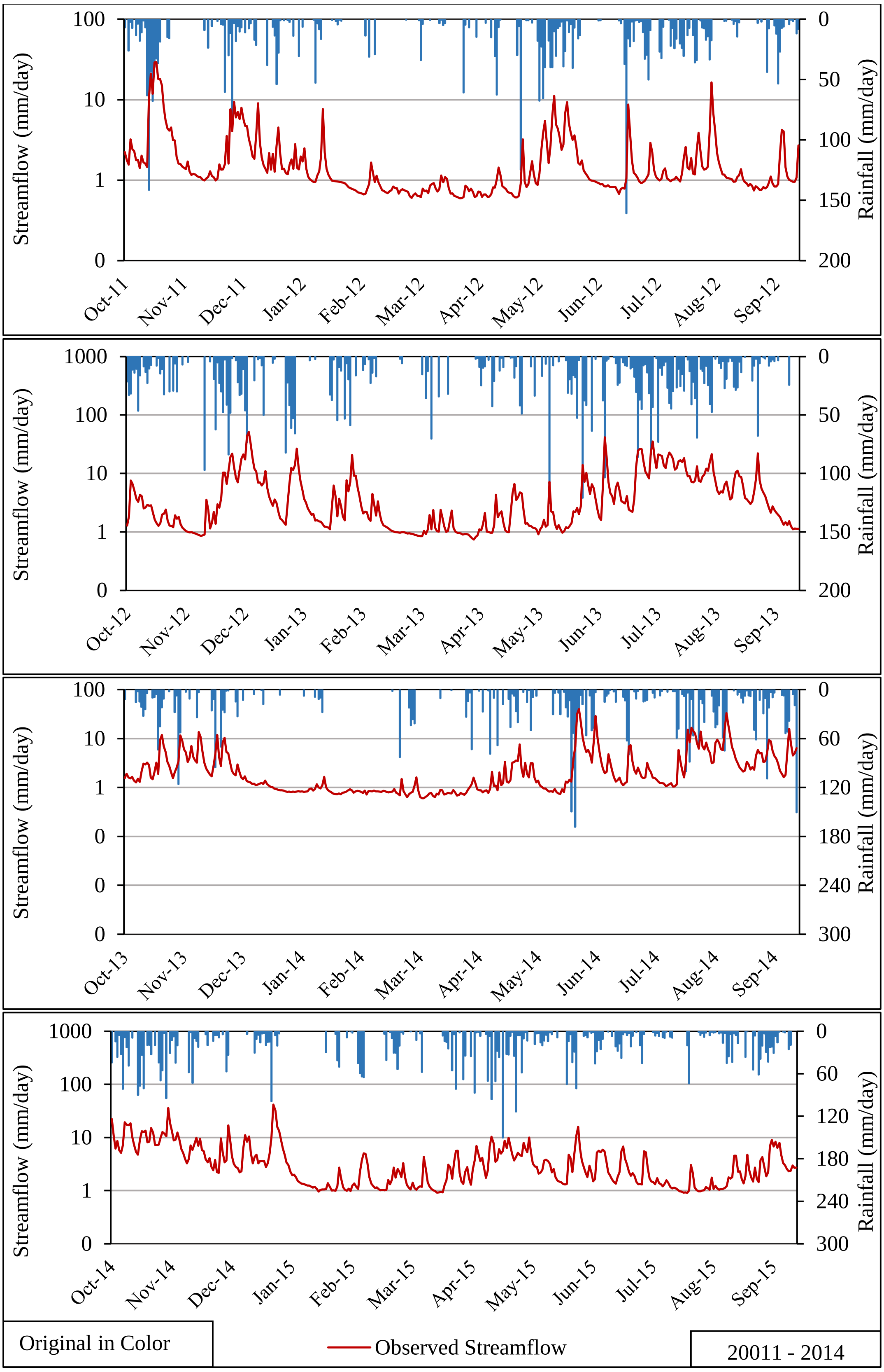

Figure A - 16 Streamflow with response to Rainfall for Kitulgala Station for the Water Year 2011-2014 in Semi-log Hydrograph

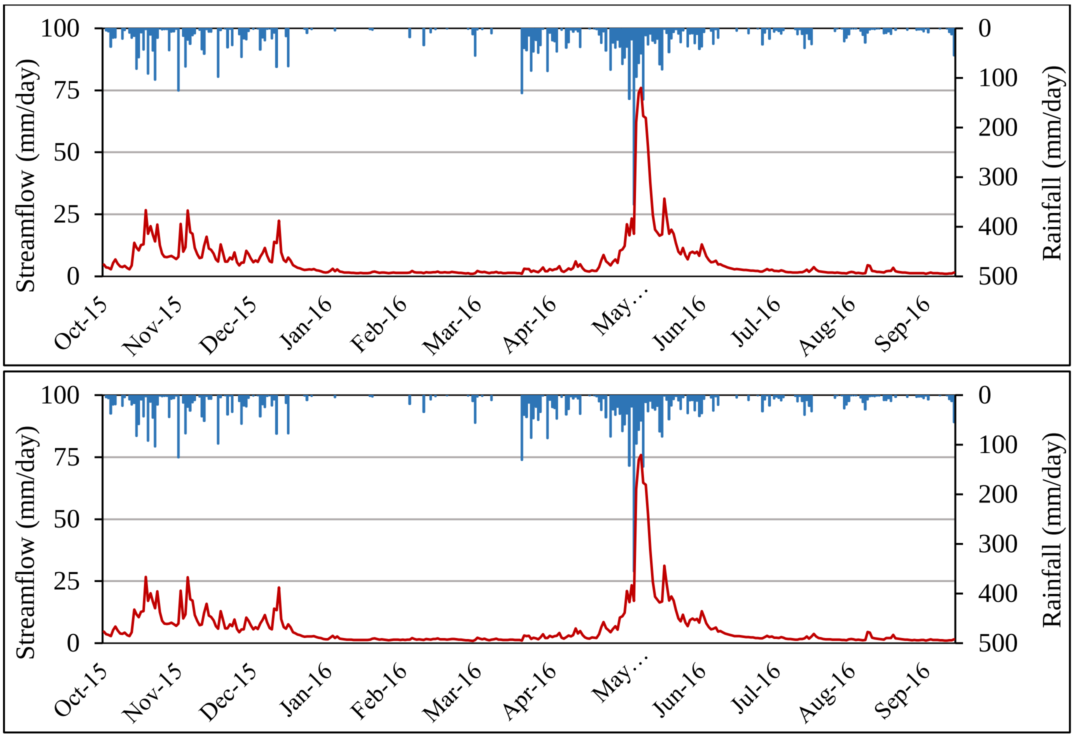

Figure A - 17 Streamflow with response to Rainfall for Kitulgala Station for the Water Year 2015 - 2016 in Normal Hydrograph

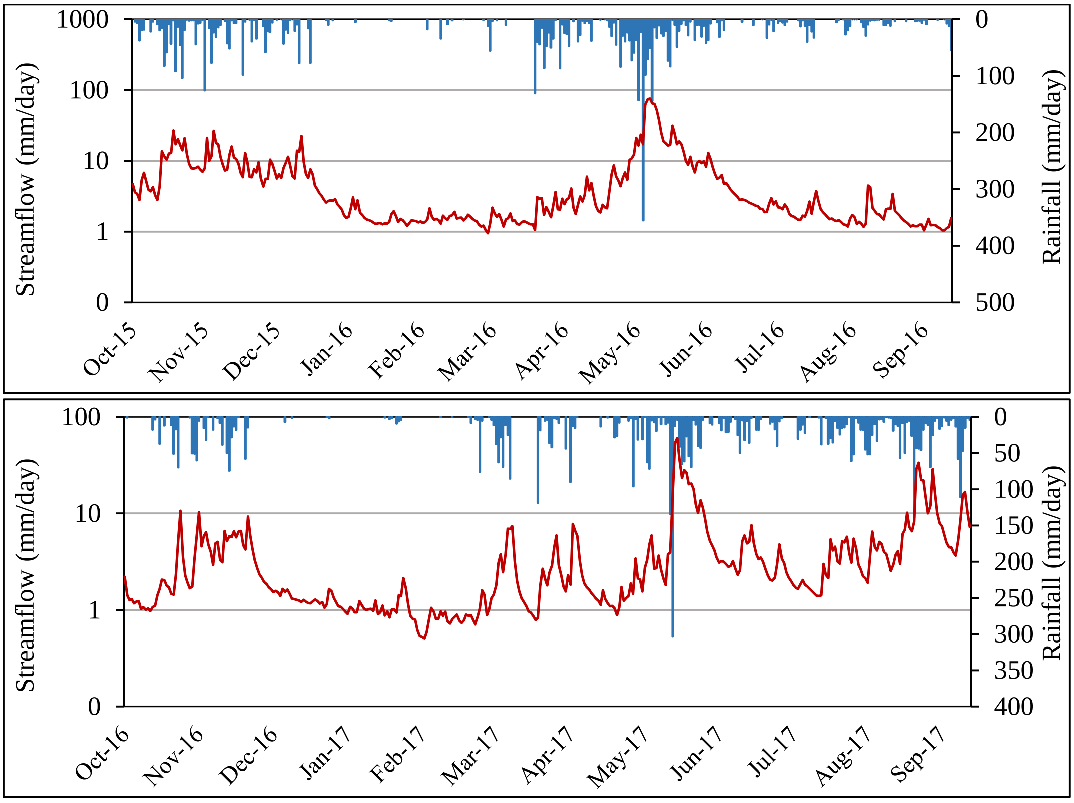

Figure A - 18 Streamflow with response to Rainfall for Kitulgala Station for the Water Year 2015-2016 in Semi-log Hydrograph

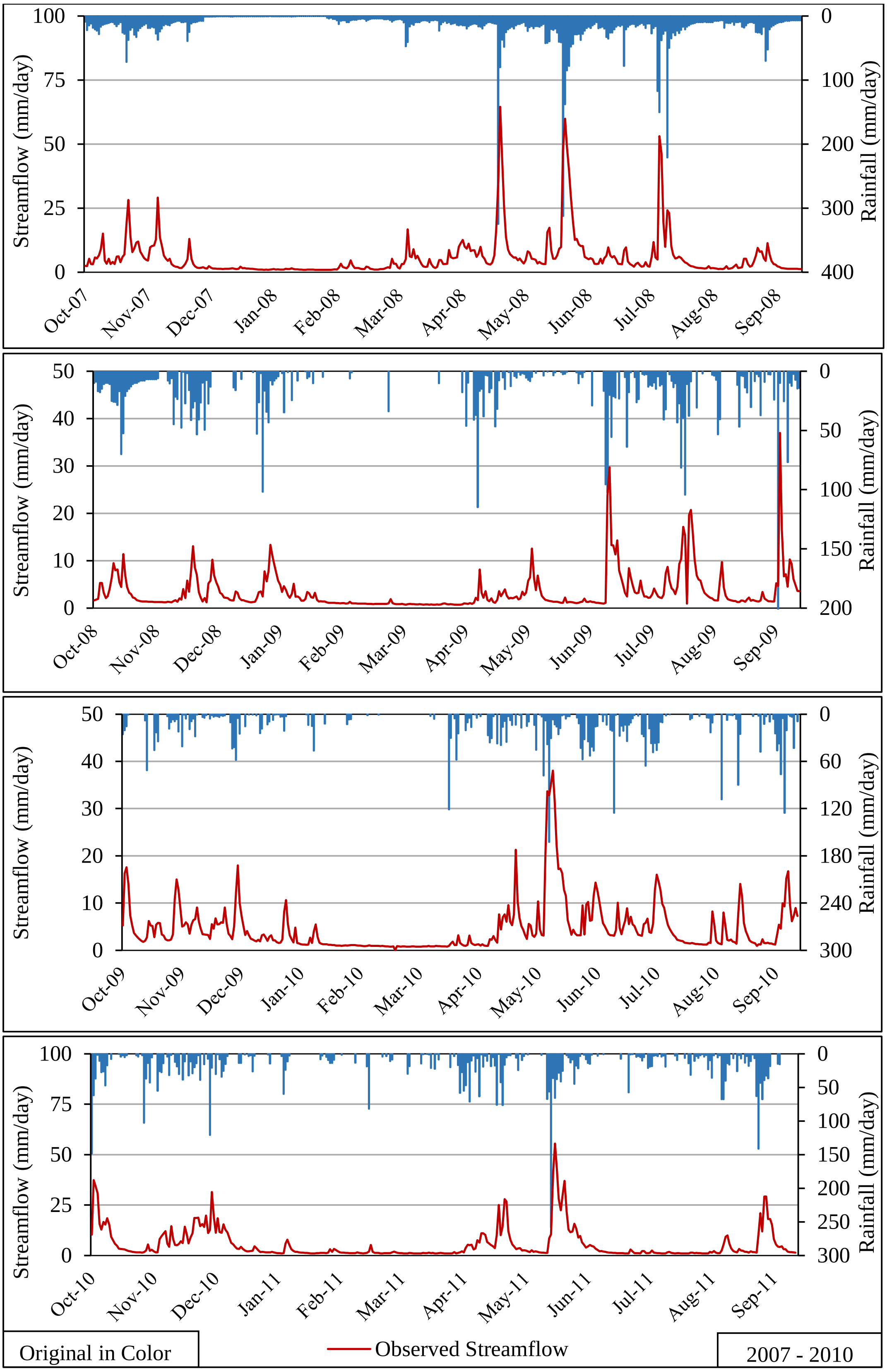

Figure A - 19 Streamflow with response to Rainfall for Holombuwa Station for the Water Year 2007-2010 in Normal Hydrograph

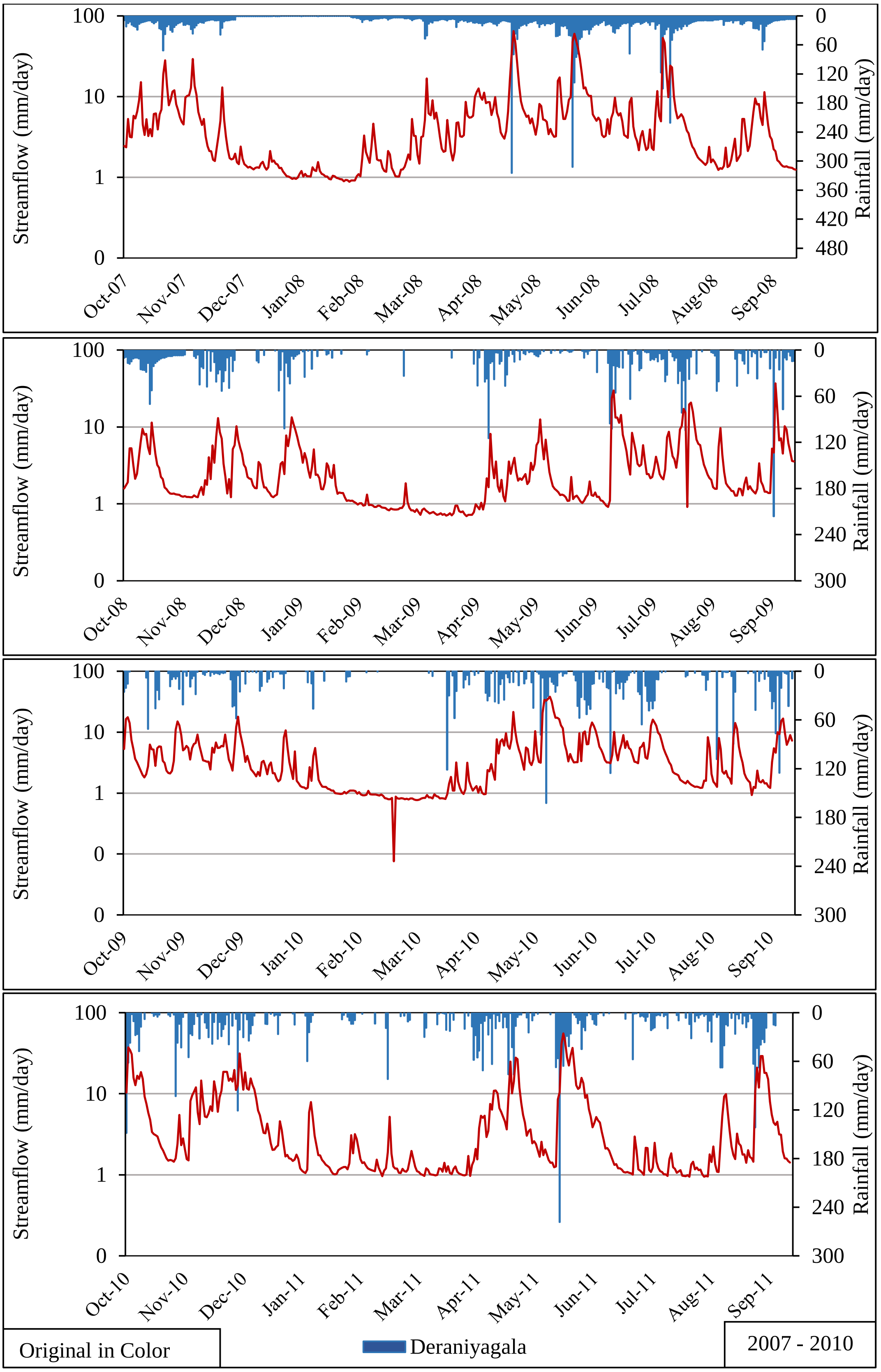

Figure A - 20 Streamflow with response to Rainfall for Holombuwa Station for the Water Year 2007-2010 in Semi-log Hydrograph

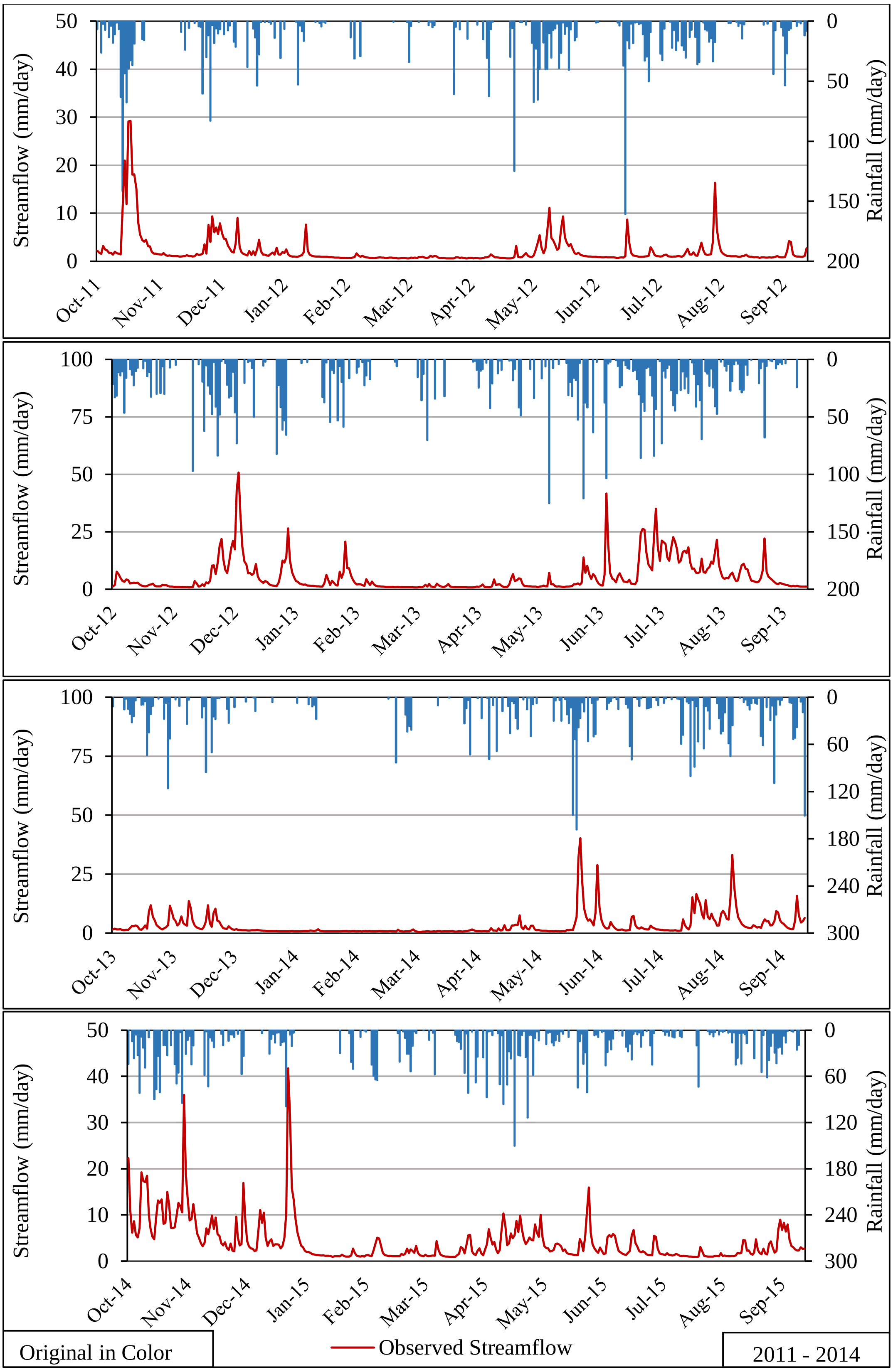

Figure A - 21 Streamflow with response to Rainfall for Holombuwa Station for the Water Year 20011-2014 in Normal Hydrograph

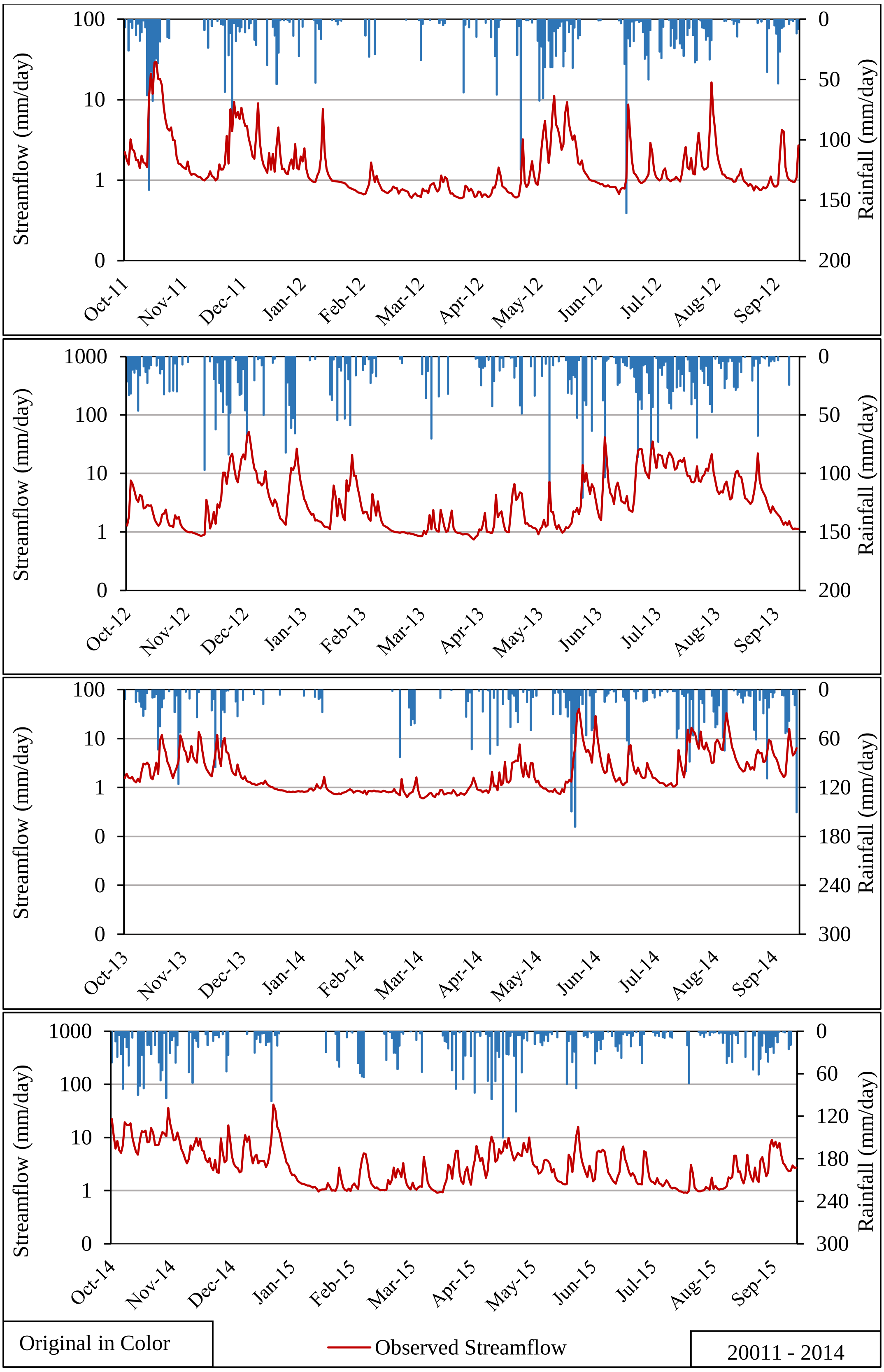

Figure A - 22 Streamflow with response to Rainfall for Holombuwa Station for the Water Year 2011-2014 in Semi-log Hydrograph

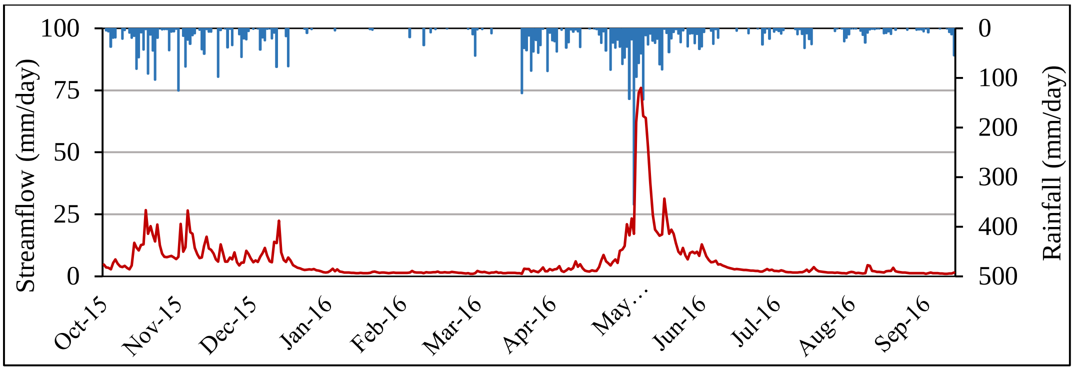

Figure A - 23 Streamflow with response to Rainfall for Holombuwa Station for the Water Year 2015 - 2016 in Normal Hydrograph

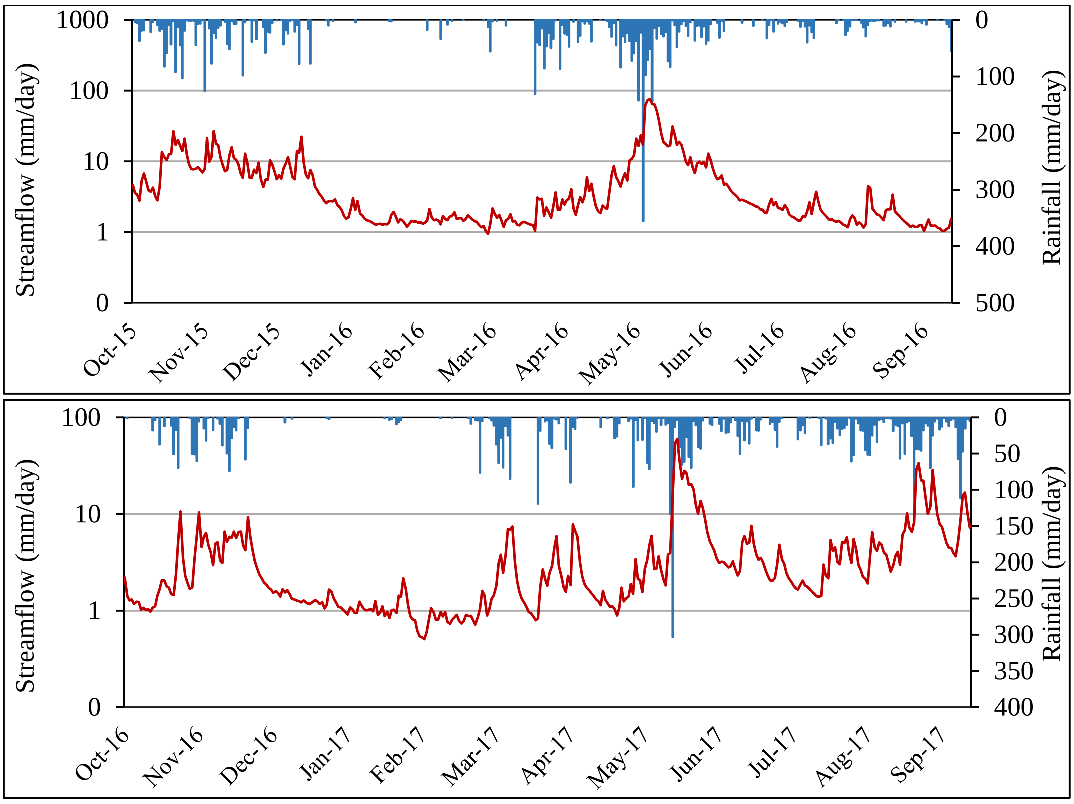

Figure A - 24 Streamflow with response to Rainfall for Holombuwa Station for the Water Year 2015-2017 in Semi-log Hydrograph

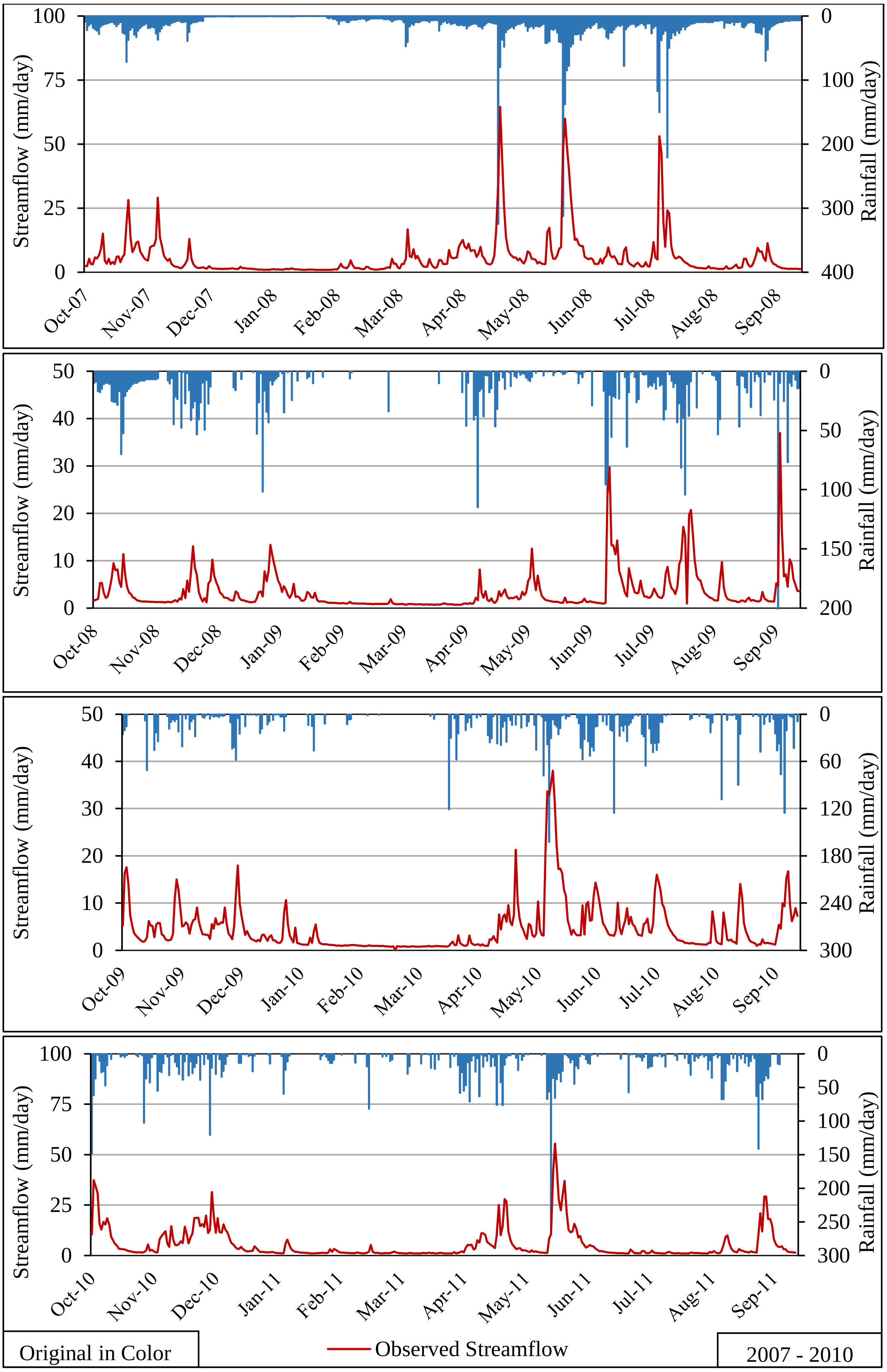

Figure A - 25 Streamflow with response to Rainfall for Glencorse Station for the Water Year 2007-2010 in Normal Hydrograph

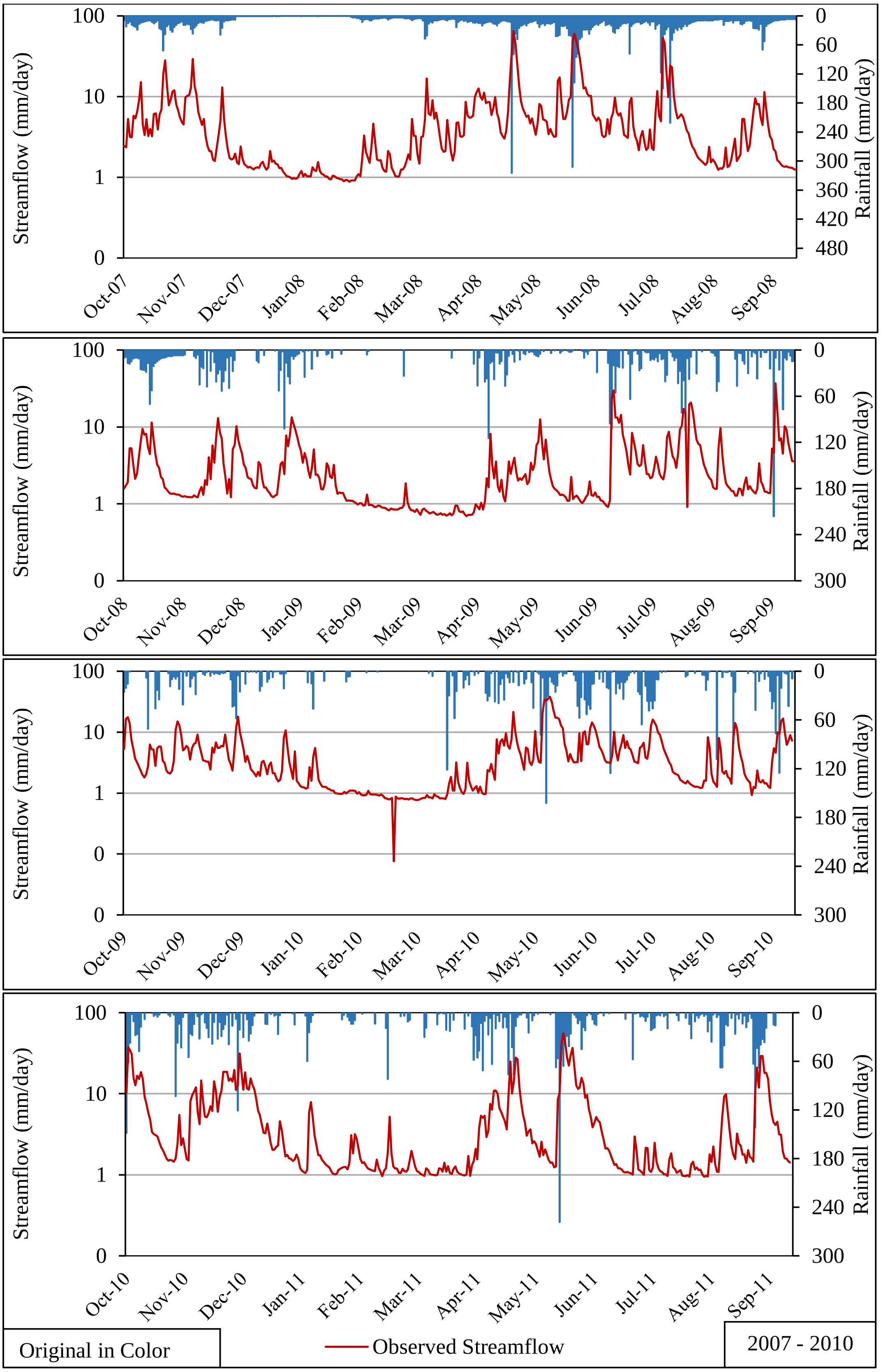

Figure A - 26 Streamflow with response to Rainfall for Glencorse Station for the Water Year 2007-2010 in Semi-log Hydrograph

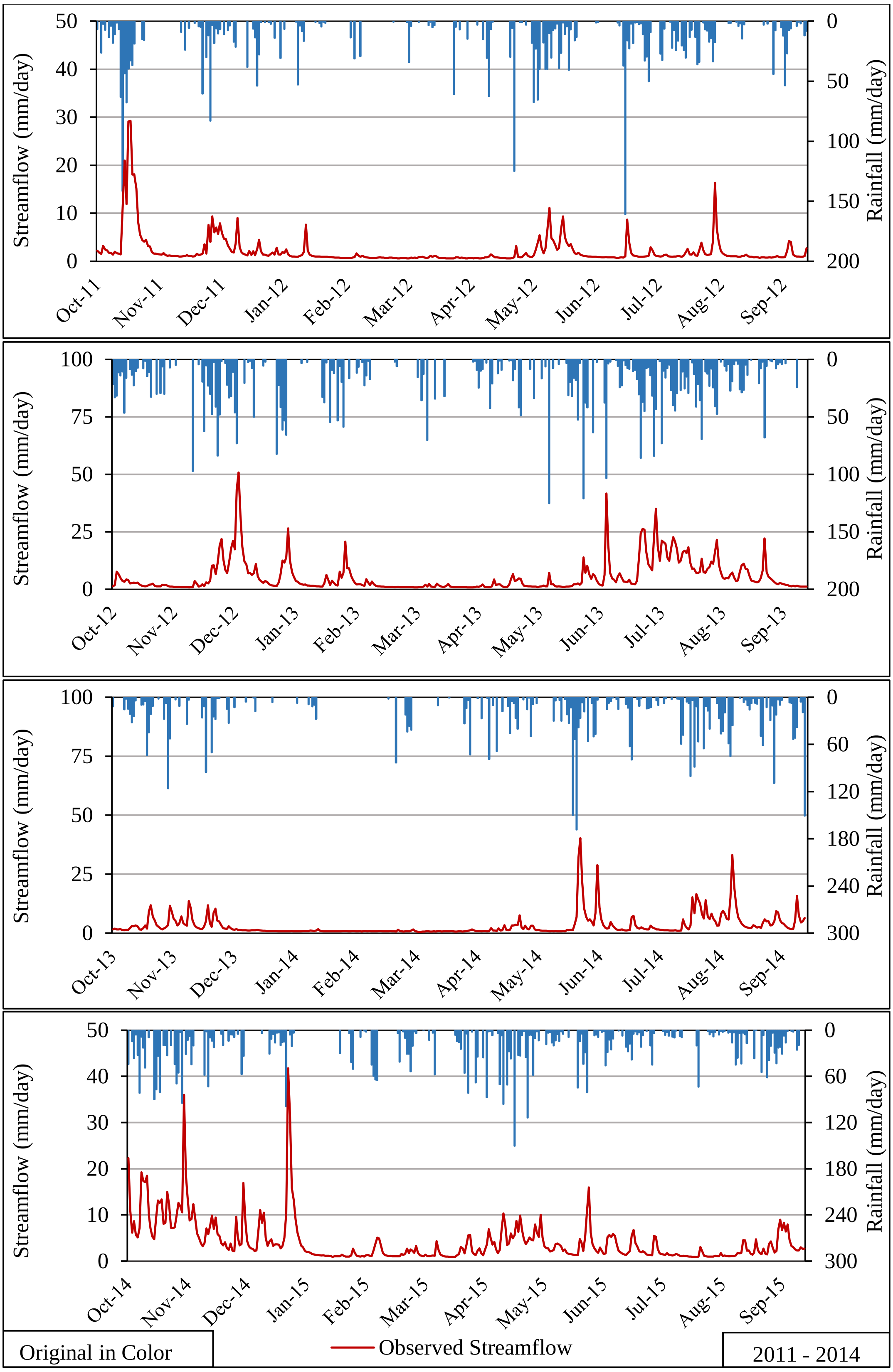

Figure A - 27 Streamflow with response to Rainfall for Glencorse Station for the Water Year 2011-2014 in Normal Hydrograph

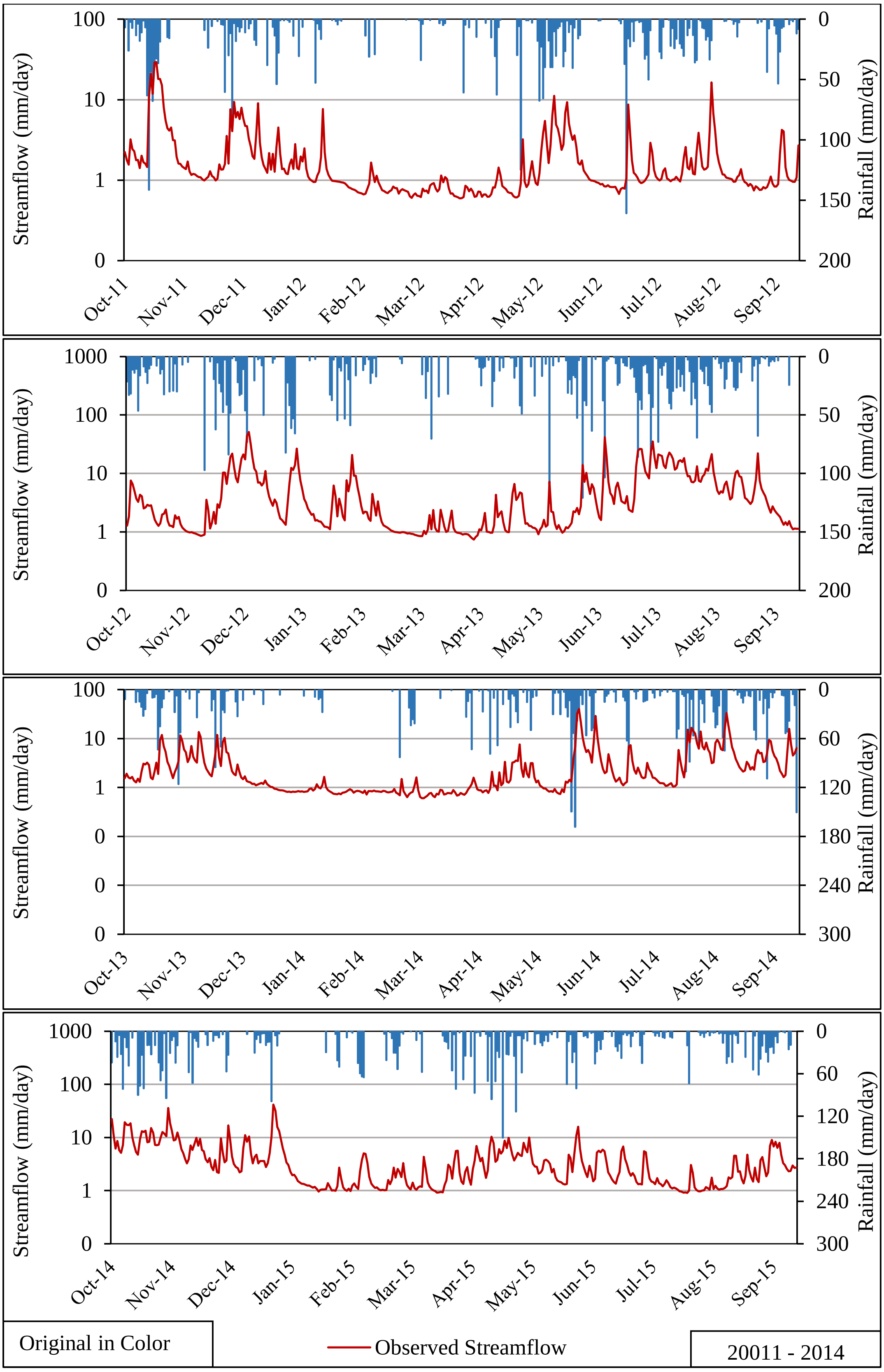

Figure A - 28 Streamflow with response to Rainfall for Glencorse Station for the Water Year 2011-2014 in Semi-log Hydrograph

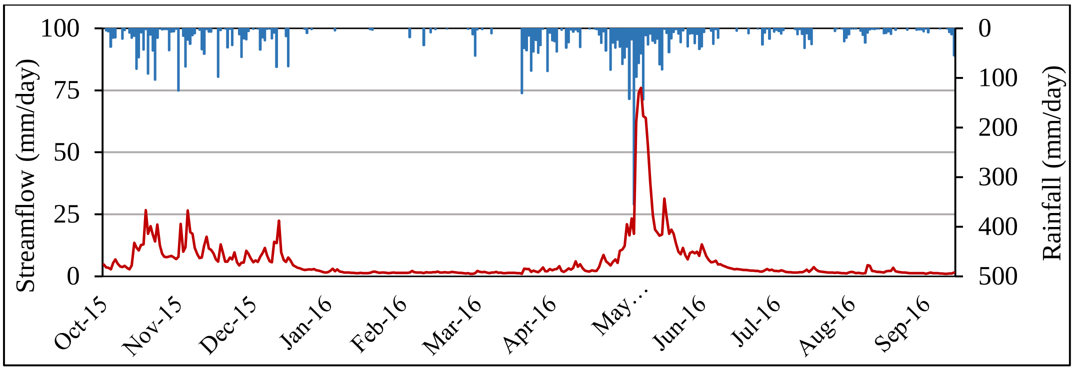

Figure A - 29 Streamflow with response to Rainfall for Glencorse Station for the Water Year 2015 - 2016 in Normal Hydrograph

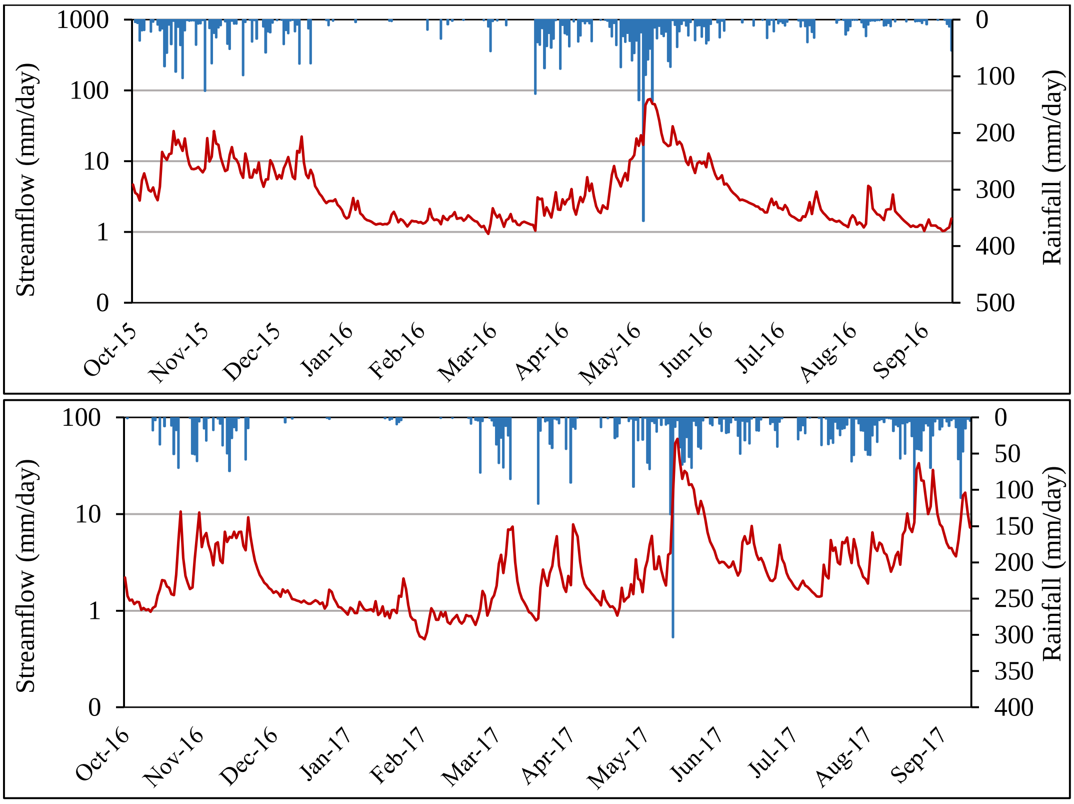

Figure A - 30 Streamflow with response to Rainfall for Glencorse Station for the Water Year 2015-2017 in Semi-log Hydrograph

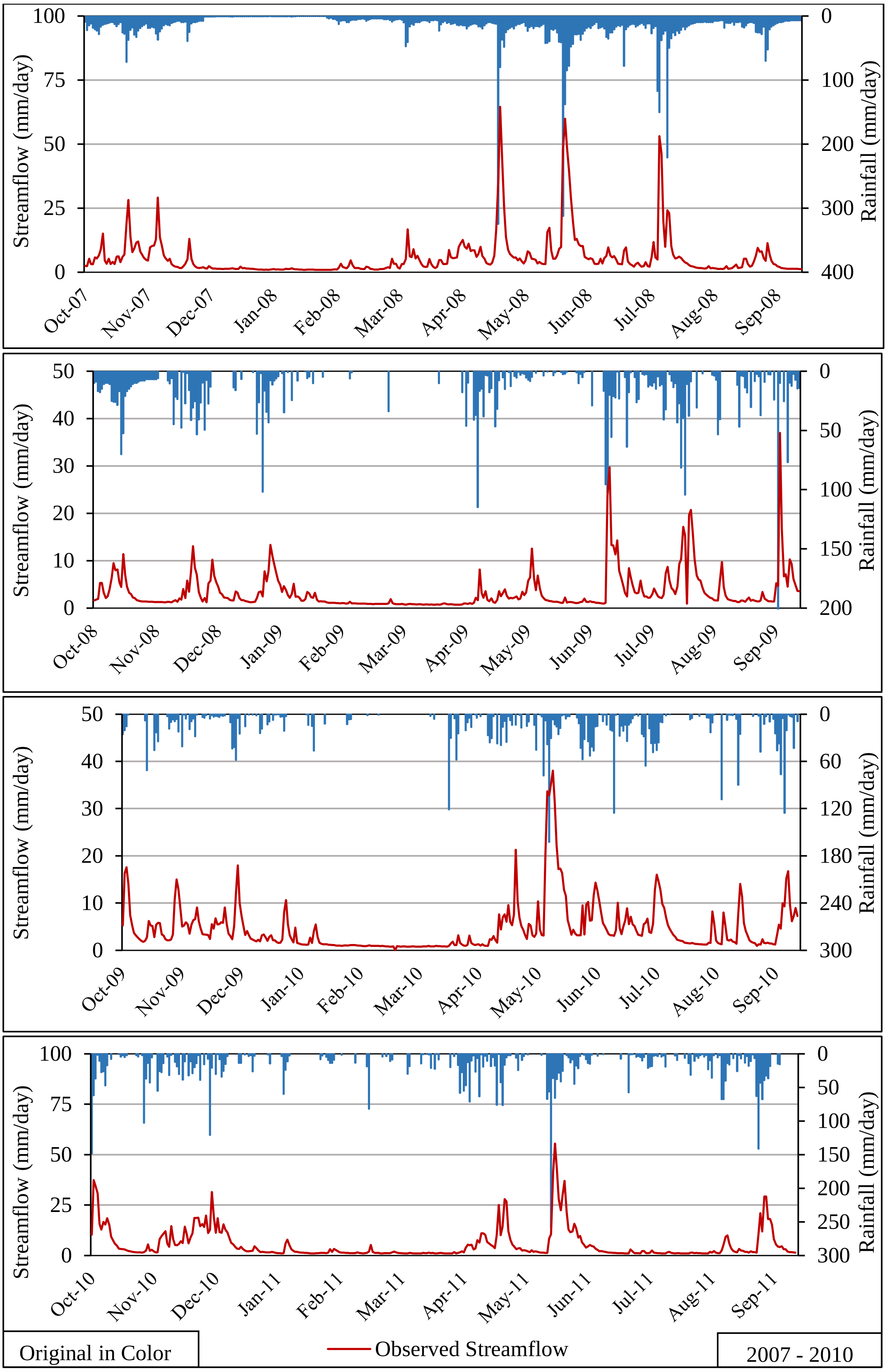

Figure A - 31 Streamflow with response to Rainfall for Hanwella Station for the Water Year 2007-2010 in Normal Hydrograph

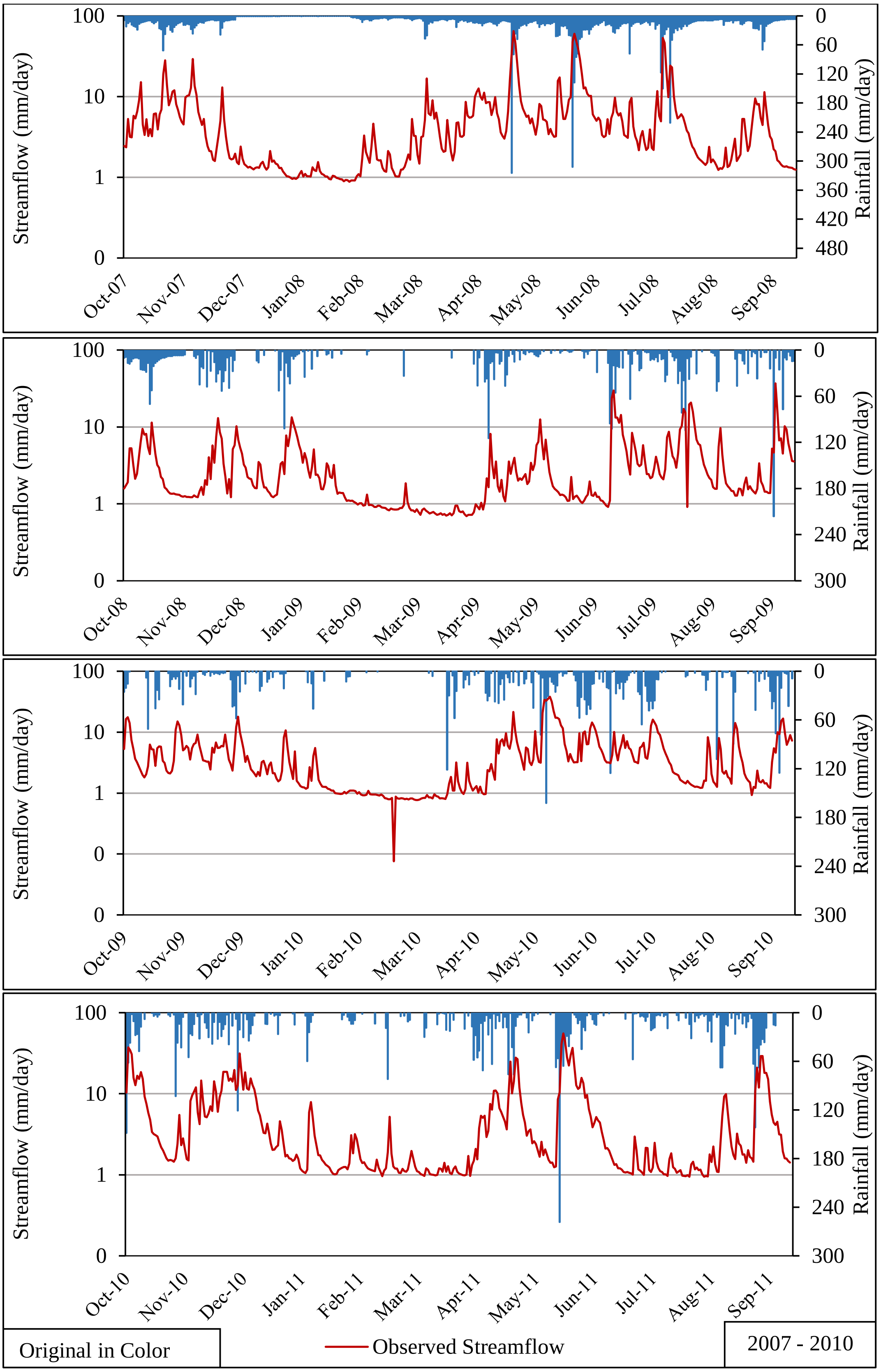

Figure A - 32 Streamflow with response to Rainfall for Hanwella Station for the Water Year 2007-2010 in Semi-log Hydrograph

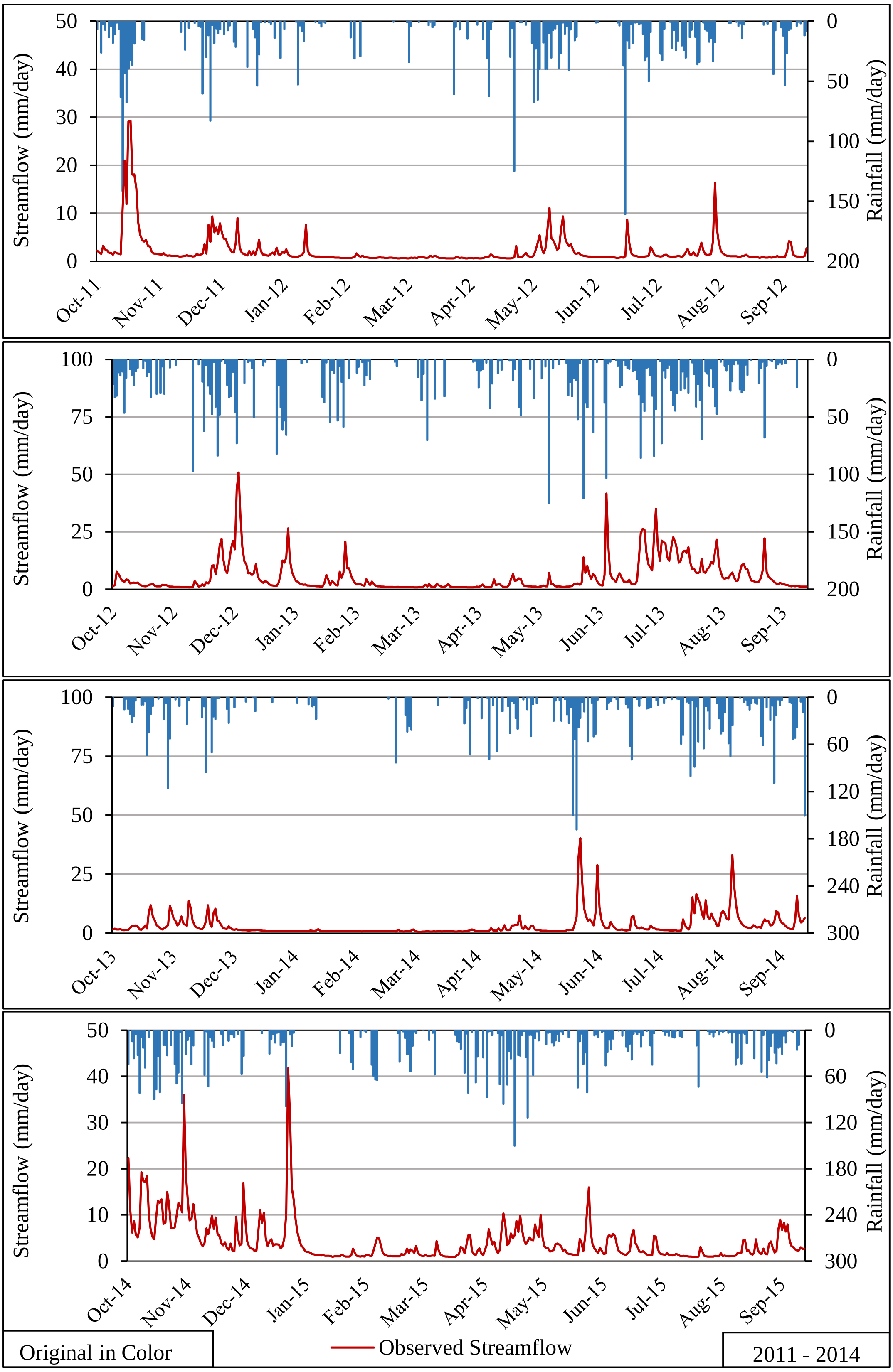

Figure A - 33 Streamflow with response to Rainfall for Hanwella Station for the Water Year 2011-2014 in Normal Hydrograph

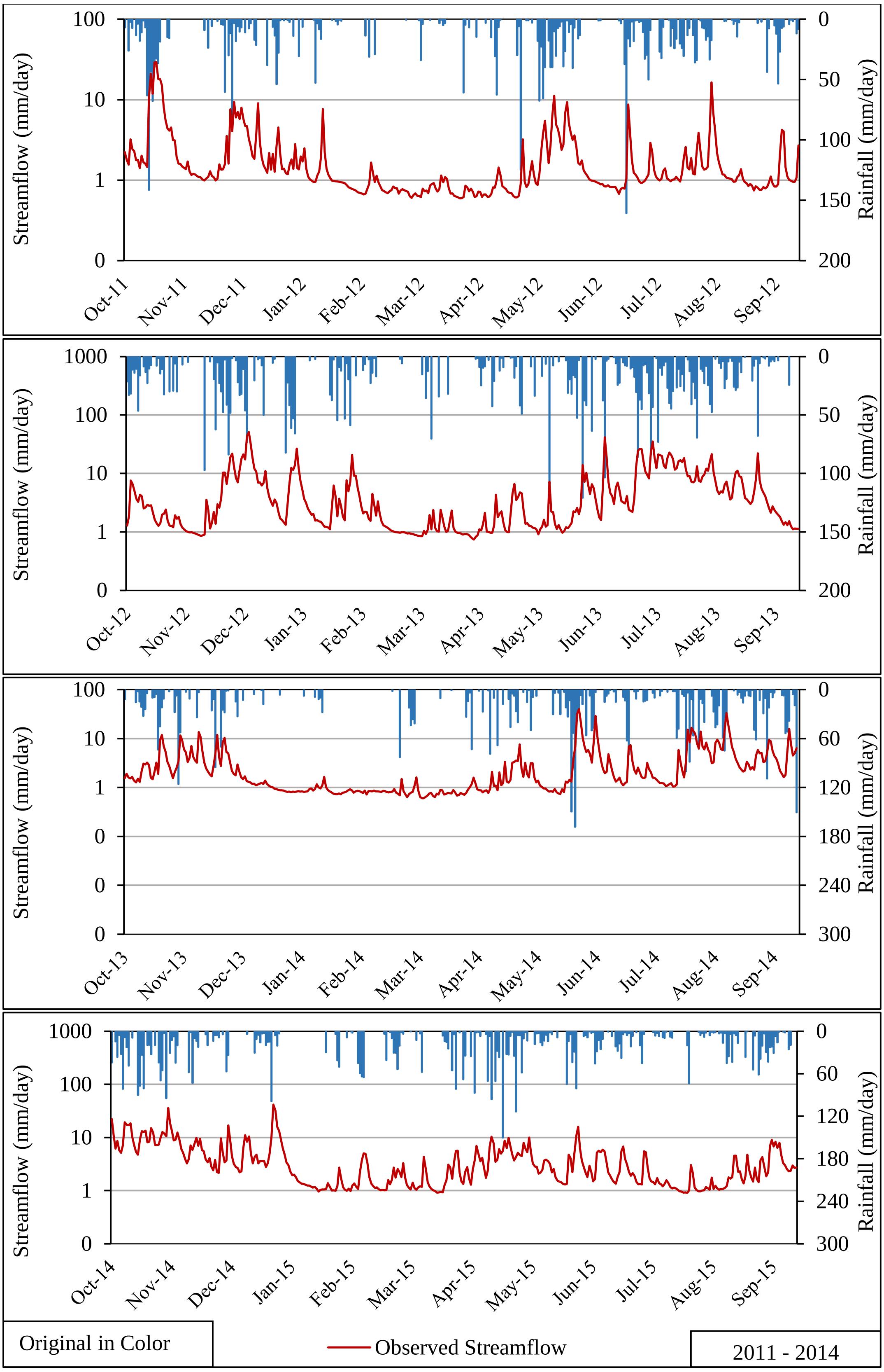

Figure A - 34 Streamflow with response to Rainfall for Hanwella Station for the Water Year 2011-2014 in Semi-log Hydrograph

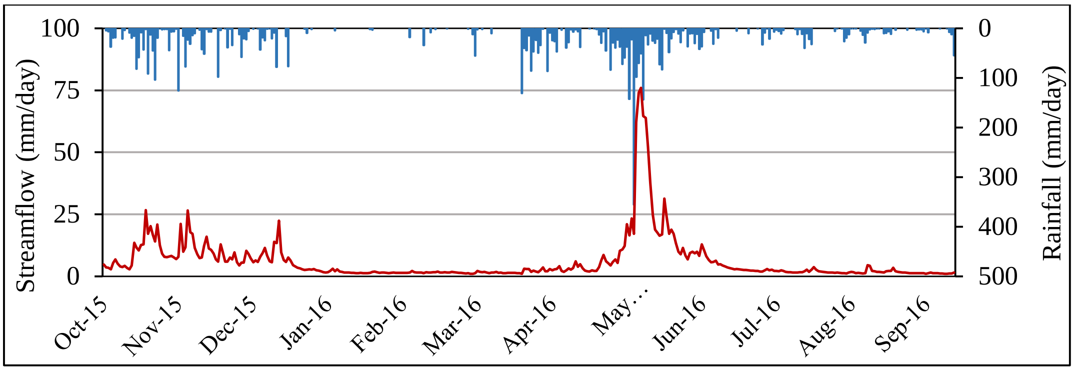

Figure A - 35 Streamflow with response to Rainfall for Hanwella Station for the Water Year 2015 - 2016 in Normal Hydrograph

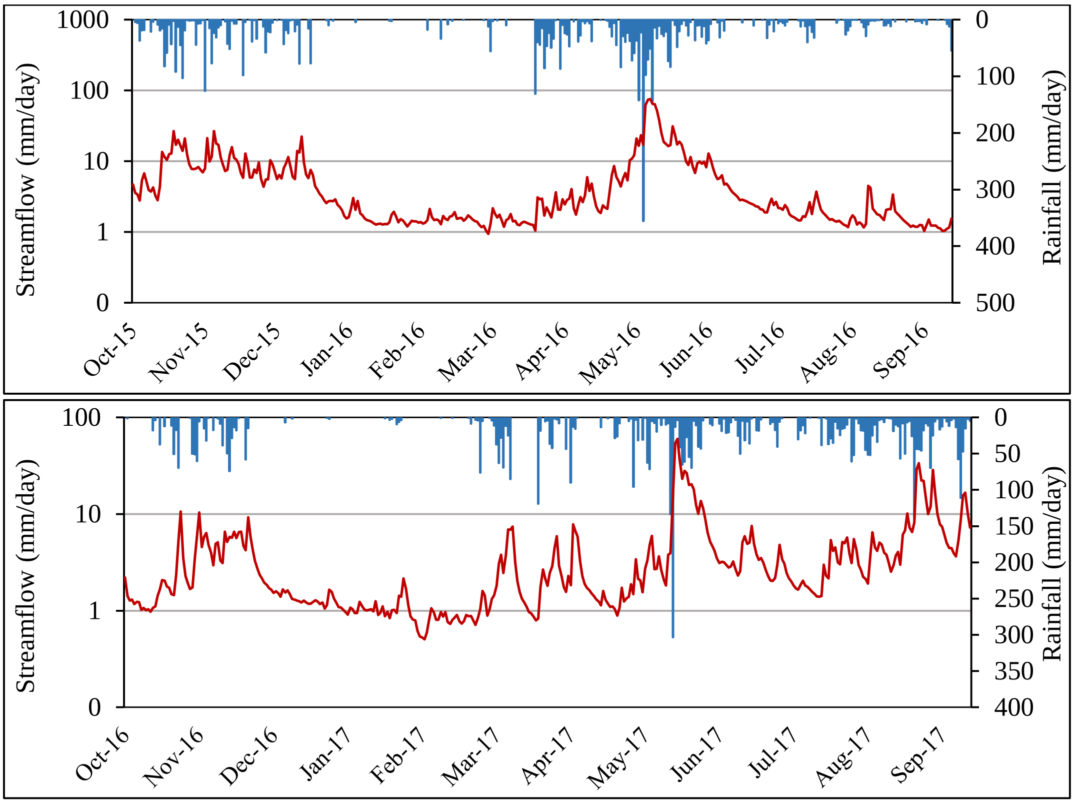

Figure A - 36 Streamflow with response to Rainfall for Hanwella Station for the Water Year 2015-2017 in Semi-log Hydrograph

APPENDIX B: MONTHLY RAINFALL COMPARISON FOR EACH GAUGING STATIONS

Table B 1 Monthly Rainfall Comparison for Norwood Station

Month	2007-08	2008-09	2009-10	2010-11	2011-12	2012-13	2013-14	2014-15	2015-16	2016-17
Oct	379.00	346.50	509.50	273.00	193.50	663.00	234.10	393.80	450.10	78.70
Nov	148.00	243.00	371.50	384.50	169.00	247.00	149.10	175.80	246.30	193.60
Dec	96.50	115.50	219.50	299.00	67.00	120.00	95.60	415.20	125.10	17.30
Jan	49.00	58.50	34.50	279.00	50.00	174.00	105.40	41.90	85.30	0.00
Feb	208.00	20.00	34.30	176.00	179.00	98.00	28.10	182.20	18.10	0.00
Mar	247.20	229.40	274.00	114.50	178.00	432.00	70.10	85.70	108.90	366.70
Apr	657.50	228.50	425.00	428.50	193.00	189.40	455.90	341.40	286.00	126.90
May	194.00	659.50	387.10	184.00	17.00	481.60	56.70	125.20	734.10	388.54
Jun	311.00	302.00	338.50	155.50	95.00	620.00	447.10	207.10	122.50	137.90
Jul	300.00	191.00	357.00	198.00	209.00	347.50	200.50	196.80	107.70	100.00
Aug	131.00	230.50	364.00	183.00	212.00	355.50	170.00	134.80	137.70	107.83
Sep	116.50	303.00	188.50	184.50	74.00	199.60	198.10	226.40	69.90	133.76
Total	**2837.70**	**2927.40**	**3503.40**	**2859.50**	**1636.50**	**3927.60**	**2210.70**	**2526.30**	**2491.70**	**1651.23**

Table B 2 Monthly Rainfall Comparison for Kitulgala Station

Month	2007-08	2008-09	2009-10	2010-11	2011-12	2012-13	2013-14	2014-15	2015-16	2016-17
Oct	555.70	460.30	350.30	602.40	453.20	571.60	488.80	621.70	834.70	232.90
Nov	246.60	212.80	290.50	753.50	153.00	478.10	130.70	300.90	534.60	318.00
Dec	63.10	114.80	259.00	261.60	99.90	332.70	17.80	374.20	317.70	44.20
Jan	77.60	19.10	194.30	171.80	56.30	103.30	92.40	69.60	57.20	42.90
Feb	296.60	40.30	28.80	103.60	73.70	157.40	112.40	151.60	94.30	8.80
Mar	365.60	454.00	129.10	156.40	214.80	212.50	45.80	236.20	220.40	224.00
Apr	690.10	307.60	421.50	483.20	560.80	262.30	312.60	295.90	473.30	112.30
May	734.40	683.40	649.30	1178.10	240.90	711.20	237.60	524.20	1434.10	771.00
Jun	479.00	643.30	669.00	356.30	318.50	757.80	660.10	492.40	301.00	443.20
Jul	624.80	310.60	451.80	238.20	292.20	644.50	315.80	311.70	244.60	264.40
Aug	271.10	572.90	864.10	377.40	347.40	218.40	688.20	450.50	244.80	565.70
Sep	249.50	406.50	380.80	553.20	205.10	600.30	653.90	521.50	151.40	636.20
Total	**4654.10**	**4225.60**	**4688.50**	**5235.70**	**3015.80**	**5050.10**	**3756.10**	**4350.40**	**4908.10**	**3663.60**

Table B 3 Monthly Rainfall Comparison for Holombuwa Station

Month	2007-08	2008-09	2009-10	2010-11	2011-12	2012-13	2013-14	2014-15	2015-16	2016-17
Oct	295.40	574.60	347.70	347.20	408.10	713.80	242.50	511.70	429.90	173.30
Nov	195.80	377.30	260.80	662.10	156.80	299.70	189.40	265.90	480.90	163.90
Dec	76.60	104.50	387.90	339.10	146.70	338.80	23.30	603.70	370.60	45.30
Jan	33.70	96.90	128.50	161.80	66.00	104.40	33.00	6.10	18.50	53.60
Feb	193.40	2.60	31.60	124.30	205.20	105.60	170.90	65.00	29.40	9.20
Mar	454.20	307.00	120.70	126.60	112.00	348.50	56.70	243.70	137.80	317.50
Apr	571.70	297.70	657.70	588.20	303.50	139.10	361.90	381.80	268.70	67.80
May	421.50	356.80	308.80	552.20	31.00	374.60	271.20	209.20	940.50	312.40
Jun	201.30	210.30	266.10	112.90	218.90	511.40	392.50	221.70	154.10	195.10
Jul	535.10	114.40	180.90	77.80	114.70	201.30	174.40	80.70	77.80	197.24
Aug	104.10	439.50	115.00	285.00	186.40	160.70	325.20	206.70	24.00	223.90
Sep	89.50	235.40	226.30	197.30	105.30	383.70	472.80	289.00	34.90	506.91
Total	**3117**	**3032**	**3574.5**	**2054.6**	**3681.6**	**2713.8**	**3085.2**	**2967.1**	**2266.15**	**2266.15**

Table B 4 Monthly Rainfall Comparison for Hanwella Station

Month	2007-08	2008-09	2009-10	2010-11	2011-12	2012-13	2013-14	2014-15	2015-16	2016-17
Oct	442.50	532.20	320.80	188.80	331.20	645.00	254.60	531.40	450.10	78.70
Nov	246.70	254.30	359.80	426.50	134.20	205.40	357.30	277.10	246.30	193.60
Dec	74.66	146.60	307.30	205.80	166.20	229.70	47.50	352.60	125.10	17.30
Jan	92.60	52.40	74.40	127.50	149.60	50.30	55.10	92.40	85.30	0.00
Feb	314.40	30.70	25.50	69.60	158.50	200.80	10.60	231.10	18.10	0.00
Mar	247.20	238.20	170.40	181.70	146.30	352.60	162.20	272.70	108.90	366.70
Apr	664.40	349.10	574.80	484.60	339.10	192.20	354.20	257.30	286.00	126.90
May	429.30	252.10	823.20	487.60	197.30	416.40	162.10	180.60	734.10	388.54
Jun	427.60	375.30	254.20	153.60	135.60	516.40	438.40	375.90	122.50	137.90
Jul	218.70	166.00	237.60	125.40	90.50	254.20	137.40	88.00	107.70	100.00
Aug	156.10	164.50	56.10	255.60	269.70	141.00	400.60	156.50	137.70	107.83
Sep	217.40	264.70	486.10	274.90	220.30	271.50	283.20	395.40	69.90	133.76
Total	**3531.56**	**2826.1**	**3690.2**	**2981.6**	**2338.5**	**3475.5**	**2663.2**	**3211**	**2491.70**	**1651.23**

Table B 5 Monthly Rainfall Comparison for Deraniyagala Station

Month	2007-08	2008-09	2009-10	2010-11	2011-12	2012-13	2013-14	2014-15	2015-16	2016-17
Oct	627.3	535.2	323.6	609.7	279.9	616.4	508.4	946.9	450.10	78.70
Nov	455.6	348.8	245.3	452.5	250.4	490.7	325.6	360	246.30	193.60
Dec	30	101.3	213.7	328.2	97.5	309.6	76.6	345.9	125.10	17.30
Jan	19.784	41.3	107.7	143.9	74.7	84.7	66.2	126.1	85.30	0.00
Feb	168.8	10.2	9	157.8	117.9	201.1	85.1	333.9	18.10	0.00
Mar	345.47	498.2	248.7	144	301.3	265.9	155.9	302.7	108.90	366.70
Apr	802.94	62.2	320.3	620.8	532.2	379.6	400.4	854.6	286.00	126.90
May	988.59	494.1	533.7	744.2	266.3	643.7	442.8	440.3	734.10	388.54
Jun	938.67	570.5	662.1	189.9	382.6	710	607.9	443.1	122.50	137.90
Jul	1139.27	286.2	398.9	206.1	195.9	451.9	288	165.8	107.70	100.00
Aug	354.89	581.5	300.3	405.5	307.3	162.8	729.2	306.6	137.70	107.83
Sep	480.92	414.7	478.4	536.7	326.1	629.3	686.4	475.48	69.90	133.76
Total	**6352.234**	**3944.2**	**3841.7**	**4539.3**	**3132.1**	**4945.7**	**4372.5**	**5101.38**	**2491.70**	**1651.23**

Table B 6 Monthly Rainfall Comparison for Glencorse Station

Month	2007-08	2008-09	2009-10	2010-11	2011-12	2012-13	2013-14	2014-15	2015-16	2016-17
Oct	446.66	480.57	400.98	406.70	317.48	638.80	338.48	585.54	565.51	213.08
Nov	285.68	267.48	270.09	491.30	163.29	330.74	237.72	273.84	473.08	346.38
Dec	81.06	116.51	227.63	277.06	157.62	259.95	51.11	406.87	291.47	34.92
Jan	54.16	88.66	169.28	166.49	135.61	99.13	71.12	69.71	70.01	53.45
Feb	269.81	105.17	101.50	109.50	257.29	157.09	72.07	194.88	64.07	16.88
Mar	371.83	418.64	291.68	142.79	289.91	323.63	102.21	229.07	169.23	342.04
Apr	740.38	346.25	517.81	486.92	461.50	227.54	373.08	393.12	413.85	148.08
May	587.39	576.07	570.93	611.92	228.57	521.16	218.24	288.54	1146.86	666.91
Jun	462.61	420.19	462.51	241.74	217.14	617.48	506.99	355.25	207.40	287.62
Jul	559.27	254.11	294.69	199.22	237.44	378.67	216.93	168.03	157.12	175.56
Aug	202.78	418.72	400.26	309.70	276.59	205.30	457.44	246.62	112.39	362.81
Sep	231.67	284.21	385.94	344.18	220.92	401.07	438.18	386.12	86.39	588.46
Total	**4293.30**	**3776.57**	**4093.31**	**3787.53**	**2963.36**	**4160.55**	**3083.56**	**3597.59**	**3757.39**	**3236.20**

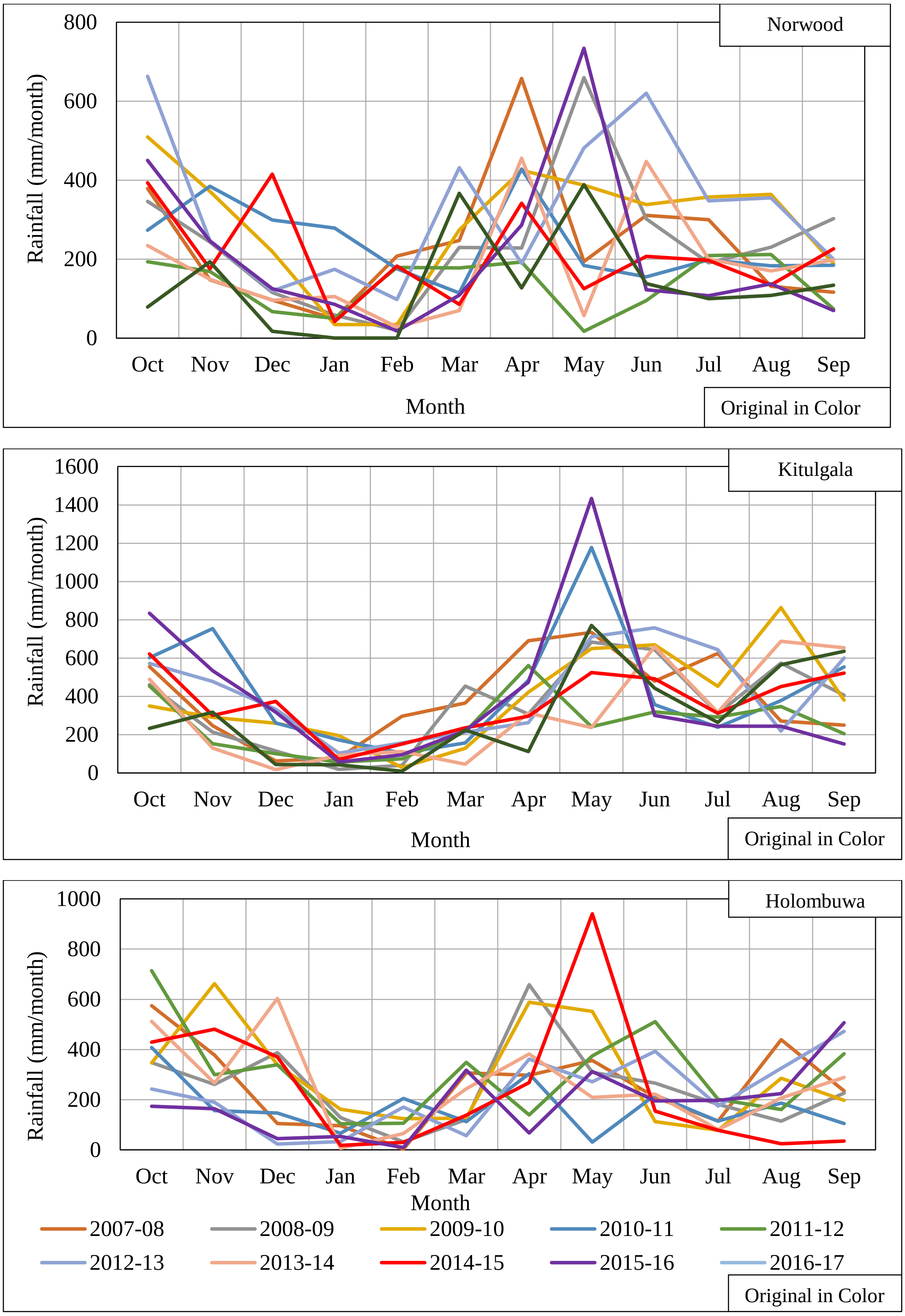

Figure B 1 Monthly Rainfall Comparison for Norwood, Kitulgala and Holombuwa Stations

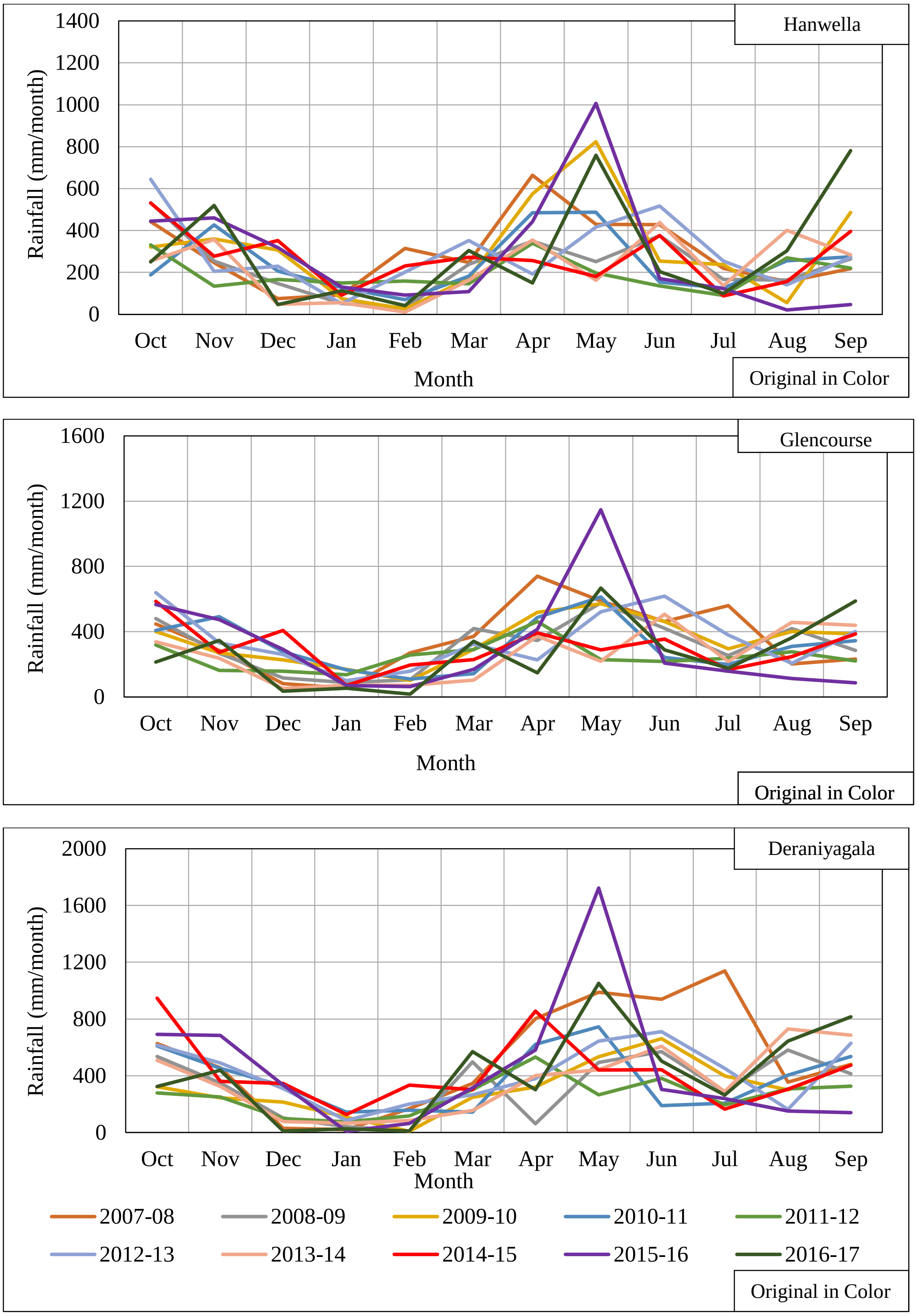

Figure B 2 Monthly Rainfall Comparison for Deraniyagala, Glencorse and Hanwella Stations

APPENDIX C: MONTHLY MAXIMUM, MINIMUM, MEAN AND ANNUAL TOTAL THEISSEN RAINFALL, STREAMFLOW AND TEMPERATURE

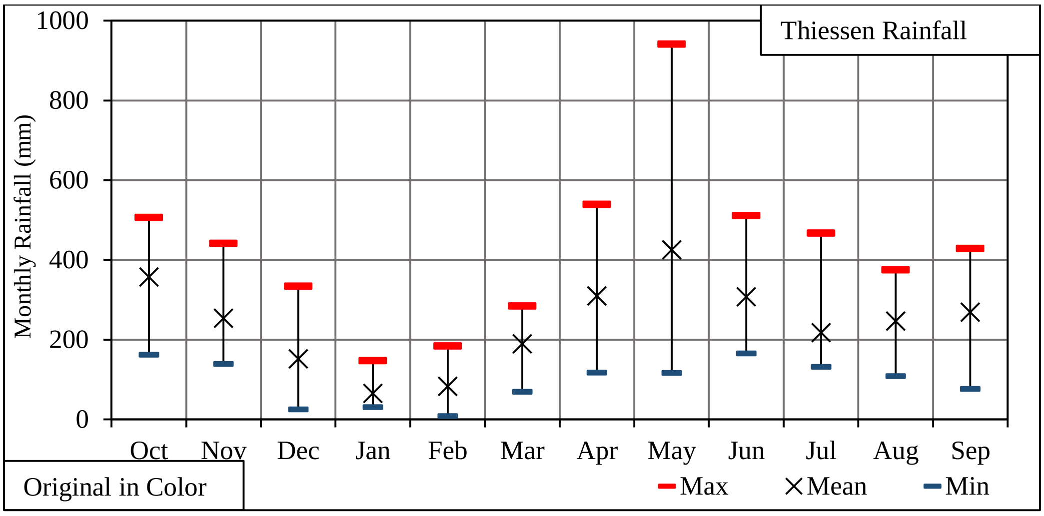

Figure C 1 Monthly Maximum, Minimum, and Mean Theissen Rainfall from 2007 – 2017

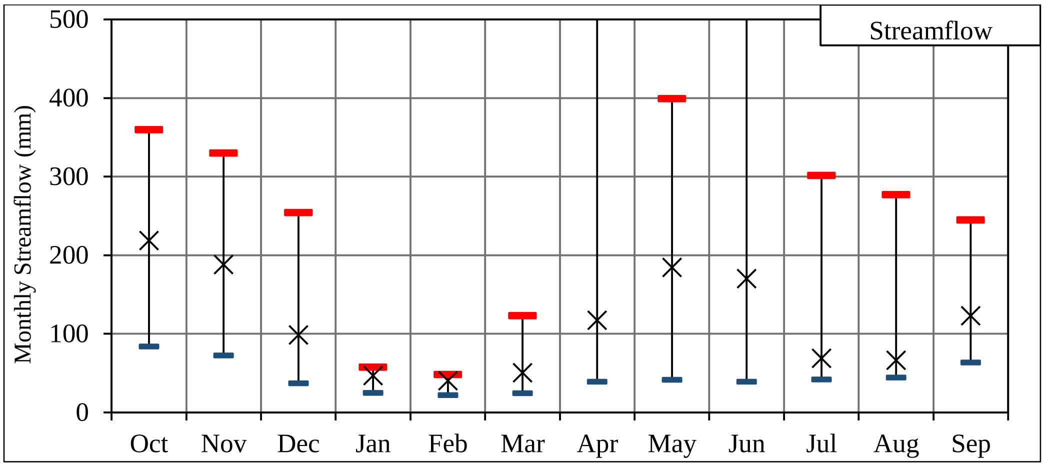

Figure C 2 Monthly Maximum, Minimum, and Mean Streamflow from 2007 – 2017

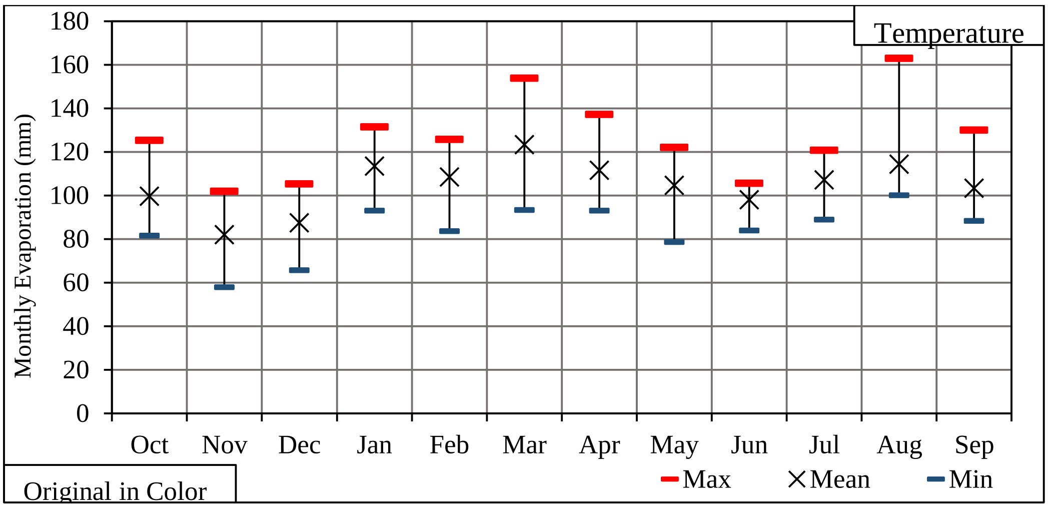

Figure C 3 Monthly Maximum, Minimum, and Mean Temperature from 2007 – 2017

Table C 1 Monthly Total Theissen Rainfall (mm) from Six Rainfall Gauging Stations

Month	2007-08	2008-09	2009-10	2010-11	2011-12	2012-13	2013-14	2014-15	2015-16	2016-17
Oct	370.32	379.41	302.53	344.97	267.38	507.19	286.53	477.11	477.11	379.05
Nov	201.79	224.79	240.79	442.17	138.97	288.83	164.81	217.30	217.30	226.52
Dec	54.53	90.39	215.26	233.14	85.33	213.08	41.41	334.92	334.92	43.49
Jan	41.80	40.83	90.87	147.95	55.40	88.86	59.88	50.86	50.86	45.44
Feb	184.89	16.96	21.09	105.20	112.73	116.12	69.90	147.73	147.73	147.03
Mar	269.30	285.16	151.07	111.97	155.96	251.68	69.11	173.43	173.43	323.60
Apr	540.18	193.56	369.14	411.60	313.98	188.32	300.81	340.62	340.62	941.37
May	447.42	425.40	410.15	528.23	116.88	436.19	185.16	251.69	251.69	172.73
Jun	373.11	347.19	372.77	165.68	190.51	512.11	417.53	278.55	278.55	132.11
Jul	468.02	178.73	274.43	143.22	158.29	326.81	188.90	150.08	150.08	108.14
Aug	166.91	338.34	324.81	243.42	213.33	176.53	375.70	214.69	214.69	76.80
Sep	181.58	267.27	265.88	289.93	142.61	345.68	380.40	305.44	305.44	162.11
Total	**3299.85**	**2788.04**	**3038.80**	**3167.48**	**1951.36**	**3451.40**	**2540.15**	**2942.41**	**2942.41**	**2758.40**

Table C 2 Monthly Total Streamflow (mm) from Hanwella Gauging Station

Month	**2007-08**	**2008-09**	**2009-10**	**2010-11**	**2011-12**	**2012-13**	**2013-14**	**2014-15**	**2015-16**	**2016-17**
Oct	232.53	116.44	180.64	274.70	84.04	204.93	100.96	359.79	359.79	305.02
Nov	181.68	110.65	156.53	292.17	72.47	330.27	151.35	194.92	194.92	212.61
Dec	43.08	75.39	134.88	223.15	42.73	122.03	37.18	254.31	254.31	51.24
Jan	32.53	29.80	51.78	57.74	24.89	50.96	27.60	49.47	49.47	44.41
Feb	46.60	21.89	25.31	46.19	22.15	34.09	23.61	48.55	48.55	47.90
Mar	123.56	60.14	30.27	36.26	26.07	63.02	24.21	50.61	50.61	82.49
Apr	343.75	88.54	93.52	157.06	100.59	48.67	39.20	133.85	133.85	775.61
May	267.68	161.42	399.41	343.51	41.43	207.47	53.64	113.08	113.08	217.18
Jun	354.14	149.49	191.11	229.56	39.08	504.41	226.42	123.82	123.82	67.25
Jul	301.84	145.89	180.09	41.78	68.55	248.07	69.14	57.47	57.47	55.08
Aug	62.25	161.49	98.26	70.18	52.13	100.30	277.31	48.07	48.07	44.32
Sep	108.48	159.79	139.62	211.87	64.55	245.16	137.52	107.90	107.90	63.61
Total	**2098.12**	**1280.92**	**1681.41**	**1984.17**	**638.68**	**2159.37**	**1168.14**	**1541.82**	**1541.82**	**1966.71**

Table C 3 Monthly Temperature (mm) from Colombo Gauging Station

Month	**2007-08**	**2008-09**	**2009-10**	**2010-11**	**2011-12**	**2012-13**	**2013-14**	**2014-15**	**2015-16**	**2016-17**
Oct	82.71	95.43	106.78	100.51	111.46	91.89	104.16	81.58	101.66	125.42
Nov	102.1	81.03	57.93	62.13	83.09	87.54	88.789	67.33	85.84	99.28
Dec	89.16	102.12	86.05	65.75	90.29	82.76	105.36	67.82	81.25	102.75
Jan	99.95	117.69	131.61	93.1	121.12	112.4	116.713	118.27	110.116	115.653
Feb	109.67	125.83	121.2	90.47	101.2	103.83	118.16	100.19	121.24	83.59
Mar	93.33	116.82	129.83	120.6	129.22	117.91	129.229	109.72	153.88	88.43
Apr	97.17	100.73	98.47	98.63	93.01	127.73	118.37	114.39	137.38	132.14
May	107.52	113.11	78.62	107.1	122.19	95.63	108.21	115.72	87.82	115.02
Jun	99.91	94.7	94.72	105.66	101.07	84.01	102.79	95.15	105.032	95.83
Jul	89	109.43	98.15	106.01	112.68	93.88	115.006	120.83	116.16	118.13
Aug	103.48	109.29	106.74	113.28	107.62	109.83	104.34	119.53	163.1	121.39
Sep	113.04	101.34	95.51	107.81	96.87	99.83	106.81	88.42	130.11	97.823
Total	**1187.04**	**1267.52**	**1205.61**	**1171.05**	**1269.82**	**1207.24**	**1317.94**	**1198.95**	**1393.59**	**1207.026**

APPENDIX D: DOUBLE MASS CURVE

Table D 1 Variation of Cumulative Rainfall

Water Year	Norwood	Kitulgala	Holombuwa	Glencourse	Hanwella	Deraniyagala
2007 - 2008	4351.76	4049.03	4295.99	4013.24	4236.12	3766.00
2008 - 2009	7761.68	7242.58	7674.31	7324.31	7662.92	7006.45
2009 - 2010	11599.16	10882.54	11590.36	11065.31	11469.27	10787.55
2010 - 2011	15470.39	14357.74	15342.43	14760.68	15320.15	14378.82
2011 - 2012	18035.39	16692.86	17837.74	17180.01	17768.15	16694.55
2012 - 2013	22128.06	20598.44	21971.41	21272.68	21936.17	20617.54
2013 - 2014	25330.69	23543.51	25090.19	24335.93	25063.38	23459.87
2014 - 2015	29080.90	26989.70	28747.25	27916.81	28699.48	26780.90
2015 - 2016	33031.57	30537.64	32618.69	31638.71	32504.88	30273.87
2016 - 2017	35501.96	32832.68	35101.00	33919.65	34795.96	32395.00

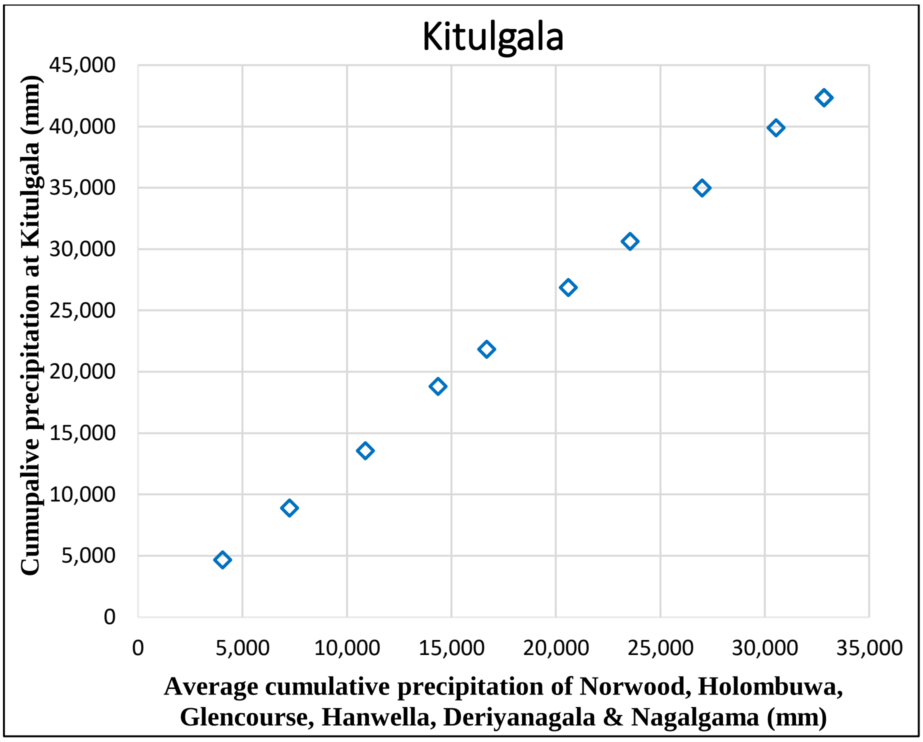

Figure D 1 Double Mass Curve for Kitulgala Station

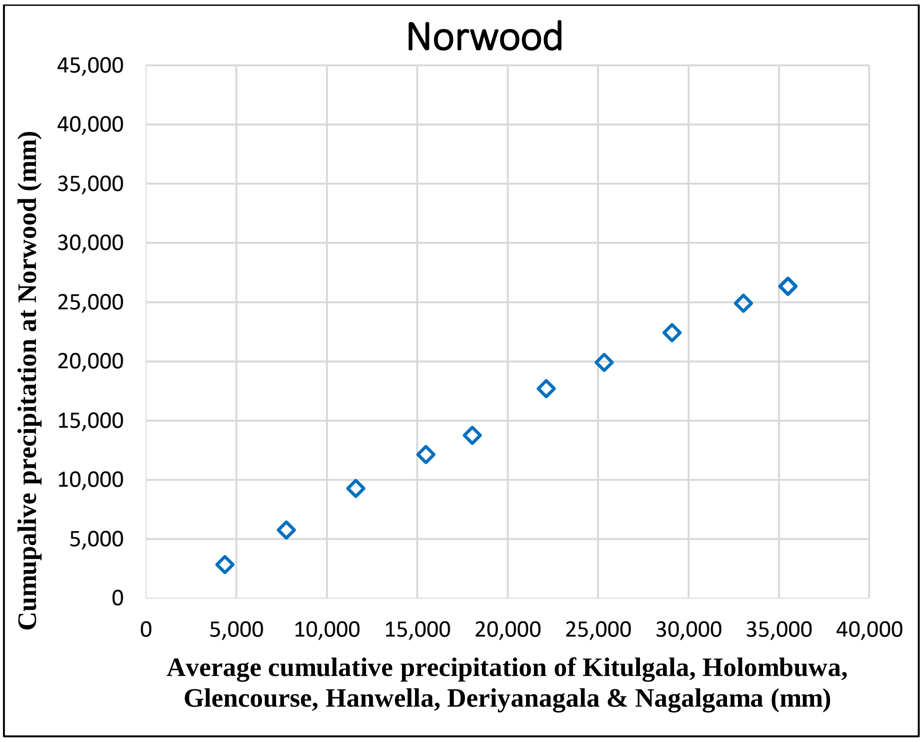

Figure D 2 Double Mass Curve for Norwood Station

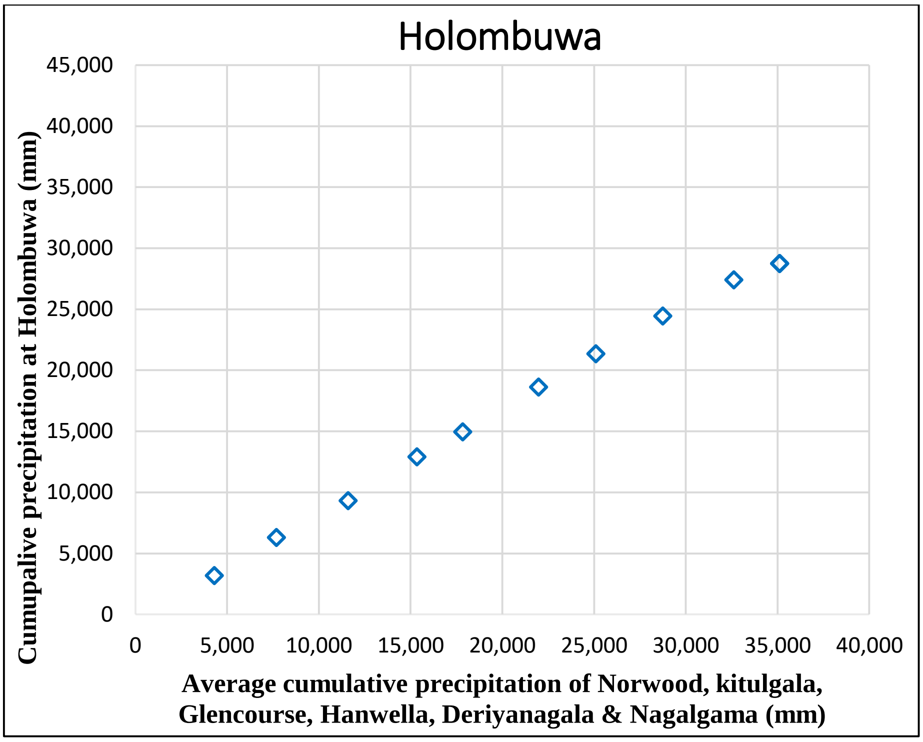

Figure D 3 Double Mass Curve for Holombuwa Station

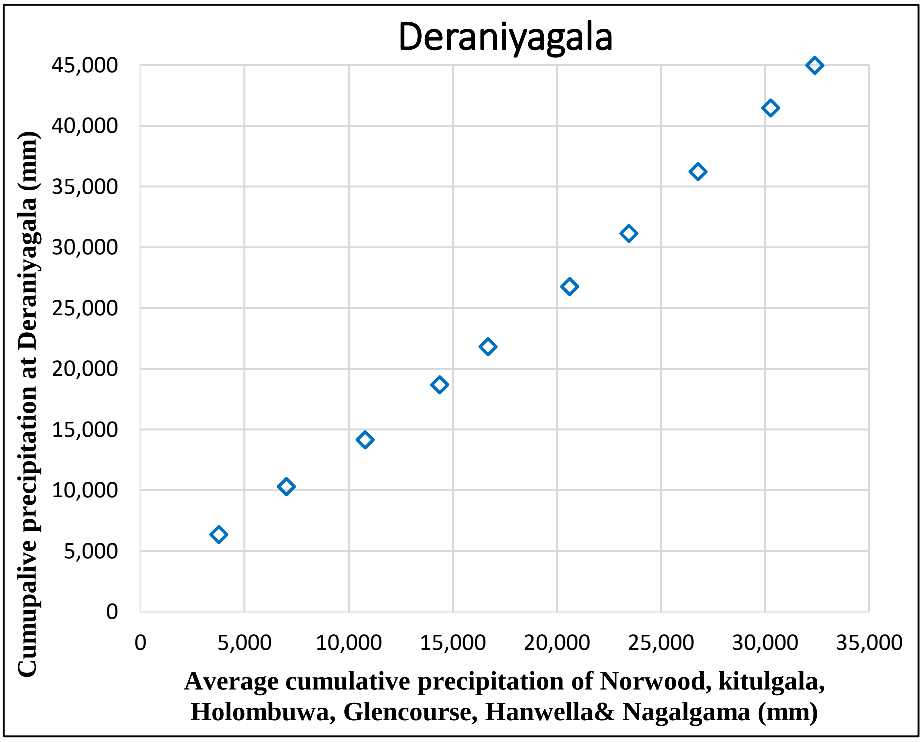

Figure D 4 Double Mass Curve for Deraniyagala Station

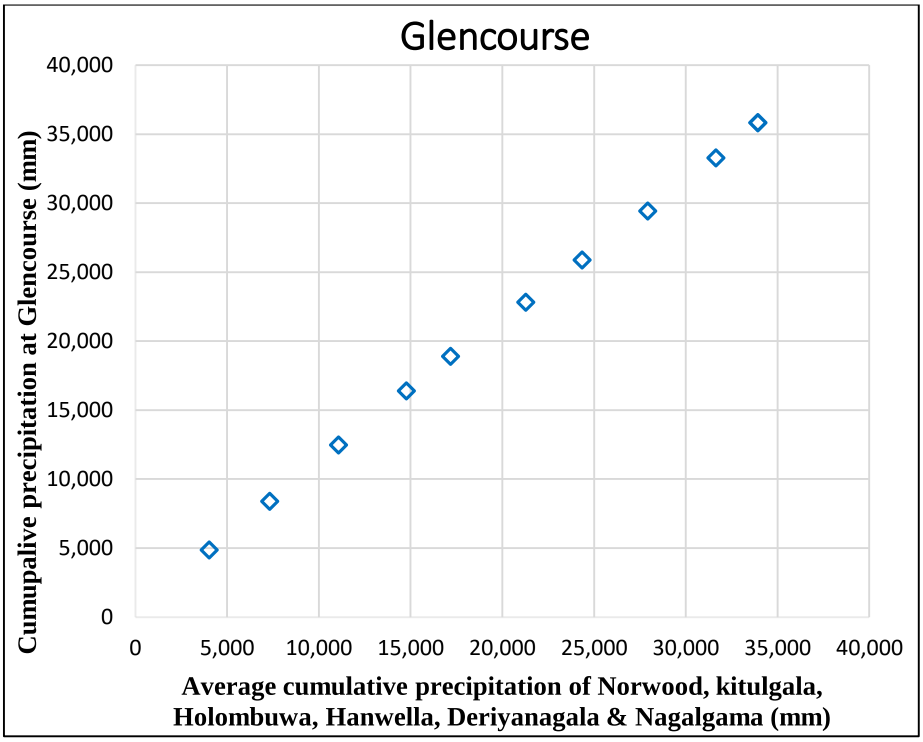

Figure D 5 Double Mass Curve for Glencorse Station

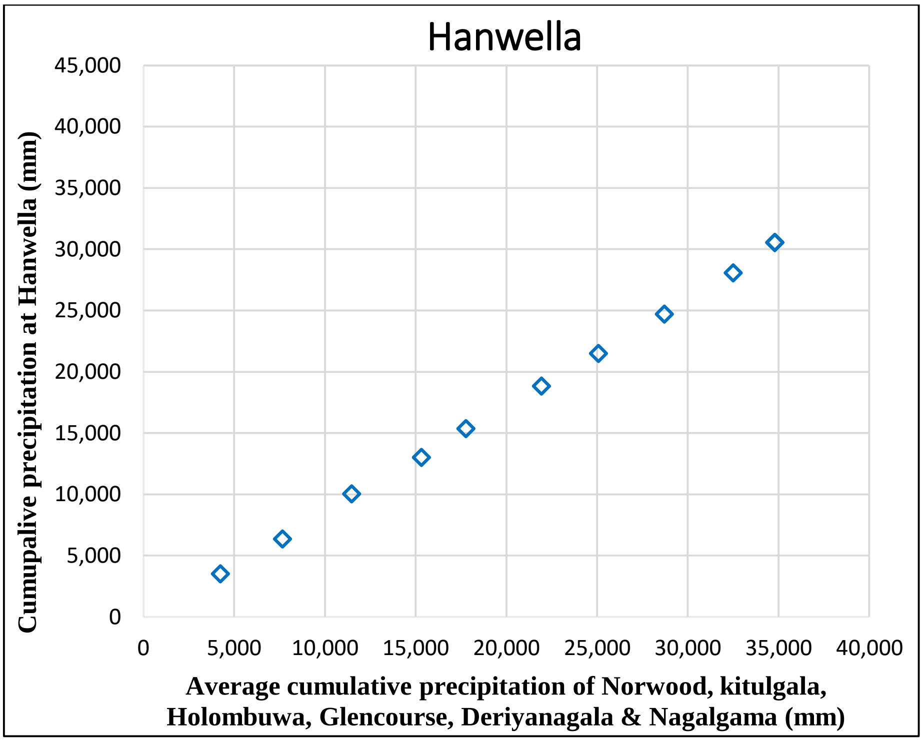

Figure D 6 Double Mass Curve for Hanwella Station

APPENDIX E: MODEL SIMULATION AND CALIBRATION

EVENT 1			
Date	Rainfall	Observed Flow	Simulated Flow
7-Nov-08	1.148	33.9	33.9
8-Nov-08	18.153	33.6	39.7
9-Nov-08	12.590	73.8	63.7
10-Nov-08	0.000	68.3	68.6
11-Nov-08	0.185	43.9	50.8
12-Nov-08	5.967	34.5	43.3
EVENT 2			
Date	Rainfall	Observed Flow	Simulated Flow
6-Jan-09	0.192	20.400	20.7
7-Jan-09	3.549	27.800	25.8
8-Jan-09	0.231	20.400	23.4
9-Jan-09	0.792	20.500	19.4
EVENT 3			
Date	Rainfall	Observed Flow	Simulated Flow
25-Jan-09	0.2	18.6	18.6
26-Jan-09	4.8	18.6	12.5
27-Jan-09	40.6	20.3	22.7
28-Jan-09	4.3	39	36.6
29-Jan-09	0	22.4	32.2
30-Jan-09	0	18.8	22.1
31-Jan-09	0	17.4	14.8
EVENT 4			
Date	Rainfall	Observed Flow	Simulated Flow
21-Feb-09	0.690	16	16
22-Feb-09	8.603	15	12.4
23-Feb-09	6.520	16	13.6
24-Feb-09	8.569	20	19.9
25-Feb-09	0.000	20.1	23.1
26-Feb-09	0.000	17	15.6
27-Feb-09	0.031	16.4	16
28-Feb-09	0.000	16.2	14.9
1-Mar-09	0.000	15.4	13.9

EVENT 5			
Date	Rainfall	Observed Flow	Simulated Flow
25-Jul-09	0.122426	30.78	31.2
26-Jul-09	7.025532	27	25
27-Jul-09	19.74869	27	23.2
28-Jul-09	4.360493	33.38	24.5
29-Jul-09	2.443287	32.84	21.2
30-Jul-09	13.34698	27.2	20.2
31-Jul-09	16.91082	38.2	32.1
1-Aug-09	7.588688	46.6	42.4
2-Aug-09	18.36129	32.57	47.7
3-Aug-09	0.765921	35.8	48.9
4-Aug-09	3.623949	32.3	31.6
5-Aug-09	1.661961	30.4	24.3
6-Aug-09	8.884722	28.8	26.2
7-Aug-09	22.46639	33.11	54.6
8-Aug-09	1.580506	71.25	77.4
9-Aug-09	1.949241	41.4	49.8
10-Aug-09	0.061517	36.6	38.1
11-Aug-09	0.825963	30.4	30.4
12-Aug-09	1.253862	30.39	24.2
EVENT 6			
Date	Rainfall	Observed Flow	Simulated Flow
12-Oct-09	15.904	38.200	38.200
13-Oct-09	10.813	43.000	45
14-Oct-09	50.282	57.800	65
15-Oct-09	5.764	131.800	142
16-Oct-09	2.523	110.880	115
17-Oct-09	0.000	109.000	100.9
18-Oct-09	36.938	59.250	72.3
19-Oct-09	15.346	115.260	120
20-Oct-09	16.110	122.670	130
21-Oct-09	1.524	122.340	120
22-Oct-09	0.000	71.250	70
23-Oct-09	0.000	66.050	55
24-Oct-09	0.000	49.600	40.2

EVENT 7			
Date	Rainfall	Observed Flow	Simulated Flow
8-Jan-10	0.031	24.960	25
9-Jan-10	26.606	26.000	16.8
10-Jan-10	0.830	56.350	26.7
11-Jan-10	22.200	33.380	38.9
12-Jan-10	26.088	85.000	86.3
13-Jan-10	10.635	116.120	120
14-Jan-10	0.256	60.700	69
15-Jan-10	0.000	34.750	32
16-Jan-10	1.987	30.020	28.2
17-Jan-10	0.720	27.000	20.1
EVENT 8			
Date	Rainfall	Observed Flow	Simulated Flow
9-Feb-10	0.288	19.4	19.4
10-Feb-10	17.347	19.8	16.0
11-Feb-10	0.000	24.0	26.0
12-Feb-10	0.000	21.3	21.0
13-Feb-10	0.544	21.1	19.0
14-Feb-10	0.000	20.8	20.0
15-Feb-10	0.000	20.0	20.0
EVENT 9			
Date	Rainfall	Observed Flow	Simulated Flow
15-Dec-10	2.449	69.82	70
16-Dec-10	7.402	68.40	58.5
17-Dec-10	4.932	90.47	62
18-Dec-10	0.323	68.65	63.4
19-Dec-10	0.232	52.08	49
20-Dec-10	0.000	42.83	40
21-Dec-10	4.444	43.18	45
22-Dec-10	6.316	46.54	48
23-Dec-10	33.028	48.58	57.6
24-Dec-10	7.543	96.75	95.7
25-Dec-10	0.000	75.48	76.8
26-Dec-10	0.348	51.10	45.5
27-Dec-10	0.000	35.69	25.6
28-Dec-10	1.537	37.09	26.7
29-Dec-10	0.173	33.73	22.4
30-Dec-10	0.148	33.21	23.2
31-Dec-10	2.732	31.22	25
1-Jan-11	4.420	32.61	27
2-Jan-11	1.537	37.36	28
3-Jan-11	0.384	33.31	29

4-Jan-11	0.308	25.35	28
5-Jan-11	0.000	23.82	22
6-Jan-11	0.123	22.90	20
EVENT 10			
Date	Rainfall	Observed Flow	Simulated Flow
3-Oct-11	0.317	24.526	24.526
4-Oct-11	2.087	25.187	27.800
5-Oct-11	0.192	24.873	24.873
6-Oct-11	0.551	23.840	23.840
EVENT 11			
Date	Rainfall	Observed Flow	Simulated Flow
4-Jan-12	1.71	13.98	14.0
5-Jan-12	6.52	14.34	9.1
6-Jan-12	27.64	16.58	12.4
7-Jan-12	13.46	19.05	19.8
8-Jan-12	13.54	34.98	34.1
9-Jan-12	1.34	25.98	28.1
10-Jan-12	12.53	20.02	20.5
EVENT 12			
Date	Rainfall	Observed Flow	Simulated Flow
3-Feb-12	2.14	13.35	13.4
4-Feb-12	14.68	13.04	10.0
5-Feb-12	4.25	16.51	17.0
6-Feb-12	0.00	15.36	17.3
7-Feb-12	0.19	15.75	16.8
8-Feb-12	0.11	14.50	16.0
9-Feb-12	5.34	18.11	20.0
10-Feb-12	17.33	19.00	22.0
11-Feb-12	0.00	19.38	22.0
12-Feb-12	0.00	16.68	16.0
13-Feb-12	11.60	15.19	12.0
14-Feb-12	27.78	16.32	14.0
15-Feb-12	0.86	24.14	28.0
16-Feb-12	10.23	19.80	19.8
17-Feb-12	6.87	23.01	20.0

EVENT 13			
Date	Rainfall	Observed Flow	Simulated Flow
27-Feb-12	27.80	12.96	13.0
28-Feb-12	14.99	18.00	13.4
29-Feb-12	0.00	17.15	14.0
1-Mar-12	8.84	15.32	13.0
2-Mar-12	0.00	16.49	12.0
3-Mar-12	0.00	15.26	13.0
4-Mar-12	0.11	13.05	12.0
5-Mar-12	7.00	13.33	14.0
6-Mar-12	0.00	15.20	16.0
7-Mar-12	0.00	15.12	16.0
8-Mar-12	0.00	13.09	12.0
9-Mar-12	0.00	14.03	11.0
10-Mar-12	2.07	14.04	10.0
11-Mar-12	0.06	13.14	10.0
12-Mar-12	6.50	13.18	11.0
13-Mar-12	14.43	14.14	12.0
14-Mar-12	4.07	17.19	17.0
15-Mar-12	23.48	17.04	19.0
16-Mar-12	26.46	21.48	24.0
17-Mar-12	12.28	30.31	32.0
18-Mar-12	0.09	24.43	25.5
19-Mar-12	0.00	17.842	17.0
20-Mar-12	0.00	17.042	16.0
21-Mar-12	0.00	16.325	14.7
EVENT 18			
Date	Rainfall	Observed Flow	Simulated Flow
22-Jan-13	0.63	20.59	19.0
23-Jan-13	6.87	20.46	18.0
24-Jan-13	8.51	20.95	20.0
25-Jan-13	3.92	20.93	20.0
26-Jan-13	1.54	20.46	19.0

EVENT 14			
Date	Rainfall	Observed Flow	Simulated Flow
27-Mar-12	7.21	12.933	12.2
28-Mar-12	21.88	13.533	7.6
29-Mar-12	42.98	19.079	32.7
30-Mar-12	7.78	67.720	47.0
31-Mar-12	2.47	20.142	38.4
1-Apr-12	3.96	17.375	30.4
2-Apr-12	13.42	18.800	31.7
3-Apr-12	9.55	26.478	36.6
4-Apr-12	10.97	36.156	39.3
5-Apr-12	0.00	24.678	34.9
6-Apr-12	0.77	19.350	24.7
7-Apr-12	11.79	18.321	26.4
8-Apr-12	32.65	25.414	25.0
9-Apr-12	25.43	49.194	52.0
10-Apr-12	30.96	81.301	92.0
11-Apr-12	16.19	114.826	124.9
12-Apr-12	0.77	61.235	56.0
13-Apr-12	14.59	34.498	30.0
14-Apr-12	35.53	56.498	63.0
15-Apr-12	39.56	135.189	171.4
16-Apr-12	8.09	234.983	235.0
17-Apr-12	12.23	103.283	110.0
18-Apr-12	4.55	91.981	101.0
19-Apr-12	1.48	71.658	78.0
20-Apr-12	11.01	50.140	83.1
21-Apr-12	41.48	58.444	100.0
22-Apr-12	15.14	145.194	155.0
23-Apr-12	4.87	197.225	201.0
24-Apr-12	7.97	106.551	111.0
25-Apr-12	3.54	81.604	91.0
26-Apr-12	13.95	66.804	72.0
27-Apr-12	3.61	75.890	67.0
28-Apr-12	1.27	55.144	50.0
29-Apr-12	6.76	34.575	30.0
30-Apr-12	4.53	32.760	28.0
1-May-12	0.15	37.084	20.0

EVENT 15			
Date	Rainfall	Observed Flow	Simulated Flow
10-May-12	0.19	19.49	19.5
11-May-12	0.15	18.65	20.0
12-May-12	0.00	18.88	21.0
13-May-12	1.78	17.70	21.0
14-May-12	0.14	17.60	17.6
EVENT 16			
Date	Rainfall	Observed Flow	Simulated Flow
17-Jul-12	0.25	24.692	24.7
18-Jul-12	1.33	22.667	17.0
19-Jul-12	0.00	22.400	18.0
20-Jul-12	0.00	22.108	18.7
21-Jul-12	0.29	21.746	18.9
22-Jul-12	5.62	20.133	20.0
23-Jul-12	5.33	20.346	20.0
24-Jul-12	7.31	23.124	22.0
25-Jul-12	4.71	24.308	23.0
26-Jul-12	0.28	28.868	30.0
27-Jul-12	0.00	21.964	21.0
28-Jul-12	0.00	20.033	20.0
29-Jul-12	0.00	19.321	17.8
30-Jul-12	0.00	17.883	16.0
EVENT 17			
Date	Rainfall	Observed Flow	Simulated Flow
4-Aug-12	0.67	17.100	17.1
5-Aug-12	2.92	15.950	14.5
6-Aug-12	3.85	16.108	12.4
7-Aug-12	0.55	17.367	10.5
8-Aug-12	0.08	16.725	9.0
9-Aug-12	19.75	17.317	9.5
10-Aug-12	9.70	19.677	11.7
11-Aug-12	3.53	23.491	12.4
12-Aug-12	1.71	19.088	11.4
13-Aug-12	1.98	17.533	10.2
14-Aug-12	10.03	17.517	11.9
15-Aug-12	35.78	18.771	28.4
16-Aug-12	28.24	45.539	55.4
17-Aug-12	9.34	88.977	82.4
18-Aug-12	4.05	84.833	80.6
19-Aug-12	0.00	30.523	42.4
20-Aug-12	0.12	23.383	31.4
21-Aug-12	4.03	21.192	25.8

EVENT 18			
Date	Rainfall	Observed Flow	Simulated Flow
22-Jan-13	0.63	20.59	19.0
23-Jan-13	6.87	20.46	18.0
24-Jan-13	8.51	20.95	20.0
25-Jan-13	3.92	20.93	20.0
26-Jan-13	1.54	20.46	19.0
EVENT 19			
Date	Rainfall	Observed Flow	Simulated Flow
4-Feb-13	6.39	17.83	18.3
5-Feb-13	1.76	22.02	15.6
6-Feb-13	24.10	19.45	14.7
7-Feb-13	24.33	23.03	21.6
8-Feb-13	4.68	40.78	31.7
9-Feb-13	34.52	23.37	35.6
10-Feb-13	0.00	49.85	48.9
11-Feb-13	0.13	24.98	25.0
12-Feb-13	0.77	21.68	25.0
13-Feb-13	20.67	21.33	27.0
14-Feb-13	6.30	50.38	54.2
15-Feb-13	0.19	36.48	32.1
EVENT 20			
Date	Rainfall	Observed Flow	Simulated Flow
3-Mar-13	0.45	16.50	16.5
4-Mar-13	1.51	15.67	15.0
5-Mar-13	0.75	17.23	14.7
6-Mar-13	11.09	18.37	21.0
7-Mar-13	4.63	23.29	27.0
8-Mar-13	14.23	22.36	25.0
9-Mar-13	26.80	28.80	34.0
10-Mar-13	2.48	44.51	54.0
11-Mar-13	0.38	21.39	18.0
12-Mar-13	0.48	21.17	21.0
13-Mar-13	0.96	20.38	18.0
14-Mar-13	23.21	20.34	13.0

EVENT 21			
Date	Rainfall	Observed Flow	Simulated Flow
30-Sep-13	2.02	34.50	34.5
1-Oct-13	7.18	32.57	30.4
2-Oct-13	5.68	40.60	28.4
3-Oct-13	0.00	33.92	25.3
4-Oct-13	8.83	32.30	23.8
5-Oct-13	0.57	34.75	22.7
6-Oct-13	0.00	29.26	19.8
7-Oct-13	11.89	27.00	20.5
8-Oct-13	0.43	31.92	21.3
9-Oct-13	11.09	27.60	22.4
10-Oct-13	24.56	45.40	32.4
11-Oct-13	15.97	65.05	44.7
12-Oct-13	17.66	62.15	54.9
13-Oct-13	5.08	68.30	59.8
14-Oct-13	0.00	60.70	56.3
15-Oct-13	0.06	33.38	50.7
16-Oct-13	3.93	31.16	47.6
17-Oct-13	27.57	44.20	59.1
18-Oct-13	4.68	68.50	70.2
19-Oct-13	54.95	39.80	98.4
20-Oct-13	28.51	195.60	199.7
21-Oct-13	19.49	250.70	257.6
22-Oct-13	6.94	146.10	160.3
23-Oct-13	1.06	113.52	120.3
24-Oct-13	1.67	70.50	106.6
25-Oct-13	0.36	57.80	85.8
EVENT 22			
Date	Rainfall	Observed Flow	Simulated Flow
6-Jan-14	3.57	17.20	17.20
7-Jan-14	0.00	17.40	14.00
8-Jan-14	0.00	17.60	13.90
9-Jan-14	0.00	19.60	16.70
10-Jan-14	0.12	20.10	19.43
11-Jan-14	0.00	18.20	17.10
12-Jan-14	11.56	19.80	19.10
13-Jan-14	4.77	24.70	25.00
14-Jan-14	6.09	21.20	20.00
15-Jan-14	13.62	20.10	20.00
16-Jan-14	23.00	23.30	20.00

EVENT 23			
Date	Rainfall	Observed Flow	Simulated Flow
20-Feb-14	0.635	17.00	17
21-Feb-14	0.108	16.80	14
22-Feb-14	1.553	17.20	14.5
23-Feb-14	19.864	17.40	15
24-Feb-14	0.000	19.60	16
25-Feb-14	0.000	16.60	16
26-Feb-14	0.000	15.80	16.7
27-Feb-14	39.543	14.60	16
28-Feb-14	12.223	31.54	41
1-Mar-14	0.000	17.80	17
2-Mar-14	0.000	15.40	14
3-Mar-14	0.000	13.40	14
4-Mar-14	8.434	15.40	14.5
5-Mar-14	14.880	16.60	14.2
6-Mar-14	12.545	17.20	14
7-Mar-14	29.193	23.20	25
8-Mar-14	1.525	34.150	37
9-Mar-14	0.000	18.600	18
10-Mar-14	0.000	13.600	13
11-Mar-14	0.000	12.800	10
12-Mar-14	0.000	12.800	9.93
EVENT 24			
Date	Rainfall	Observed Flow	Simulated Flow
1-Apr-14	3.4	16.4	16.4
2-Apr-14	0.1	15.6	10
3-Apr-14	7.0	15.0	8
4-Apr-14	17.0	16.4	9.7
5-Apr-14	15.5	19.2	12.2
6-Apr-14	22.0	21.6	15
7-Apr-14	31.8	25.0	22
8-Apr-14	4.7	33.7	35
9-Apr-14	0.0	25.7	26
10-Apr-14	3.4	19.4	18
11-Apr-14	4.8	18.4	16.3
12-Apr-14	1.6	18.2	15

EVENT 25			
Date	Rainfall	Observed Flow	Simulated Flow
10-Nov-14	1.564	68.452	68.45
11-Nov-14	27.612	82.613	51.12
12-Nov-14	0.693	150.056	87.00
13-Nov-14	20.497	123.181	101.30
14-Nov-14	27.881	161.822	161.89
15-Nov-14	4.081	208.100	222.10
16-Nov-14	25.043	147.838	131.00
17-Nov-14	2.344	199.329	210.98
18-Nov-14	6.970	122.863	142.00
19-Nov-14	0.812	116.150	125.80
20-Nov-14	1.655	82.313	102.10
21-Nov-14	17.889	71.767	87.00
EVENT 26			
Date	Rainfall	Observed Flow	Simulated Flow
22-Feb-15	0.730	21.938	21.938
23-Feb-15	3.457	21.554	12.869
24-Feb-15	13.675	21.771	14.89
25-Feb-15	2.415	33.601	19.1
26-Feb-15	12.332	27.762	22
27-Feb-15	20.749	33.895	30.89
28-Feb-15	12.824	57.632	65.87
1-Mar-15	19.544	37.282	38.1
2-Mar-15	11.724	54.189	60.78
3-Mar-15	3.268	47.343	50.4
4-Mar-15	16.894	37.918	36.5
5-Mar-15	1.261	69.408	72.3
6-Mar-15	0.000	37.448	35.3
7-Mar-15	0.000	27.069	30.6
8-Mar-15	0.000	23.999	28.46
9-Mar-15	4.647	22.183	26.17

EVENT 27			
Date	Rainfall	Observed Flow	Simulated Flow
26-Mar-15	20.836	19.53	19.5
27-Mar-15	4.116	26.96	12.1
28-Mar-15	39.448	33.18	15.9
29-Mar-15	15.477	64.98	35.4
30-Mar-15	8.167	58.71	60.1
31-Mar-15	19.845	35.67	55.2
1-Apr-15	19.163	72.63	71.3
2-Apr-15	30.318	117.71	125.3
3-Apr-15	0.134	118.97	132.0
4-Apr-15	2.841	45.75	55.0
5-Apr-15	0.000	31.28	37.2
6-Apr-15	28.122	28.34	30.1
EVENT 28			
Date	Rainfall	Observed Flow	Simulated Flow
26-Dec-15	1.183	54.108	54.1
27-Dec-15	7.432	57.433	50.0
28-Dec-15	0.080	58.117	45.0
29-Dec-15	6.290	57.469	60.0
30-Dec-15	0.000	61.142	60.0
31-Dec-15	0.000	51.303	43.0
1-Jan-16	0.440	47.548	40.0
2-Jan-16	0.112	43.127	35.0
EVENT 29			
Date	Rainfall	Observed Flow	Simulated Flow
23-Jan-16	8.304	28.892	28.9
24-Jan-16	5.069	37.342	38.0
25-Jan-16	0.790	40.940	45.0
26-Jan-16	0.647	34.993	38.0
27-Jan-16	0.000	28.896	29.3
28-Jan-16	0.000	32.029	28.0
29-Jan-16	0.000	30.730	27.0
30-Jan-16	0.000	28.044	25.0

EVENT 30			
Date	Rainfall	Observed Flow	Simulated Flow
27-Mar-16	4.518	26.708	26.71
28-Mar-16	49.130	22.175	19.20
29-Mar-16	18.487	64.983	55.30
30-Mar-16	27.078	61.019	48.50
31-Mar-16	3.148	62.618	44.00
1-Apr-16	24.359	36.005	38.90
2-Apr-16	10.775	47.025	52.10
3-Apr-16	8.614	40.663	38.90
4-Apr-16	16.630	33.802	30.00
5-Apr-16	12.089	49.505	55.00
6-Apr-16	4.278	76.689	80.00
7-Apr-16	14.025	43.738	42.00
8-Apr-16	13.520	43.347	47.00
9-Apr-16	6.608	61.480	64.00
10-Apr-16	14.155	51.710	51.00
11-Apr-16	13.841	59.984	60.00
12-Apr-16	33.413	62.645	75.00
13-Apr-16	0.078	85.927	88.00
14-Apr-16	9.536	45.728	49.00
15-Apr-16	13.974	37.162	47.00
16-Apr-16	20.196	50.740	59.00
17-Apr-16	23.112	66.173	70.00
18-Apr-16	3.751	56.103	60.00
EVENT 31			
Date	Rainfall	Observed Flow	Simulated Flow
9-Sep-16	0.56	28.72	28.7
10-Sep-16	0.58	27.06	19.8
11-Sep-16	0.00	24.98	20.0
12-Sep-16	1.07	25.98	27.0
13-Sep-16	1.02	25.02	31.0
EVENT 32			
Date	Rainfall	Observed Flow	Simulated Flow
13-Oct-16	7.67	22.61	22.6
14-Oct-16	6.20	23.51	15.9
15-Oct-16	9.05	30.06	21.9
16-Oct-16	18.49	35.06	33.9
17-Oct-16	0.00	43.76	49.1
18-Oct-16	11.29	43.10	41.1
19-Oct-16	0.00	37.64	34.0
20-Oct-16	0.79	36.43	32.0
21-Oct-16	4.45	31.27	31.0

EVENT 33			
Date	Rainfall	Observed Flow	Simulated Flow
4-Dec-16	0.56	32.39	32.4
5-Dec-16	0.00	33.52	29.9
6-Dec-16	0.00	32.05	29.0
7-Dec-16	2.38	29.58	30.0
8-Dec-16	0.88	35.00	38.0
9-Dec-16	5.20	32.57	32.6
10-Dec-16	0.55	34.36	31.0
11-Dec-16	0.00	31.27	29.0
12-Dec-16	0.41	27.90	26.0
13-Dec-16	0.33	27.49	25.0
14-Dec-16	0.58	26.90	24.0
EVENT 34			
Date	Rainfall	Observed Flow	Simulated Flow
19-Jan-17	0.22	20.11	20.1
20-Jan-17	1.33	23.43	11.9
21-Jan-17	1.04	18.50	12.0
22-Jan-17	0.17	20.57	13.0
23-Jan-17	2.59	17.74	14.2
24-Jan-17	2.14	21.38	16.0
25-Jan-17	0.00	21.58	17.3
26-Jan-17	25.98	19.95	17.8
27-Jan-17	4.24	30.24	30.0
28-Jan-17	23.13	29.59	37.5
29-Jan-17	9.93	45.41	48.0
30-Jan-17	3.48	35.52	38.0
31-Jan-17	0.00	24.18	21.0
EVENT 35			
Date	Rainfall	Observed Flow	Simulated Flow
25-Feb-17	0.76	19.04	19.0
26-Feb-17	1.95	18.45	9.0
27-Feb-17	1.96	18.65	10.0
28-Feb-17	0.23	16.70	8.9
1-Mar-17	5.00	15.03	9.0
2-Mar-17	8.88	18.00	9.0
3-Mar-17	25.86	22.04	12.0
4-Mar-17	5.97	33.87	14.0
5-Mar-17	0.00	30.39	12.0
6-Mar-17	1.19	18.73	12.0
7-Mar-17	5.52	21.70	12.0
8-Mar-17	11.94	27.97	16.0
9-Mar-17	12.04	30.41	32.0

Date	Rainfall	Observed Flow	Simulated Flow
10-Mar-17	36.62	38.08	43.5
11-Mar-17	24.38	64.80	54.3
12-Mar-17	12.05	79.91	64.2
13-Mar-17	27.27	52.05	65.0
14-Mar-17	38.15	79.35	87.0
15-Mar-17	31.16	146.46	140.0
16-Mar-17	37.71	145.77	170.0
17-Mar-17	0.00	156.22	140.0
18-Mar-17	0.00	67.09	79.0
19-Mar-17	0.00	42.37	52.2
20-Mar-17	0.00	32.97	40.0
21-Mar-17	0.00	28.12	30.0
EVENT 36			
Date	Rainfall	Observed Flow	Simulated Flow
27-Mar-17	0.29	16.70	16.7
28-Mar-17	26.63	17.54	8.1
29-Mar-17	24.38	37.04	14.7
30-Mar-17	8.98	56.47	25.0
31-Mar-17	3.96	45.11	45.0
1-Apr-17	4.18	38.11	50.0
2-Apr-17	14.87	51.79	55.0
3-Apr-17	15.17	61.19	68.0
4-Apr-17	19.51	94.34	103.0
5-Apr-17	10.70	125.11	128.1
6-Apr-17	2.82	61.97	75.5
7-Apr-17	0.00	48.01	55.0
8-Apr-17	0.00	37.01	40.0
9-Apr-17	24.34	32.95	35.0

Table D 2 Curve Number and Initial Abstraction for all events

Event ID	CN	Ia
1	72.2	3.31
2	90.5	1.34
3	65.7	2.60
4	81.1	3.30
5	43.6	3.39
6	39.7	8.95
7	53.4	2.37
8	85.2	1.43
9	42.7	2.55
10	85.2	1.08
11	55.5	5.08
12	48.9	2.97
13	38.3	4.82
14	18.1	7.44
15	89.1	0.40
16	77.8	2.11
17	43.5	1.97
18	82.8	10.53
19	41.1	3.50
20	63.6	1.93
21	28.0	4.73
22	61.3	2.94
23	46.3	4.54
24	47.4	2.66
25	37.8	9.37
26	46.0	5.72
27	35.7	9.24
28	63.4	1.43
29	82.9	2.44
30	19.0	6.85
31	85.3	2.10
32	64.5	3.77
33	67.3	1.41
34	58.7	1.98
35	26.4	6.07
36	40.3	7.26

Event Calibration Hydrograph

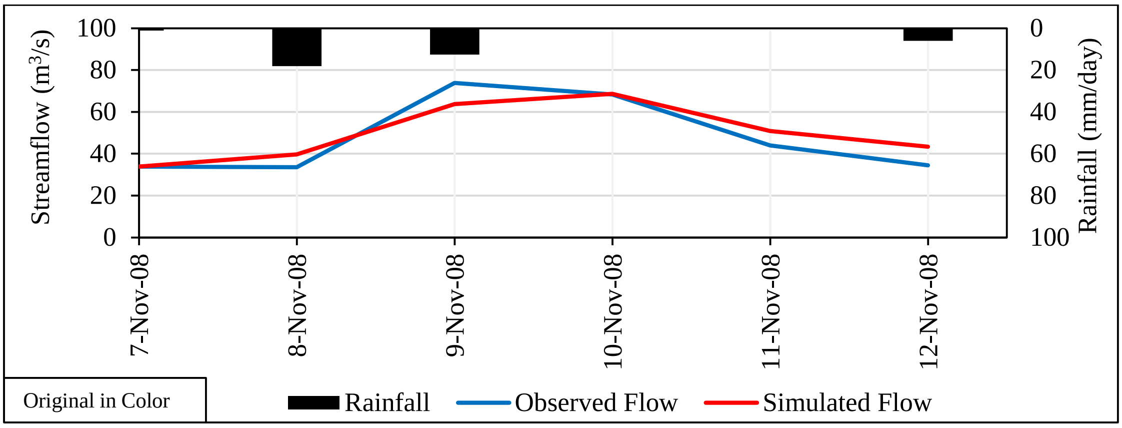

Figure E 1 Performance of event 1 lumped Kelani model

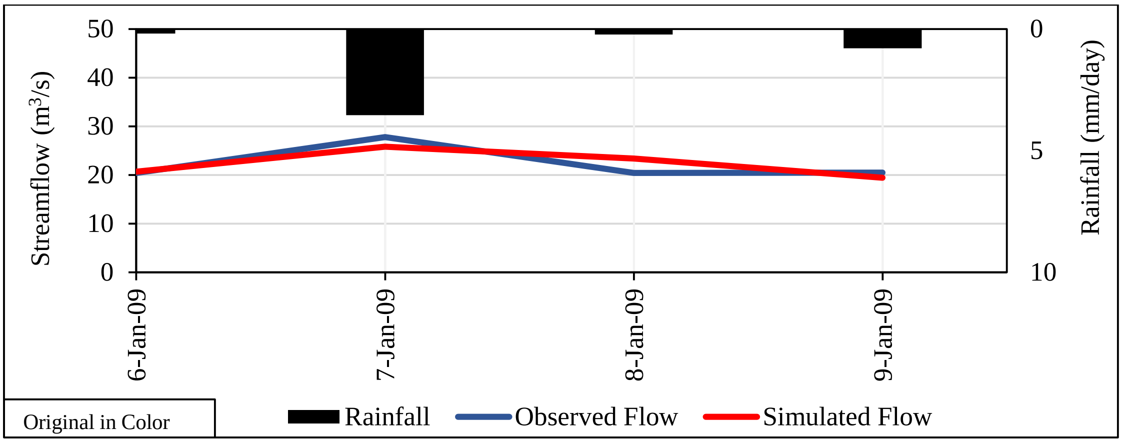

Figure E 2 Performance of event 2 lumped Kelani model

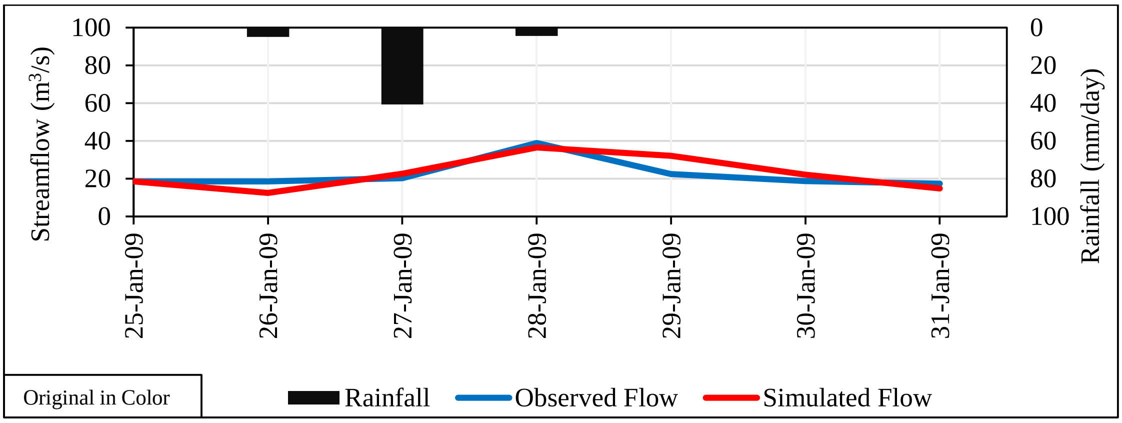

Figure E 3 Performance of event 3 lumped Kelani model

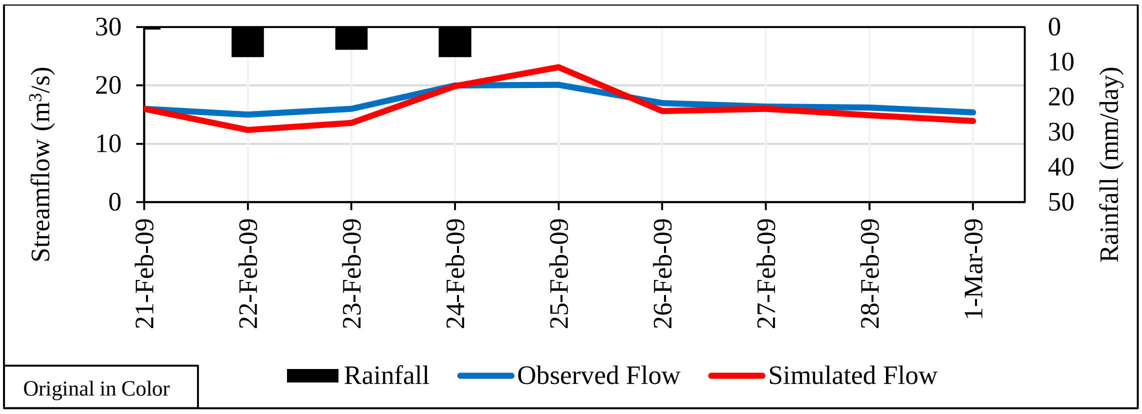

Figure E 4 Performance of event 4 lumped Kelani model

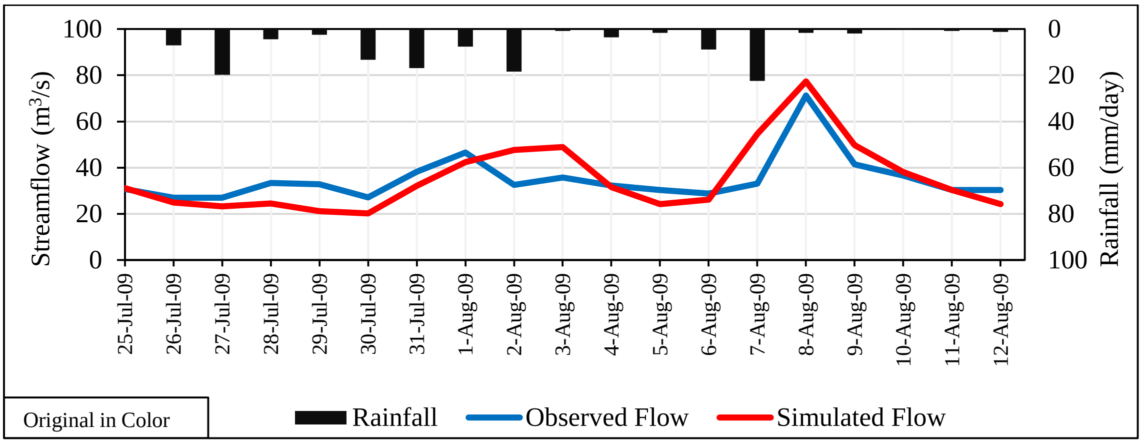

Figure E 5 Performance of event 5 lumped Kelani model

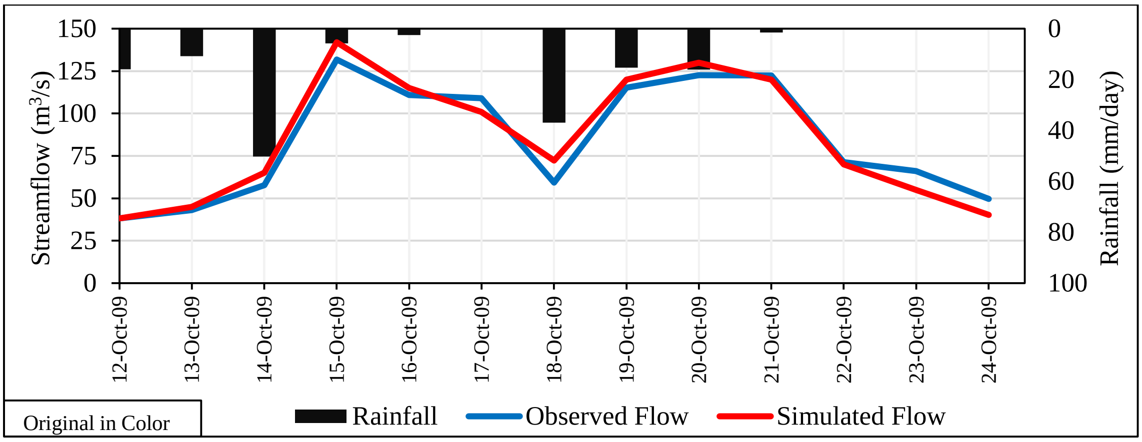

Figure E 6 Performance of event 6 lumped Kelani model

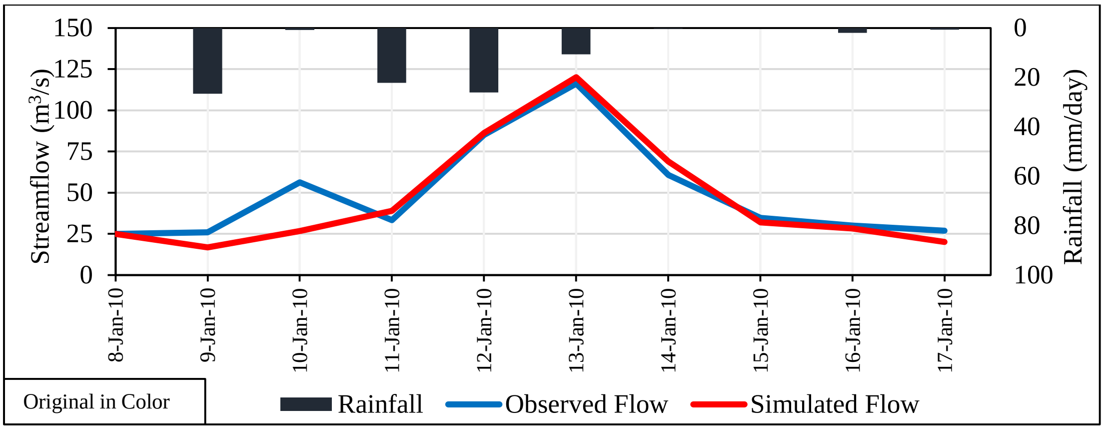

Figure E 7 Performance of event 7 lumped Kelani model

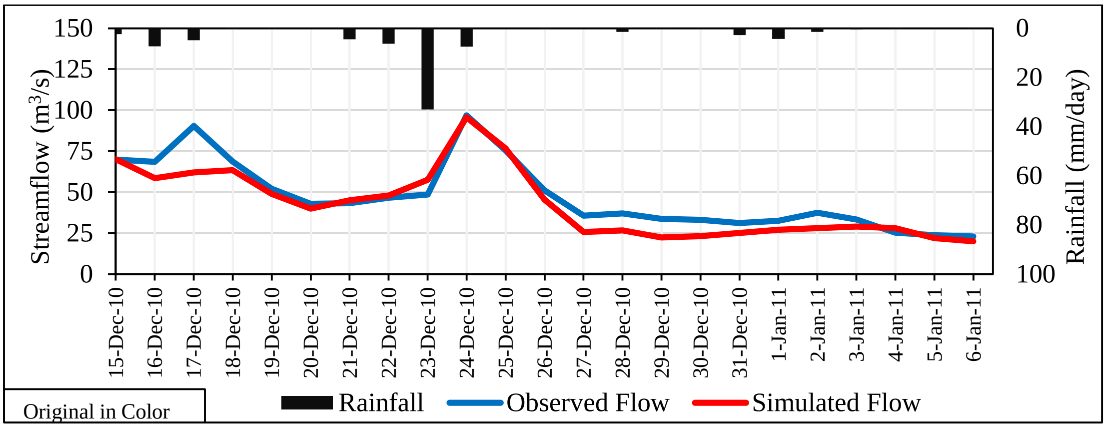

Figure E 8 Performance of event 9 lumped Kelani model

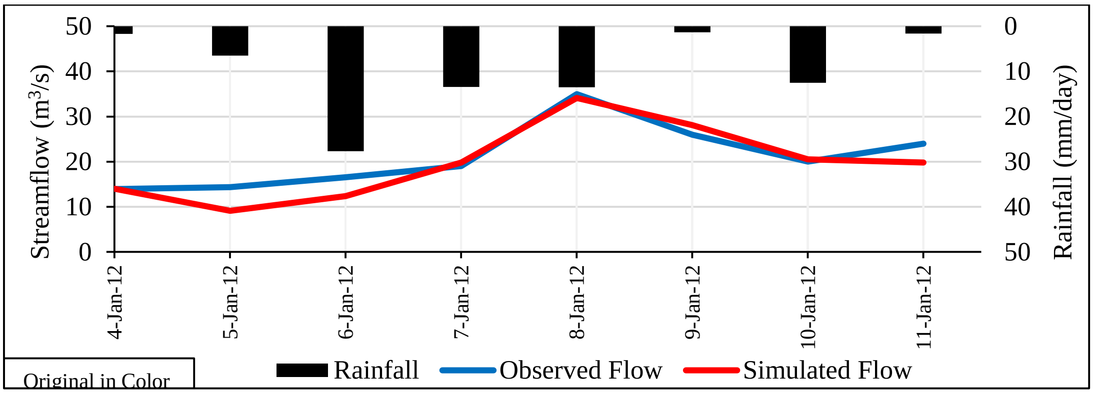

Figure E 9 Performance of event 11 lumped Kelani model

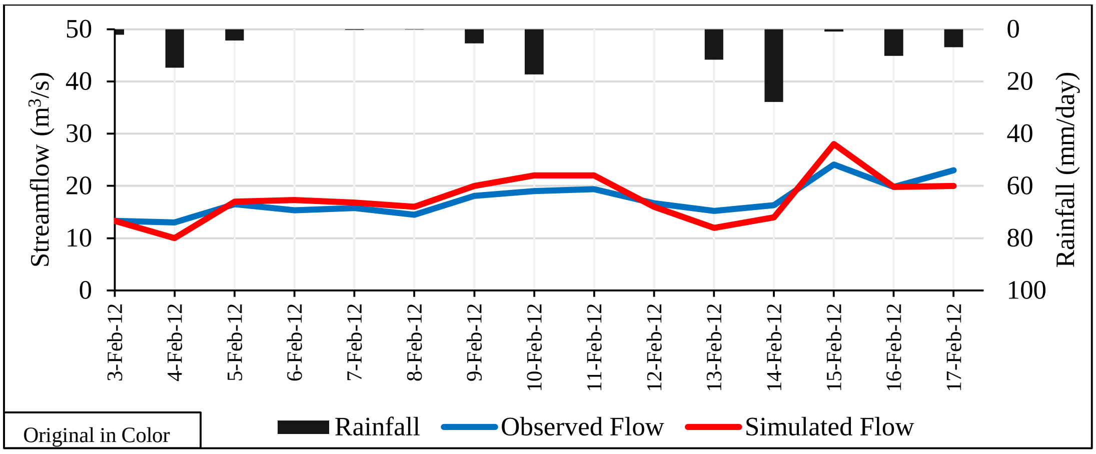

Figure E 10 Performance of event 12 lumped Kelani model

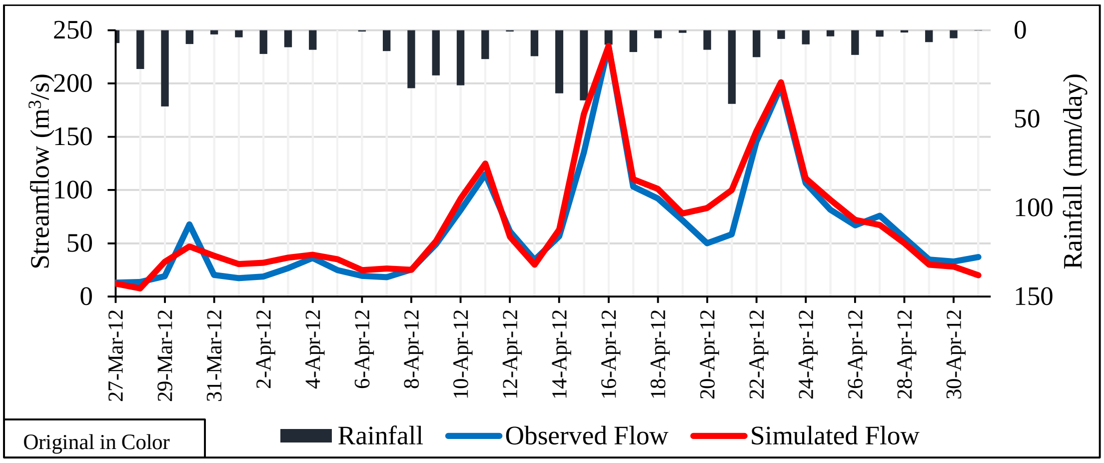

Figure E 11 Performance of event 14 lumped Kelani model

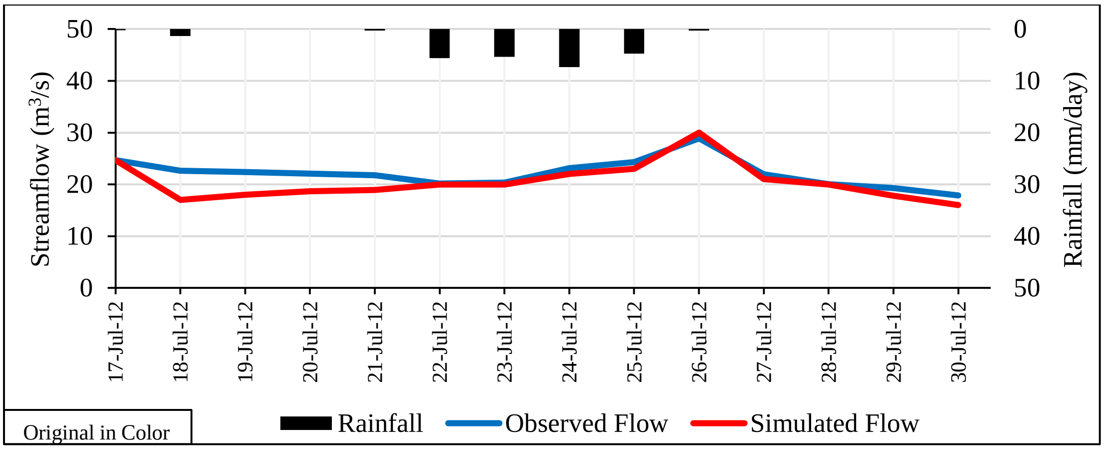

Figure E 12 Performance of event 16 lumped Kelani model

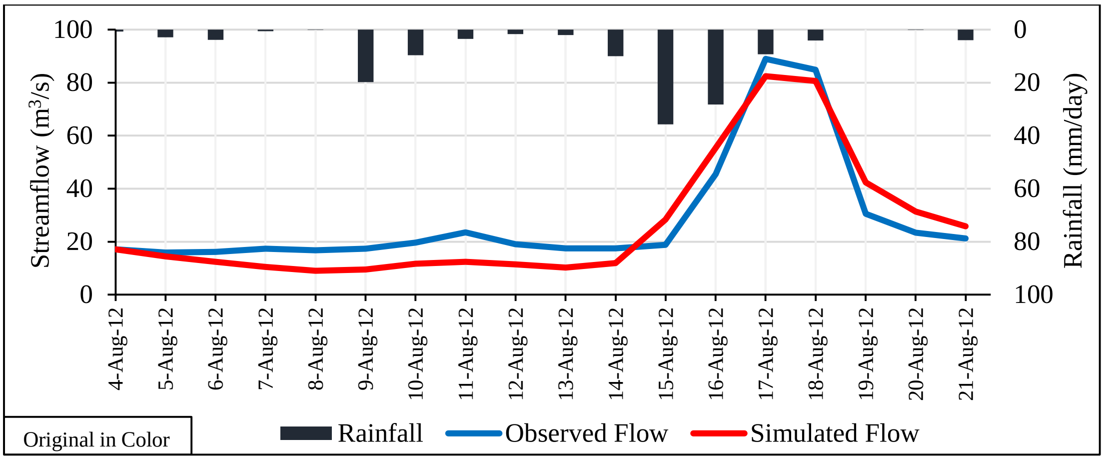

Figure E 13 Performance of event 17 lumped Kelani model

Event Verification Hydrograph

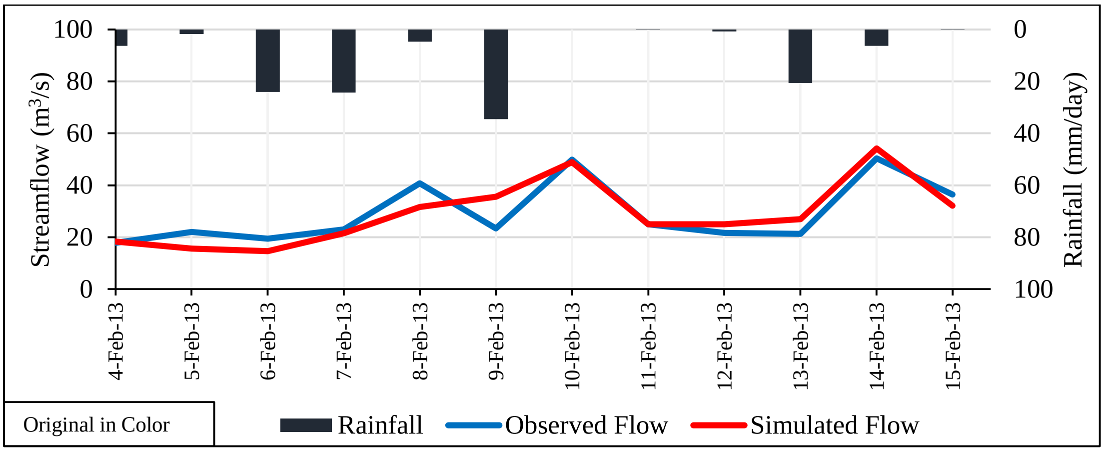

Figure E 14 Performance of event 19 lumped Kelani model

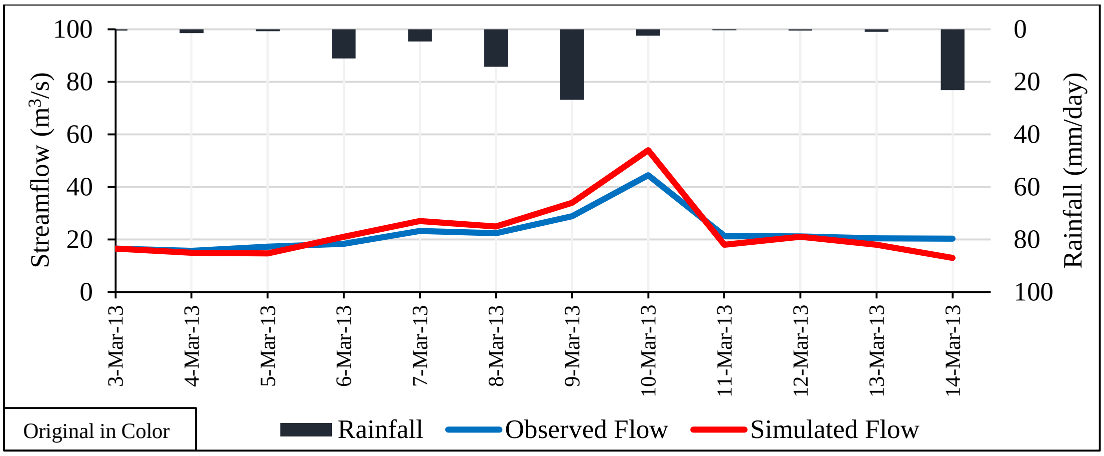

Figure E 15 Performance of event 20 lumped Kelani model

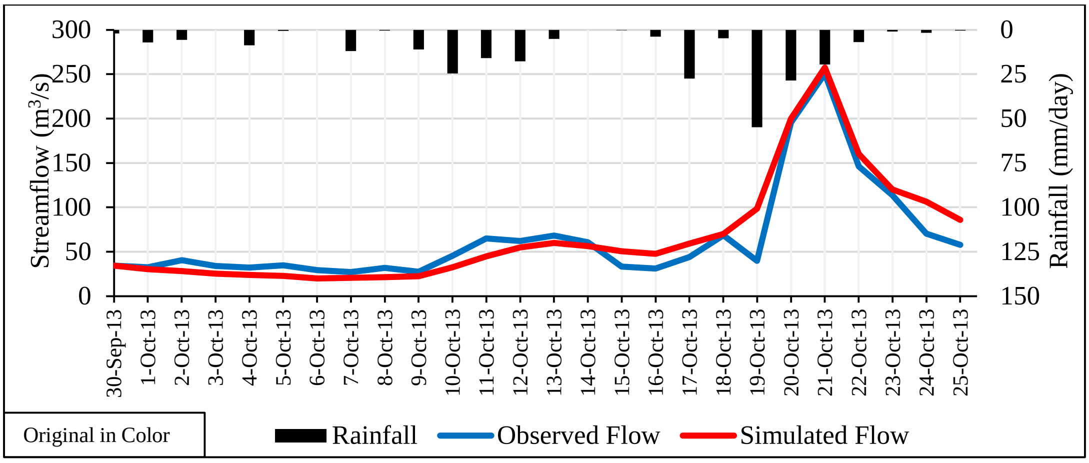

Figure E 16 Performance of event 21 lumped Kelani model

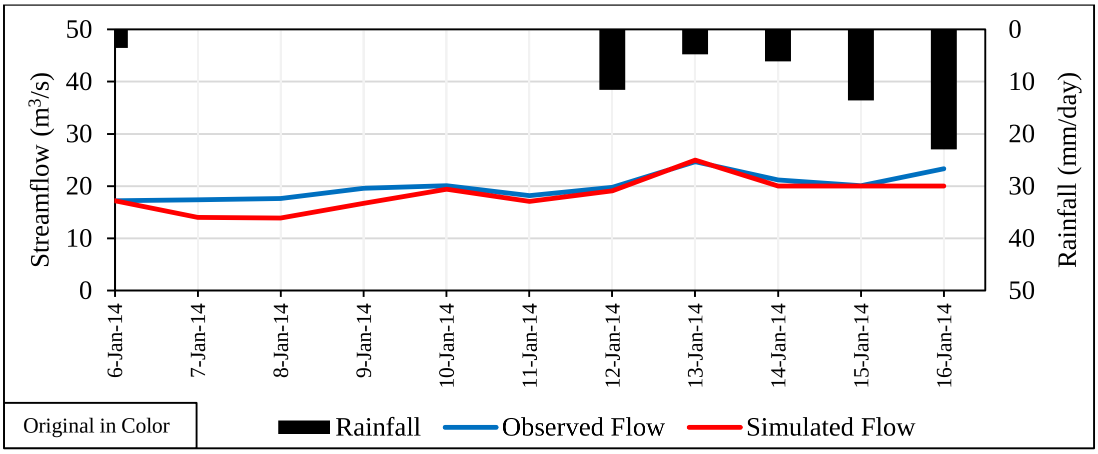

Figure E 17 Performance of event 22 lumped Kelani model

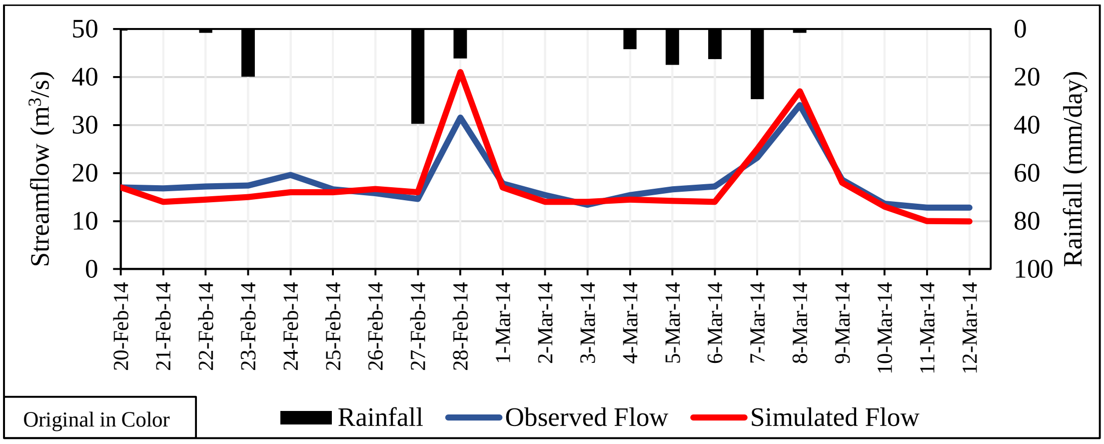

Figure E 18 Performance of event 23 lumped Kelani model

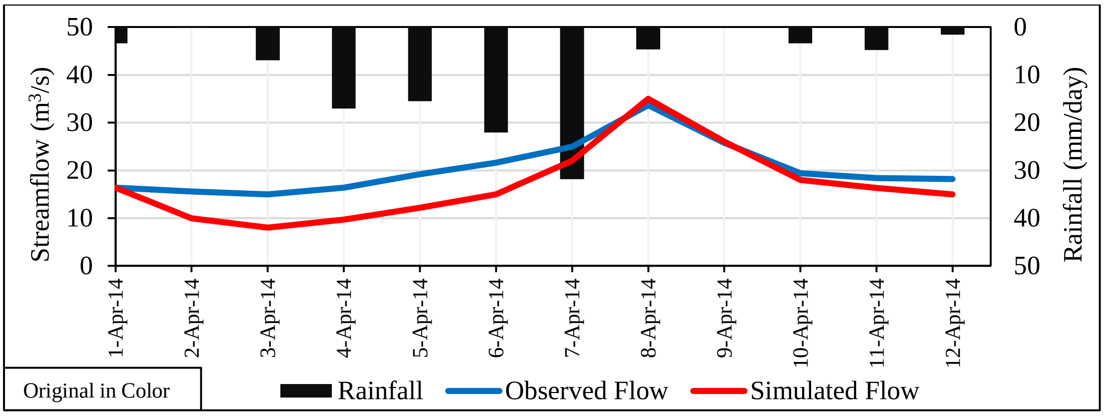

Figure E 19 Performance of event 24 lumped Kelani model

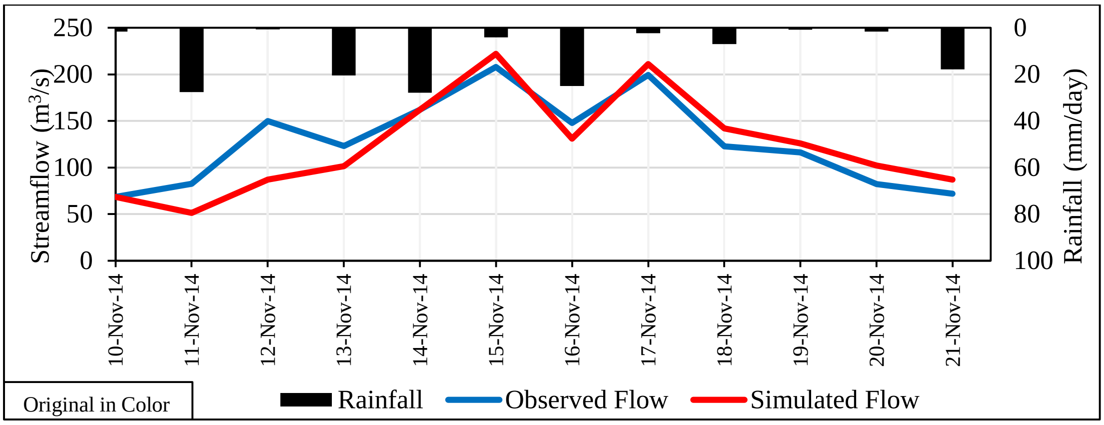

Figure E 20 Performance of event 25 lumped Kelani model

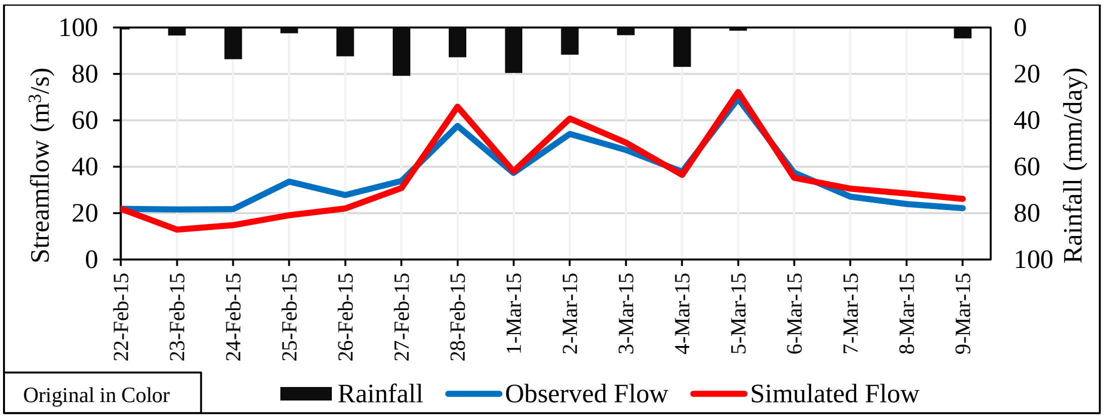

Figure E 21 Performance of event 26 lumped Kelani model

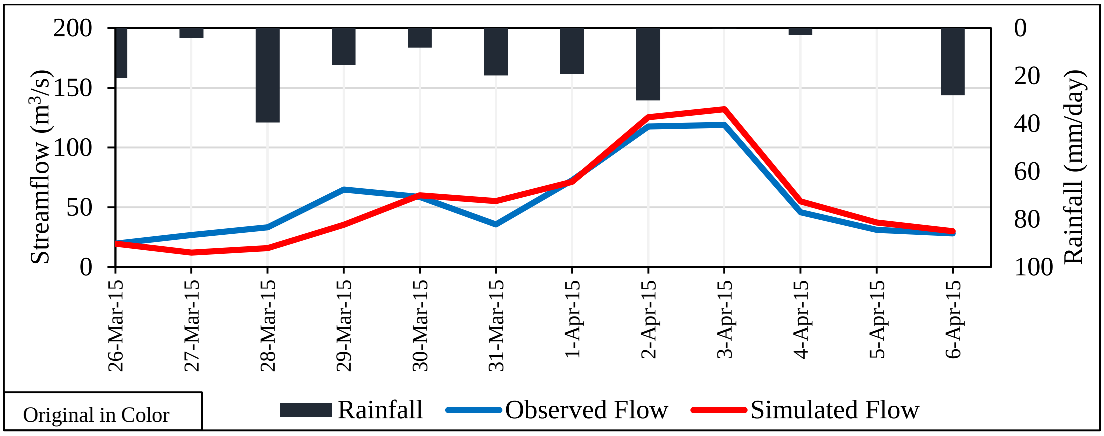

Figure E 22 Performance of event 27 lumped Kelani model

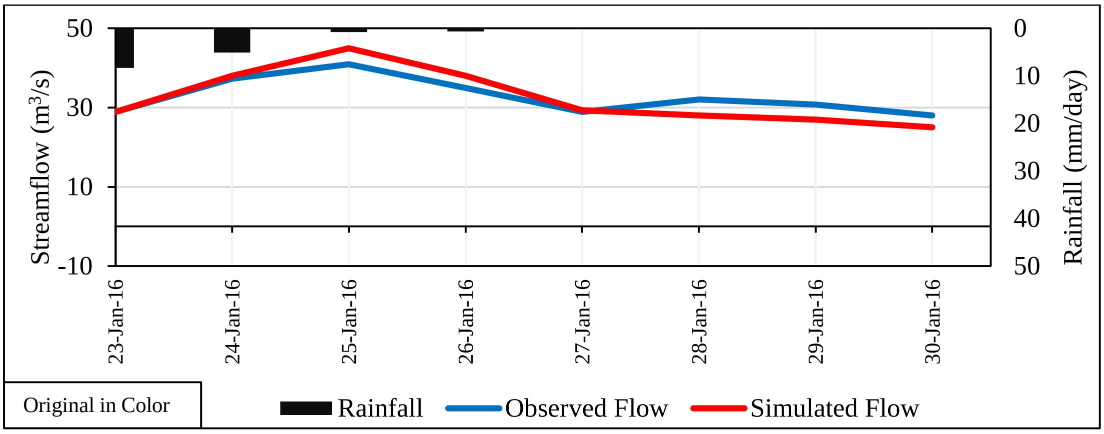

Figure E 23 Performance of event 29 lumped Kelani model

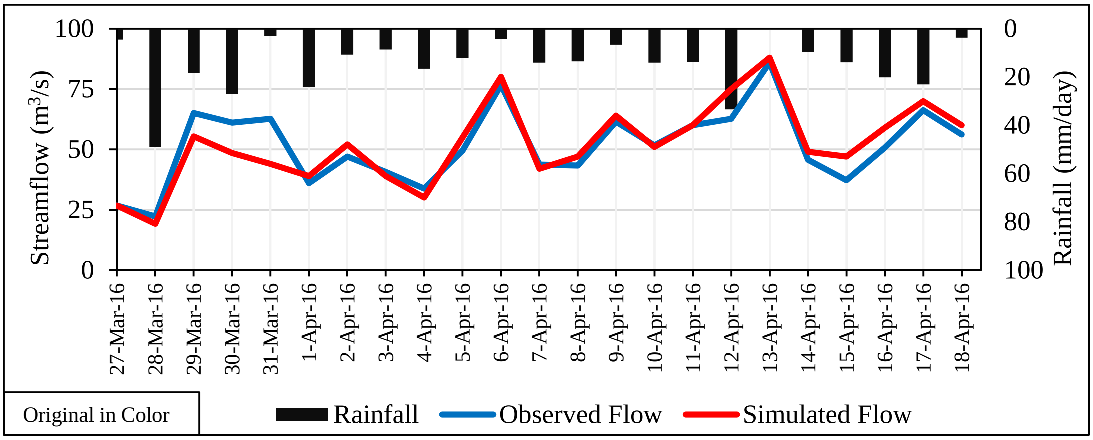

Figure E 24 Performance of event 30 lumped Kelani model

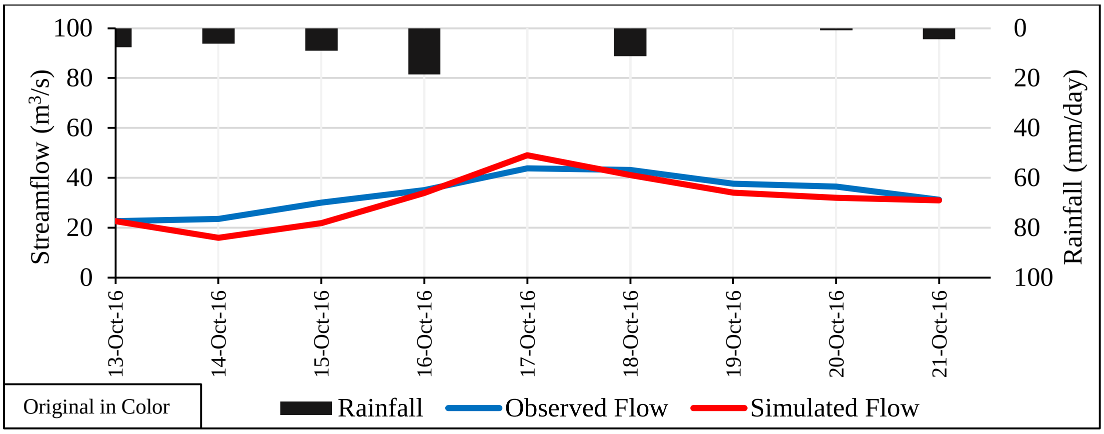

Figure E 25 Performance of event 32 lumped Kelani model

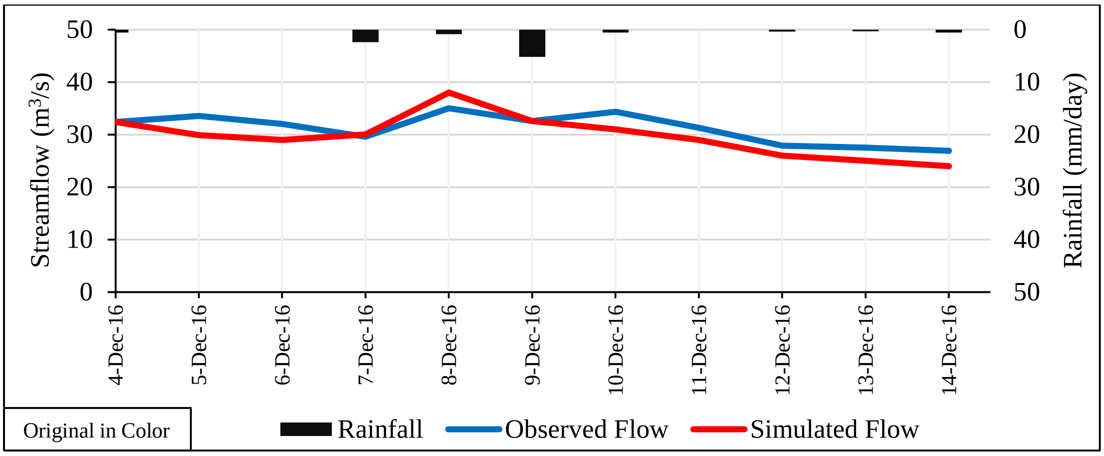

Figure E 26 Performance of event 33 lumped Kelani model

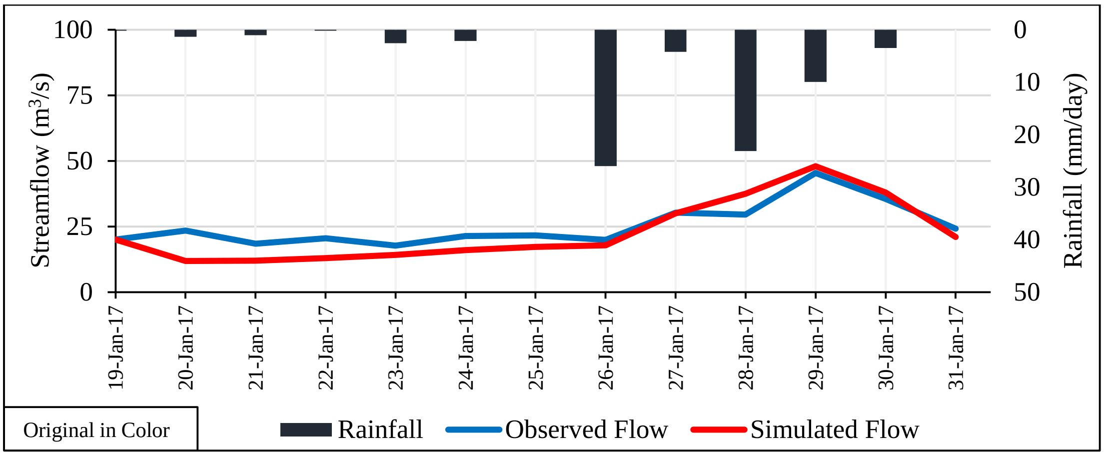

Figure E 27 Performance of event 34 lumped Kelani model

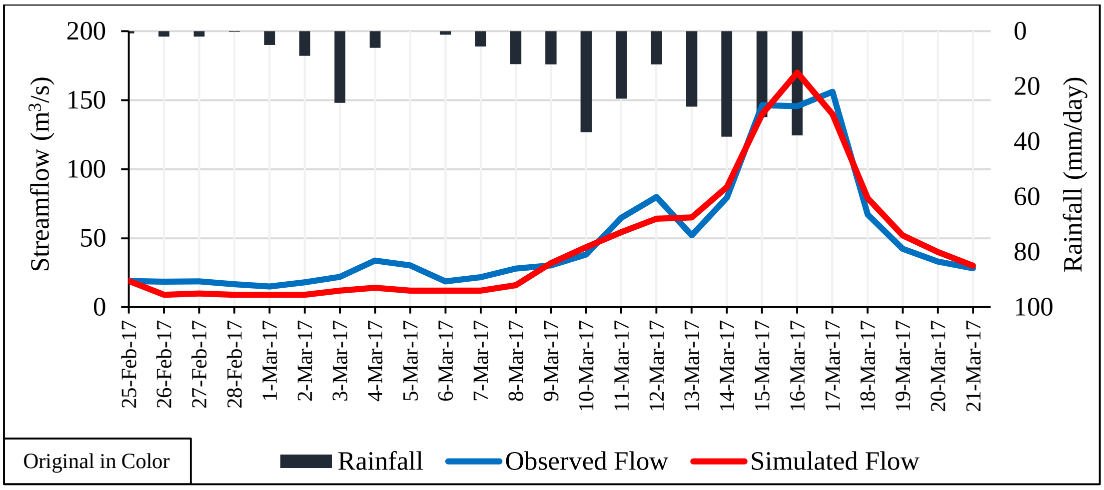

Figure E 28 Performance of event 35 lumped Kelani model

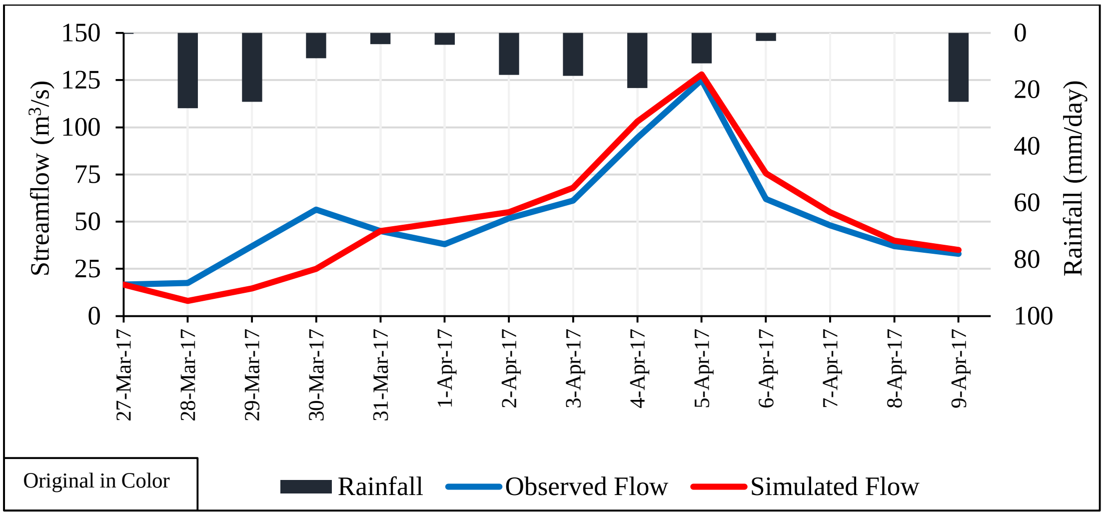

Figure E 29 Performance of event 36 lumped Kelani model